Performance Analysis of Long Term Evolution (LTE) Network

A Thesis

Submitted to

University of Technology Sydney

by

Ramprasad Subramanian

In accordance with

the requirements for the Degree of

Master of Engineering by Research

Faculty of Engineering and Information Technology

University of Technology Sydney

New South Wales, Australia

2016

CERTIFICATE OF ORIGINAL AUTHORSHIP

I, Ramprasad Subramanian declare that this thesis, is submitted in fulfilment of the requirements for the award of Master of Engineering by Research, in the Faculty of Engineering and Information Technology at the University of Technology Sydney.

This thesis is wholly my own work unless otherwise reference or acknowledged. In addition, I certify that all information sources and literature used are indicated in the thesis. This document has not been submitted for qualifications at any other academic institution. This research is supported by the Australian Government Research Training Program.

Production Note:
Signature of Candidate: Signature removed prior to publication.

Date: 20-02-2019

ACKNOWLEDGMENT

ABSTRACT

The demand for high speed network has led to the development of LTE. The LTE replaced circuit switched legacy systems into packet switched network. The high speed simultaneous transmission of data is achieved by using Orthogonal Frequency Division Multiple Access (OFDMA) in the downlink. To achieve high speed multimedia services in the downlink various packet scheduling algorithms have been proposed in the past. The LTE architecture has been simplified compared to 2G or 3G systems to a greater extent. The network elements namely Base Station Controller (BSC) and Radio Network Controller (RNC) have been replaced with eNodeB. The Radio Resource Management (RRM) functionality has been confined to eNodeB. To enable end users to achieve high data rates Heterogeneous Networks (HetNets) are used. In HetNets, the pico cells and femto cells work alongside the macro cells to deliver the required QoS. The objective of this thesis is to study the performance of LTE network through simulation and by observing the KPIs from real-time network.

The thesis starts with the performance analysis of downlink scheduling algorithms through simulations. The scheduling algorithms were simulated using NS-3 and LTE-Sim and various performance factors were studied. Thereafter, a model HetNet was simulated with a macro cell and pico cells. In the simulated LTE network environment, impact of pico cells on macro has been studied along with the scheduling algorithms.

After simulations, a more practical approach has been taken to study the performance of the LTE network. The performance analysis of Proportional Fair (PF) scheduler has been made in the real-time LTE network. In this study, the end users were classified as Gold, Silver and Bronze based on the subscription plans. A combination of various scenarios has been was tested to analyse the throughput of the scheduler. Then the performance of RAN and Evolved Packet Core has been made by observing the Key Performance Indicators (KPIs). To obtain RAN KPIs drive tests were made in various modes such as walking around the city centre, travelling in train, driving in the car and in indoor environments. The KPIs were collected using Nemo Handy RF planning tool. The final part of the thesis covers the performance analysis of EPC. The KPIs such as accessibility, retainability, traffic, mobility, and Automatic Neighbour Relations (ANR) were collected

for three months and the EPC performance was analysed. In the analysis, a critical issue in retainability was identified and this issue was impacting the accessibility of the network. After thorough analysis of KPIs, the root cause of the issue was identified as the Mobility Management Entity (MME) sending fake Serving Gateway (SGW) relocation request to eNodeB when there is only one SGW configured. This issue was identified and resolved using the KPIs.

RELATED PUBLICATIONS

Majority of the contributions included in this thesis appear in peer reviewed journal and conference papers. They are outlined as following:

Journal Articles

[1]   R. Subramanian, R. Heidari, and K. Sandrasegaran, "Interoperability and Quality Assurance for Multi-Vendor LTE Network," *International Journal of Wireless & Mobile Networks*, vol. 7, no. 5, pp. 65–76, Oct. 2015.

[2]   F. Afroz, R. Subramanian, R. Heidari, and K. Sandrasegaran, "SINR, RSRP, RSSI AND RSRQ Measurements in Long Term Evolution Networks," *International Journal of Wireless & Mobile Networks*, vol. 7, no. 4, pp. 113–123, 2015.

[3]   R. Subramanian, R. Heidari, K. Sandrasegaran, A. M. A. Dhanraj, and K. Srinivasan, "Benchmarking of Cell Throughput Using Proportional Fair Scheduler In A Single Cell Environment," *International Journal of Wireless & Mobile Networks*, vol. 7, no. 2, pp. 67–79, Apr. 2015.

[4]   R. Subramanian, P. Ghosal, S. Barua, and S. C. Lam, "Survey of LTE Downlink Schedulers Algorithms in Open access simulation Tools NS-3 and LTE-SIM," *International Journal of Wireless & Mobile Networks*, vol. 7, no. 2, pp. 01–14, Apr. 2015.

[5]   S. Xing, P. Ghosal, R. Subramanian, and K. Sandrasegaran, "Level Simulation For Two Tier Macro-Femto Cellular Network," *International Journal of Wireless & Mobile Networks*, vol. 6, no. 6, pp. 01–14, Dec. 2014.

[6]   R. Subramanian and K. Sandrasegaran, "RACH congestion in vehicular networking," *International Journal of Wireless & Mobile Networks*, vol. 6, no. 5, pp. 153–164, Oct. 2014.

[7]   R. Subramanian, S. Barua, S. C. Lam, and P. Ghosal, "Group based Algorithm to manage access technique in the vehicular networking to reduce preamble id collision and improve RACH allocation in ITS," *International Journal of Wireless & Mobile Networks*, vol. 6, no. 5, pp. 01–15, Oct. 2014.

[8]   P. Ghosal, R. Subramanian, S. Xing, and K. Sandrasegaran, "A Novel Approach For Mobility Management In Lte Femtocells," *International Journal of Wireless & Mobile Networks*, vol. 6, no. 5, pp. 45–58, Oct. 2014.

[9]   H.A. Kim, R. Subramanian, F. Afroz and K.Sandrasegaran, "Comparison of Performance of Packet Scheduling Algorithms in LTE-A HetNets," *Wireless Personal Communication*, vol 97, Issue 2, pp. 1947-1965, DOI 10.1007/s11277-017-4380-3.

Conference Papers

[1]   R. Subramanian, K. Sandrasegaran, and X. Kong, "Benchmarking of Real-Time LTE Network in Dynamic Environment," in *IEEE Asia Pacific Communication Conference (APCC)*, Indonesia: IEEE.

[2]   S. C. Lam, R. Subramanian, K. Sandrasegaran, P. Ghosal, and S. Barua, "Performance of well-known frequency reuse algorithms in LTE downlink 3GPP LTE systems," in *IEEE International Conference on Signal Processing and Communication Systems*, Cairns: IEEE, 2016.

CONTENTS

LIST OF FIGURES

LIST OF TABLE

ACRONYMS

ABS	Almost Blank Sub-frames
AC	Admission Control
AODV	Ad hoc On-demand Distance Vector
APN	Access Point Node
APN-AMBR	APN Aggregate Maximum Bit Rate
ARP	Address Resolution Protocol
ARQ	Automatic Repeat Request
BCCH	Broadcast Control Channel
BET	Blind Equal Throughput
BGCF	Breakout Gateway Control Function
BPSK	Binary Phase Shift Keying
BSC	Base Station Controller
BTS	Base Transceiver Station
BW	Bandwidth
CA	Carrier Aggregation
CAPEX	Capital Expenditure
CC	Congestion Control
CDMA	Code Division Multiple Access
CIFQ	Channel Independent Fair Queuing
CN	Core Network
CoMP	Coordinated Multi Point
CP	Cycle Prefix
CPRI	Common Public Radio Interface
CQI	Channel Quality Indicator
CRC	Cyclic Redundancy Check
CS	Circuit Switched
CSCF	Call Session Control Function
DCI	Downlink Control Information
DFT	Discrete Fourier Transform
DL	Downlink
DL - SCH	Downlink Shared Channel
DMRS	Demodulation Modulation Reference Signal
DVB	Digital Video Broadcasting
DwPTS	Downlink Pilot Timeslot
eICIC	Enhanced ICIC
E-MBMS	Enhanced Multimedia Broadcast Multicast Services
eNB	eNodeB
EPC	Evolved Packet Core
EPRE	Energy Per Resource Element

EPS	Evolved Packet Core
eRAB	enhanced Radio Access Bearer
E-UTRA	Evolved UMTS Terrestrial Radio Access
E-UTRAN	Evolved UMTS Terrestrial Radio Access Network
EVDO	Evolution Data Only/Optimized
ExPF	Exponential Proportional Fair
FDD	Frequency Division Duplex
FIFO	First In First Out
FTP	File Transfer Protocol
GBR	Guaranteed Bit Rate
GERAN	GSM EDGE Radio Access Network
GGSN	Gateway GPRS Support Node
GP	Guard Period.
GPRS	General Radio Packet Service
HARQ	Hybrid Automatic Repeat Request
HDR	High Data Rates
HetNet	Heterogeneous Network
HOC	Handover Control
HOL	Head Of Line
HSDPA	High Speed Downlink Packet Access
HSPA	High Speed Packet Access
HSS	Home Subscriber Server
HSUPA	High Speed Uplink Packet Access
HTTP	Hyper Text Transfer Protocol
ICC	Interference Coordination and Control
ICI	Inter Cell Interference
ICIC	Inter Cell Interference Cancellation
I-CSCF	Interrogating Call Session Control Function
IFFT	Inverse Fast Fourier Transform
IM-MGW	IP Multimedia Gateway
IMS	IP Multimedia Sub-system
ISI	Inter Symbol Interference
KPI	Key Performance Indicator
LC	Load Control
LTE	Long Term Evolution
LWDF	Largest Weighted Delay First
MAC	Medium Access Control
MBMS	Multimedia Broadcast Multicast Services
MBR	Maximum Bit Rate
MCS	Modulation and Coding Scheme
MGCF	Media Gateway Controller Function
MIB	Master Information Block

MIMO	Multiple Input Multiple Output
MLWDF	Modified Largest Weighted Delay First
MME	Mobility Management Entity
MT	Maximum Throughput
MTU	Message Transfer Unit
MU-MIMO	Multi User MIMO
NS-3	Network Simulator -3
OFDMA	Orthogonal Frequency Division Multiple Access
OLSR	Optimized Link State Routing Protocol
OPEX	Operational Expenditure
PBCH	Physical Broadcast Channel
PC	Power Control
PCFICH	Physical Control Format Indicator Channel
PCI	Physical Cell ID
PCRF	Policy Control and charging Rules Function
P-CSCF	Proxy Call Session Control Function
PDCCH	Physical Downlink Control Channel
PDCP	Packet Data Convergence Protocol
PDN	Packet Data Network
PDSCH	Physical Downlink Shared Channel
PF	Proportional Fair
PGW	PDN Gateway
PHICH	Physical Hybrid ARQ Indicator Channel
PHY	Physical layer
PLR	Packet Loss Ratio
PS	Packet Switched
PSS	Priority Set Scheduler
PVI	Pre-emption Vulnerability Indicator
QAM	Quadrature Amplitude Modulation
QCI	QoS Class Identifier
QoS	Quality of Service
QPSK	Quadrature Phase Shift Keying
RACH	Random Access Channel
RAN	Radio Access Network
RB	Resource Blocks
RBG	Resource Block Group
RLC	Radio Link Control
RNC	Radio Network Controller
RR	Round Robin
RRC	Radio Resource Control
RRM	Radio Resource Management
RSRP	Reference Signal Received Power
RSRQ	Reference Signal Received Quality

RSSI	Reference Signal Strength Indicator
SBFA	Server Based Fairness Approach
SC-FDMA	Single Carrier Frequency Division Multiple Access
SGSN	Serving GPRS Support Node
SGW	Serving Gateway
SINR	Signal to Interference Noise Ratio
SLF	Subscriber Location Function
SMS	Short Message Service
SNR	Signal to Noise Ratio
SRS	Sounding Reference Signal
TBFQ	Token Bank Fair Queue Scheduler
TDD	Time Division Duplex
TEMS	Test Mobile System
TPC	Transmission Power Control
TTA	Throughout To Average
TTI	Transmission Time Interval
TxD	Transmit Diversity
UDP	User Datagram Protocol
UE	User Equipment
UL	Uplink Link
UL - SCH	Uplink Link Shared Channel
UMTS	Universal Mobile Telecommunications System
VoIP	Voice over IP
VoLTE	Voice over LTE
WCDMA	Wideband Code Division Multiple Access
WFQ	Weighted Fair Queuing
WFS	Work Flow Scheduling
WiFi	Wireless Fidelity
WiMAX	Worldwide Interoperability for Microwave Access
WLAN	Wireless Local Area Network

LIST OF SYMBOLS

s_m	OFDM symbol
N	Narrowband modulated subcarriers
PL	Pathloss
SH	Shadowing
PN	Penetration loss
i, j	Users
t	Subframe index
k	Resource blocks
$M_{i,k}(t)$	Modulation coding scheme
B	Transport block in bits for resource blocks
$R_i(k, t)$	Achievable rate
τ	TTI duration
$T_j(t)$	Past throughput
α	Time constant
$\widehat{T}_j(t)$	Actual throughput
$\widehat{M}_j(t)$	Modulation coding scheme index
t_i	Packet arrival rate (byte/sec)
r_i	Token generation rate (byte/sec)
p_i	Token pool size (byte)
E_i	Number of token borrowed from or given
$p_k^1(t)$	Priority metric
$\frac{B}{N}$	FD-BET
R_i^{fb}	Full achievable bandwidth of a UE
T_{fdtbfq}^I	Total TBFQ throughput

T_{pss}^{I}	Total PSS throughput
nbs	Number of bits per symbol
nss	Number of symbols per slot
nts	Represents the number of slots per TTI
nsr	Represents the number of sub-carriers per RB
$pdiscard_i(t)$	Discarded or lost packet
$ptransmit_i(t)$	Transmitted packets
P_t	Transmitted power at BS
h_k	Channel gain
σ_s^2	Log normal distribution with zero mean and variance
S_k	Shadowing effect
m_k	Multipath fading
Z_k	SNR of user k
P_n	Denotes background noise power including thermal noise and other Gaussian interference.
ρ	Noise level of wireless environment
D	Radius of the cells
Z_k	Average SNR of user k
$R_k[n]$	Possible user rate in time slot n
t_c	Time constant

1. INTRODUCTION TO LTE

Cellular networks in major countries in the world have been upgraded to High Speed Packet Access (HSPA) to enable customer to enjoy high speed data. HSPA is a combination of high speed in uplink and downlink. In uplink it is referred to as High Speed Uplink Packet Access (HSUPA) and in downlink it is referred as High Speed Downlink Packet Access (HSDPA). The services, HSDPA and HSUPA were introduced in 3GPP Release 5 and 6. Eventually, the HSPA service fell short of expectation and resulted in the introduction of HSPA+. This was introduced with several enhancements in subsequent 3GPP releases namely 7, 8, 9 and 10. The main objective of introducing of HSPA+ was to serve several objectives such as high spectrum efficiency, peak data rate and latency, to exploit the potential of Wideband Code Division Multiple Access (WCDMA) based 5 MHz operation. Features of HSPA+ include downlink Multiple Input Multiple Output (MIMO), higher modulation schemes for efficient uplink and downlink such as 16QAM and 64 QAM, enhancement in layer 2 protocols, and continuous packet connectivity were released in Release 7. The other significant enhancements such as combination of 64QAM and MIMO, up to four and two carrier operations in downlink and uplink were introduced in Release 8, 9, and 10. These enhancements enabled to achieve theoretical max of 168 Mbps in downlink and 23 Mbps in uplink respectively. In addition, to complement the advancements in air interface, standardization body focused on improving circuit-switched services over HSPA+ in Release 8 [1].

To ensure competitiveness of Universal Mobile Telecommunications System (UMTS) service, concepts of UMTS Long Term Evolution (LTE) were introduced in 3GPP Release 8 for the first time. The main objective of LTE was to focus on high speed data rates, lower latency on user and control planes, and packet optimized radio access technology. LTE is referred as Evolved UMTS Terrestrial Radio Access (E-UTRA) and Evolved UMTS Terrestrial Radio Access Network (E-UTRAN). The terms LTE, E-UTRA or E-UTRAN are used interchangeably in the following sections of the thesis. LTE supports various ambitious requirements such as high speed data rate, high capacity, spectrum efficiency, and lower latency so as to become a true mobile broadband technology. To fulfil some of these requirements, LTE was proposed with several new

technical principles such as, Orthogonal Frequency Division Multiple Access (OFDMA) in downlink, Single Carrier Frequency Division Multiple Access (SC-FDMA) in uplink and MIMO antenna schemes. Several major design changes were carried out in existing UMTS protocol concepts to facilitate for LTE. The impact on overall architecture including in core network is referred to System Architecture Evolution (SAE) [1].

LTE supports two modes of operation such as Frequency Division Duplex (FDD) and Time Division Duplex (TDD) commonly referred as TD-LTE and FD-LTE. This chapter provides adequate coverage for introduction to LTE technology, including both FDD and TDD modes of operation [1].

1.1 Requirements for UMTS Long Term Evolution

Several important requirements for an LTE system were identified in the beginning of the standardization process in the year 2004 [2] and they include:

Data rate: Achieving data rate of 50 Mbps in uplink and 100 Mbps in down link is expected in LTE.

Throughput: Achieving average user throughput of 3-4 times better than 3GPP Release 6 in downlink and 2-3 times better in uplink than Release 6.

Spectrum Efficiency: The data rate and spectrum efficiency requirement for LTE is summarized in the Table 1.1.

Table 1.1: Data rate and spectrum efficiency requirement defined for LTE

Downlink (20 MHz)			Uplink (20 MHz)		
Unit	Mbps	bps/Hz	Unit	Mbps	bps/Hz
Requirement	100	5	Requirement	50	2.5
2x2 MIMO	172.8	8.6	16QAM	57.6	2.9
4x4 MIMO	326.4	16.3	64QAM	86.4	4.3

Latency: The latency can be classified as user and control plane latency. The user plane latency is the one way transit time of packets that are available in the device or Radio Access Network (RAN) at the IP layer. The availability of the packet in the device or RAN must be less than 30 ms.

The time taken for the device connection to change from passive (IDLE state) to active (CONNECTED state) is defined as control plane latency. The latency must be less than 100 ms.

Bandwidth: LTE supports various bandwidths such as 1.4, 3, 5, 10, 15 and 20 MHz.

Interworking: The interworking between E-UTRAN and other systems (3GPP and non 3GPP systems) must be ensured. The multimode wireless terminals support seamless handover between E-UTRAN and UTRAN/GERAN. The handover between E-UTRAN and UTRAN/GERAN shall be less than 300 ms for real time services and 500 ms for non-real time services.

Multimedia Broadcast Multicast Services (MBMS): The MBMS service was enhanced in LTE and referred as Enhanced-MBMS (E-MBMS). The Release 8 focused on physical layer aspect for E-MBMS and the standardization support for higher layers was carried out in Release 9.

Mobility: The LTE system must be capable of supporting both high (travelling in high speed train) and low speed (0-15 Km/h) mobile customers.

Spectrum allocation: The LTE system is designed to be operated in paired (Frequency Division Duplex - FDD mode) and un-paired (Time Division Duplex – TDD mode) spectrum.

Co-existence: LTE system is designed to support co-existence with legacy networks such as GERAN/UTRAN in the same geo-graphical location. Similarly, the support must be extended to co-exist with other service providers in adjacent bands.

Quality of Service (QoS): QoS must be supported and Voice over Internet Protocol (VoIP) must be supported similarly as voice traffic over UMTS based networks.

Costs: LTE system natively supports reduced Capital Expenditure (CAPEX) and Operational Expenditure (OPEX). Interfaces specified in LTE system must support multi-vendor equipment interoperability with reasonable system complexity, cost and power consumption.

1.2 LTE Downlink Transmission Scheme - OFDMA

The downlink transmission scheme in E-UTRA in both FDD and TDD is based on OFDM. As per the OFDM transmission scheme, the available spectrum is divided into several sub- carriers and modulated independently by a low rate data stream. Furthermore, OFDM is widely used on various technologies such as Wireless LAN (WLAN), WiMAX, and broadcast technologies such as Digital Video Broadcasting (DVB). OFDM offers several advantages such as robustness against multipath fading and provide efficient receiver architecture [3].

Figure 1 represents the OFDM signal with 5 MHz bandwidth. As shown in the figure, the data symbols are modulated independently and transmitted by closely spaced orthogonal sub-carriers.

In time domain, guard intervals are added to each data symbol to combat Inter-Symbol-Interference (ISI). The guard interval is chosen based on greater the maximum expected delay spread and it is inserted as cyclic prefix prior to each OFDM symbol. The delay used in guard interval can be defined as the time duration between the first multi-path signal and the last multipath signal. In a typical scenario the duration of the delay is expected to be in micro-seconds depending on the environment such as indoor, rural, urban, and sub-urban [3].
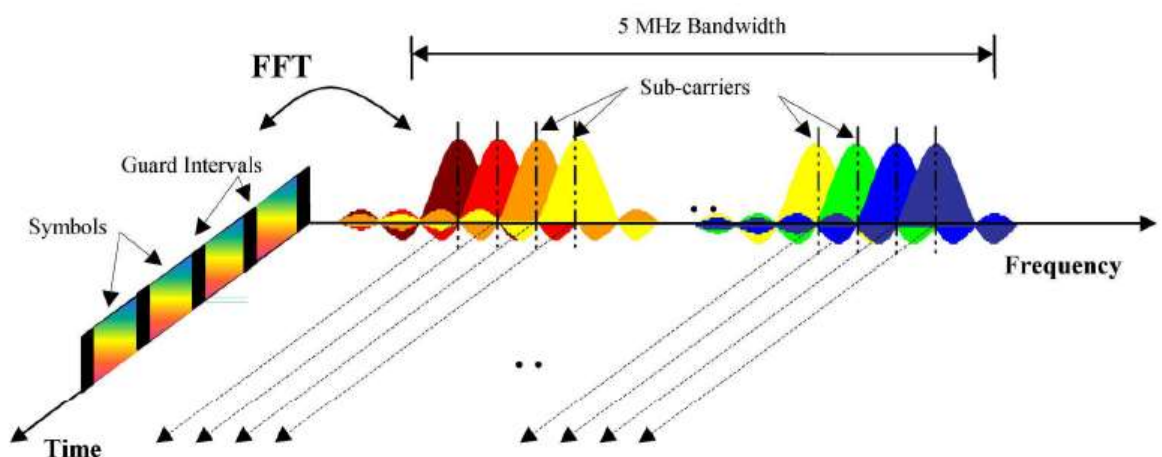
Figure 1.1: Frequency-time representation of an OFDM signal [3]

In practice, OFDM signal is generated by using Inverse Fast Fourier Transform (IFFT), in which the data symbols in frequency domain, is converted to time domain. The block

diagram explaining the conversion process is illustrated in Figure 1.2 where $a(mN + n)$ refers to n^{th} subcarrier of the modulated data symbol at the time period

$$mT_u < t \le (m + 1)T_u.$$
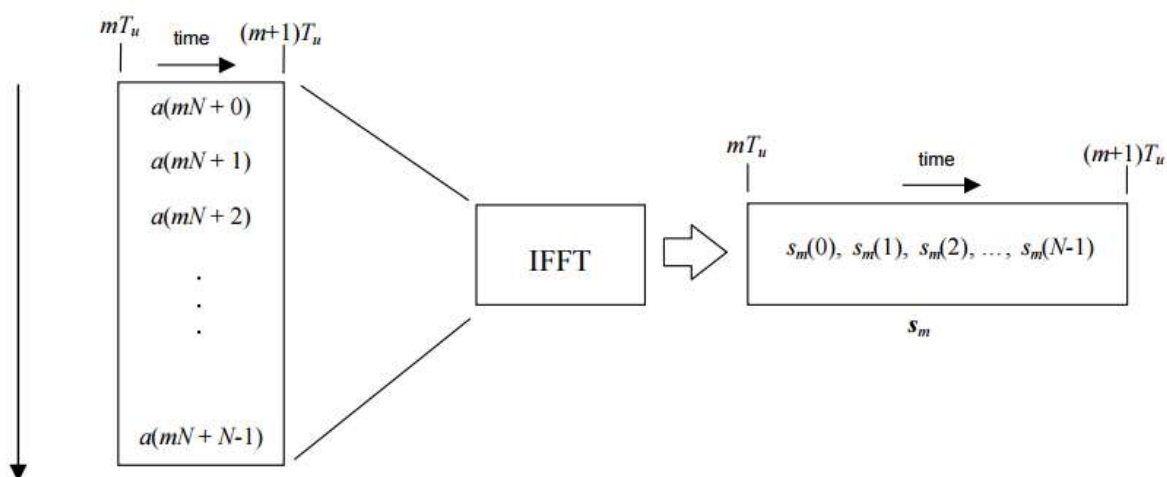
Figure 1.2: OFDM useful symbol generation using an IIFT [3]

As shown in the figure, the useful OFDM symbol s_m and time superposition of N narrowband modulated subcarriers forms a parallel stream of N sources of data, modulating independently.

In frequency domain, mapping of QAM serial data to N parallel streams to be used by IFFT is illustrated in Figure 1.3. The N point time domain blocks from IFFT are then serialized to create time domain signal.
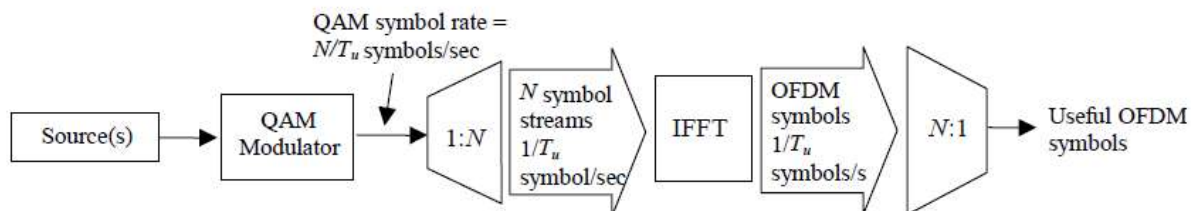
Figure 1.3: OFDM signal generation chain [3]

In OFDMA, users are allocated specific time-frequency resource and allowed to access available bandwidth unlike the OFDM transmission scheme. In E-UTRA, users share the

data channels and for every Transmission Time Interval (TTI), a new scheduling decision regarding the allocation of time/frequency resources to its users is taken [3].

1.2.1   OFDMA parameterization

The frame structure types such as frame structure Type 1 for FDD and frame structure type 2 for TDD are defined for E-UTRA [4]. In frame structure type 1, the radio frame of 10 ms is equally divided in to 20 slots of 0.5 ms and two of these slots make one subframe making it 10 subframes in one radio frame as illustrated in Figure 1.4.
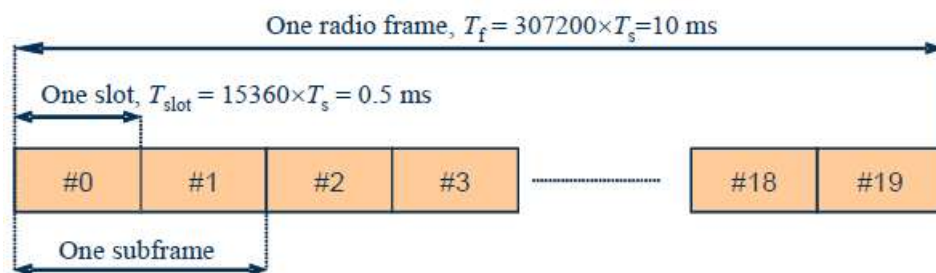
Figure 1.4: Frame structure type 1 [4]

The basic time unit in LTE is referred to as T_s (sampling time) which is corresponding to a sampling frequency of 30.72 MHz. This sampling frequency is obtained from the subcarrier spacing of $\Delta f = 15\ kHz$ which is a maximum FFT size to generate 2048 OFDM symbols. Since, this frequency is a multiple of the chiprate defined for WCDMA (30.72 MHz/8= 3.84 Mcps) and CDMA 2000 (30.72 MHz/25 = 1.2288 Mcps). These parameters ensure the implementation of multi-standard devices [4].

In frame structure Type 2, the radio frame (which is 10 ms) is divided as two half frames of 5 ms in length. Each half frame is further divided into five subframes which are of 1ms each, as shown in the Figure 1.5 below. Barring special subframes, the remaining subframes consist of two slots which are of length 0.5 ms each. The special subframes consist of fields such as Downlink Pilot Timeslot (DwPTS), Guard Period (GP), and Uplink Pilot Timeslot (UpPTS). The individual lengths of these fields are configurable

within the total length of 1 ms. These fields are already known and maintained in LTE-TDD.
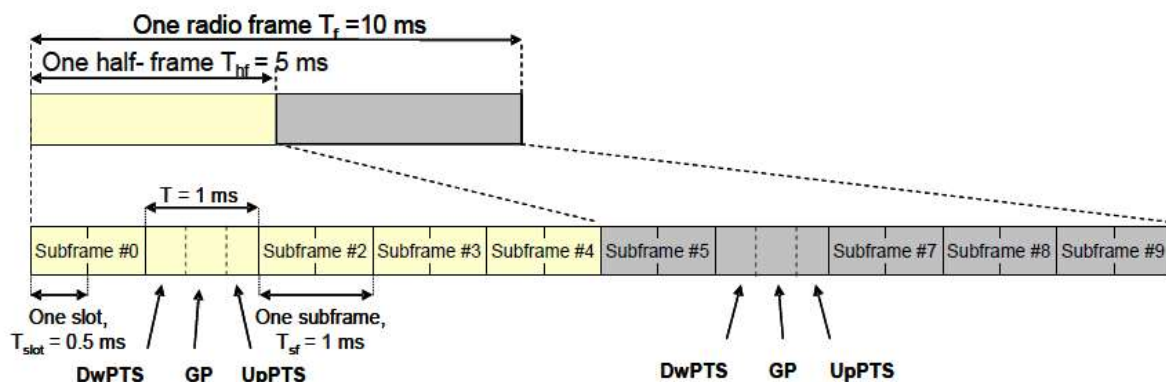
Figure 1.5: Frame structure type 2 [4]

Frame structure type 2 supports seven uplink-downlink configuration with different lengths such as 5 ms or 10 ms in downlink-uplink switch-points. In case of 5 ms switch-point, the special frame structure exists in both half frames and in 10 ms switch-point periodicity, the special frame exists in the first half frame. The subframes DwPTS, 0, and 5 are reserved for downlink transmission. The UpPTS and the subframe which follows the special subframe are reserved for uplink transmission. Table 1.2 denotes the uplink-downlink configurations, where D denotes the subframe reserved for downlink, U represents uplink, and S denotes the special subframe.

Table 1.2: Uplink-Downlink configuration for LTE-TDD [4]

Uplink-downlink configuration	Downlink-to-Uplink Switch-point-periodicity	Subframe number									
		0	1	2	3	4	5	6	7	8	9
0	5 ms	D	S	U	U	U	D	S	U	U	U
1	5 ms	D	S	U	U	D	D	S	U	U	D
2	5 ms	D	S	U	D	D	D	S	U	D	D
3	10 ms	D	S	U	U	U	D	D	D	D	D
4	10 ms	D	S	U	U	D	D	D	D	D	D
5	10 ms	D	S	U	D	D	D	D	D	D	D
6	5 ms	D	S	U	U	U	D	S	U	U	D

As illustrated in the Table 1.2, special subframe is associated when there is switching from DL to UL and it is referred as Guard Period (GP). The GP is required in DL to UL switching because GP enables transmission from different User Equipments (UE) to arrive at the same time at BS receiver [4]. On the other hand, in switching from UL to DL, only BS is involved in transmitting DL hence, do not require guard period. Besides UL-DL configurations, several other configurations such as configuration for 9 special subframes, length of DwPTS, different lengths of GP to support cell size up to 100 km, and UpPTS are given in [4].

Table 1.3: Special subframe configurations in TD-LTE [4]

Special subframe config.	Normal cyclic prefix in downlink				Extended cyclic prefix in downlink			
	DwPTS	Guard Period	UpPTS Normal cyclic prefix	UpPTS Extended cyclic prefix	DwPTS	Guard Period	UpPTS Normal cyclic prefix in uplink	UpPTS Extended cyclic prefix in uplink
0	3	10	1	1	3	8	1	1
1	9	4			8	3		
2	10	3			9	2		
3	11	2			10	1		
4	12	1	2	2	3	7	2	2
5	3	9			8	2		
6	9	3			9	1		
7	10	2			-	-	-	-
8	11	1			-	-	-	-

It is important to note that downlink and uplink in TD-LTE utilize different cyclic prefixes compared to LTE-FDD. The Figure 1.6 shows the downlink resource grid for FDD and TDD.
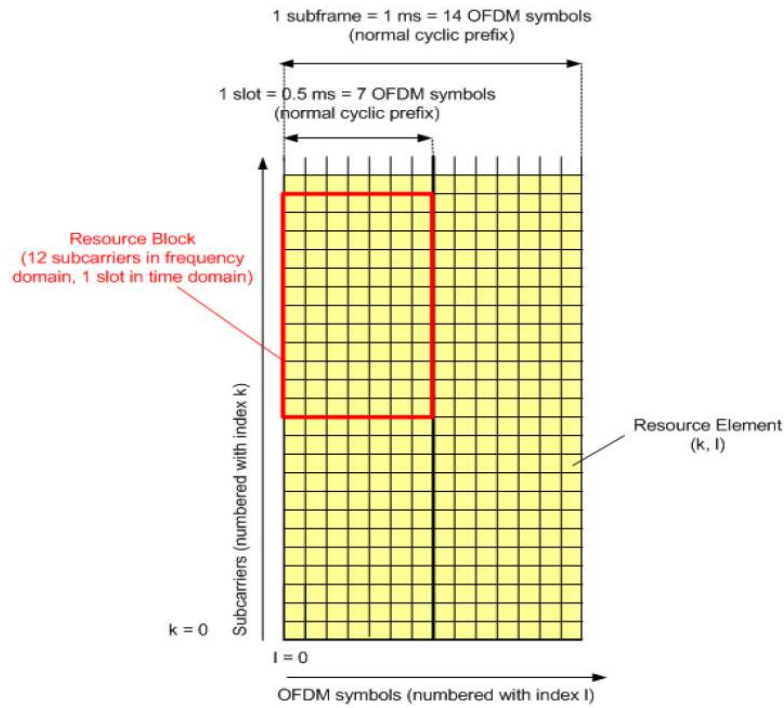
Figure 1.6: Downlink resource grid [4]

In frequency domain, 12 subcarriers with 15 KHz of spacing form one Resource Block (RB) and together they occupy a bandwidth of 180 kHz. The number of RBs in corresponding channel bandwidths is shown in Table 1.4.

Table 1.4: Number of RBs for different LTE bandwidths (TDD and FDD) [5]

Channel bandwidth [MHz]	1.4	3	5	10	15	20
Number of resource blocks	6	15	25	50	75	100

Every downlink slot consists of 6 or 7 OFDM symbols depending on the type of Cyclic Prefix (CP) configured. The extended CP covers larger cell sizes with higher delay spread of radio channel and with reduced number of symbols [4]. The CP length in samples and CP length in μs are summarized in Table 1.5.

Table 1.5: Downlink frame structure parameterization (FDD and TDD) [4]

Configuration	Resource block size N_{symb}^{RB}	Number of Symbols N_{symb}^{DL}	Cyclic prefix length in samples	Cyclic prefix length in µs
Normal cyclic prefix Δf=15kHz	12	7	160 for first symbol 144 for other symbols	5.2 µs for first symbol 4.7 µs for other symbols
Ext. cyclic prefix Δf=15kHz	12	6	512	16.7 µs

The sampling frequency of 30.72 MHz consists of 307200 samples in 10 ms frame i.e., 15360 samples are available in 0.5 ms time slot. Each OFDM symbols consists of 2048 samples and with the usage of normal CP, 7 OFDM symbols are available (7*2048) and making it to 14336 samples per time slot. The remaining samples of 1024 are the basis for CP. The first OFDM symbol uses CP length of 160 samples and the remaining 6 OFDM symbols use 144 samples as CP length [4].

1.2.2 Downlink Data Transmission

The allocation of data to UE is performed in terms of RB. The RBs that are allocated to the individual UE are allocated as integer multiples of one RB in frequency domain and these allocated RBs do not have to be adjacent to each other. In time domain, the scheduling decision to allocate RBs is modified for every Transmission Time Interval (TTI). The Base Station (BS) performs scheduling decision for uplink and downlink based on various factors such as radio link quality of individual UEs, overall interference situation, Quality of Service (QoS) requirements, and service priorities. Figure 1.7 shows the allocation of user data for different UEs in downlink (1-6). The Physical Downlink Shared Channel (PDSCH) carries user data in downlink and can be modulated by various schemes namely Quadrature Phase Shift Keying (QPSK), 16 Quadrature Amplitude Modulation (QAM), or 64 QAM [5].
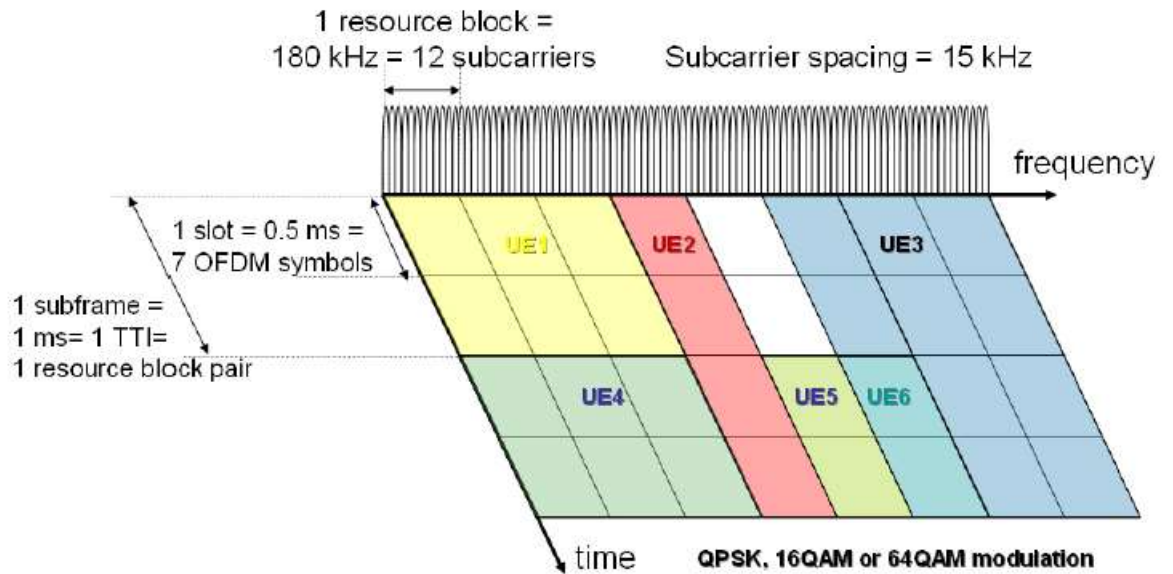
Figure 1.7: OFDMA time-frequency multiplexing for normal CP [5]

1.2.3 Downlink Control Channels

The Physical Downlink Control Channel (PDCCH) is located in the first OFDM symbol of a subframe and conveys scheduling decisions made by BS to individual UEs in downlink. PDCCH is always mapped to first two OFDM symbols of DwPTS field in frame structure Type 2. The Physical Control Format Indicator Channel (PCFICH) indicates the number of symbols used for PDCCH (1, 2, 3, or 4 symbols) and this is carried on the first OFDM symbol in each subframe. The information conveyed by PCFICH helps to understand the load on PDCCH, as it can vary depending on the number of users in the cell and signalling formats. The symbols that are used to carry PDCCH depend on the configured bandwidth. For example, in channel bandwidth of 1.4 MHz, minimum required symbol is 2 and the maximum required is 4 [5]. Table 1.6 shows different formats of Downlink Control Information (DCI) carried by PDCCH and its purpose as described by 3GPP.

Table 1.6: DCI formats carried by PDCCH as defined by 3GPP Release 8 [5]

DCI Format	Content and Tasks	Allocation Type used
0	Scheduling of PUSCH	2
1	Scheduling of one PDSCH codeword	0, 1
1A	Compact scheduling of one PDSCH codeword and random access procedure initiated by a PDCCH order	2
1B	Compact scheduling of one PDSCH code word with pre-coding	2
1C	Very compact scheduling of one PDSCH codeword, RACH response and dynamic BCCH scheduling	2
1D	Compact scheduling of one PDSCH codeword with precoding and power offset information	2
2	Scheduling PDSCH to UE's configured in closed-loop spatial multiplexing mode	0, 1
2A	Scheduling PDSCH to UE's configured in open loop spatial multiplexing mode	0 ,1
3	Transmission of TPC commands for PUCCH and PUSCH with 2-bit power adjustments	-
3A	Transmission of TPC commands for PUCCH and PUSCH with single bit power adjustments	-

In Table 1.7, the contents of DCI Format 1 have been given as an example. The Format 1 is used for assigning downlink shared channel resource when spatial multiplexing is not used. This information helps UE to identify when to receive PDSCH in that subframe and how to decode it [6].

Table 1.7: DCI format 1 contents carried on PDCCH [6]

Information type	Number of bits in PDCCH	Purpose
Resource allocation header	1	Indicates the resource allocation type being used such as Type 0 or Type 1.
RB assignment	Depending on the type of resource allocation	Indicated the RB number to be assigned for a device.
Modulation and coding scheme	5	Indicates modulation scheme, allocated physical RBs and transport block size.
Hybrid Automatic Repeat Request (HARQ) process number	3 for TDD and 4 for FDD	Identifies the packet associated with the HARQ.
New data indicator	1	Indicates whether the packet belongs to new transmission or re-transmission.
Redundancy version	2	Identifies the redundancy version for coding the packet.
Transmit Power Control (TPC) command for PUCCH	2	TPC commands to adapt transmit power on Physical Uplink Control Channel (PUCCH).
Downlink assignment index in TDD.	2	Number of downlink subframes for uplink ACK/NACK (Acknowledgement).

The UE monitors the beginning of each subframe transmitted by higher layers to know its identity. This identity of the UE is assigned during random access procedure by the network. Similarly, there are several pre-reserved identities used to serve for different purpose such as to inform about scheduling and paging information to the system or to provide a response to a network access attempt. This helps to save signalling resources on PDCCH. In Table 1.8, various transmission modes and related DCI formats are defined as specified by 3GPP Release 8 [6].

Table 1.8: LTE transmission modes [6]

Transmission Mode (TM)	DCI format	Transmission scheme of PDSCH corresponding to PDCCH
Mode 1	DCI format 1A	Single-antenna port, port 0 (SISO)
	DCI format 1	Single-antenna port, port 0 (SISO)
Mode 2	DCI format 1A	Transmit diversity (TxD)
	DCI format 1	Transmit diversity (TxD)
Mode 3	DCI format 1A	Transmit diversity (TxD)
	DCI format 2A	Large delay CDD or Transmit diversity (TxD)
Mode 4	DCI format 1A	Transmit diversity (TxD)
	DCI format 2	Closed-loop spatial multiplexing or TxD
Mode 5	DCI format 1A	Transmit diversity (TxD)
	DCI format 1D	Multi-user MIMO (MU-MIMO)
Mode 6	DCI format 1A	Transmit diversity (TxD)
	DCI format 1B	Closed-loop spatial multiplexing using a single transmission layer
Mode 7	DCI format 1A	If the number of PBCH antenna ports is one, Single-antenna port, port 0 is used otherwise TxD
	DCI format 1	Single-antenna port; port 5

The DCI formats 2 and 2A specified in the Table 1.8 provide shared channel assignment in the downlink for closed loop spatial multiplexing (Transmission Mode – TM4) or open loop spatial multiplexing (Transmission Mode –TM3) respectively. In closed loop spatial multiplexing, UE provides feedback on MIMO transmission whereas in open-loop spatial multiplexing, UE feedback is not provided. Additionally, DCI formats 3 and 3a convey uplink Transmit Power Control (TPC) commands and perform power control for the devices that are semi persistently scheduled such as VoIP call [6].

1.2.4   Downlink Reference Signal Structure and Cell Search

The reference signal structure in downlink is significant in several aspects such as initial acquisition and cell search, coherent detection and demodulation, channel estimation and radio link quality measurements. It enables UE to distinguish between transmit antennas used in eNodeBs. Figure 1.8 indicates the structure of downlink reference signal for up to four transmit antennas. In frequency domain, the cell specific reference signal is carried by pre-defined specific resource elements. In this domain, every six subcarrier carries a portion of reference signal which repeats for every fourth OFDM symbol. The reference signal sequence is derived from pseudo-random sequence and results in a QPSK type constellation. The reference signal undergoes frequency shifts when mapped to subcarriers. During cell search UE gathers different information from reference signal related to symbol and radio frame timing, frequency and cell identification, overall transmission, bandwidth, antenna configuration and CP length [6].

The initial step of cell search in LTE begins with specific synchronization signal which is based on hierarchical cell search similar to WCDMA. The synchronization signals are transmitted twice for every 10 ms interval at pre-defined slots. Figure 1.8 and 1.9 show primary and secondary synchronization signals for FDD and TDD. In frequency domain, 62 subcarriers are used to transmit synchronization signals. LTE supports 504 Physical Cell Identities (PCI), which is divided into 168 Cell ID groups with 3 Cell Ids per group (i.e. 168*3 = 504). Each group consists of three unique identities such as 0, 1, or 2 carried by primary synchronization signal [6].
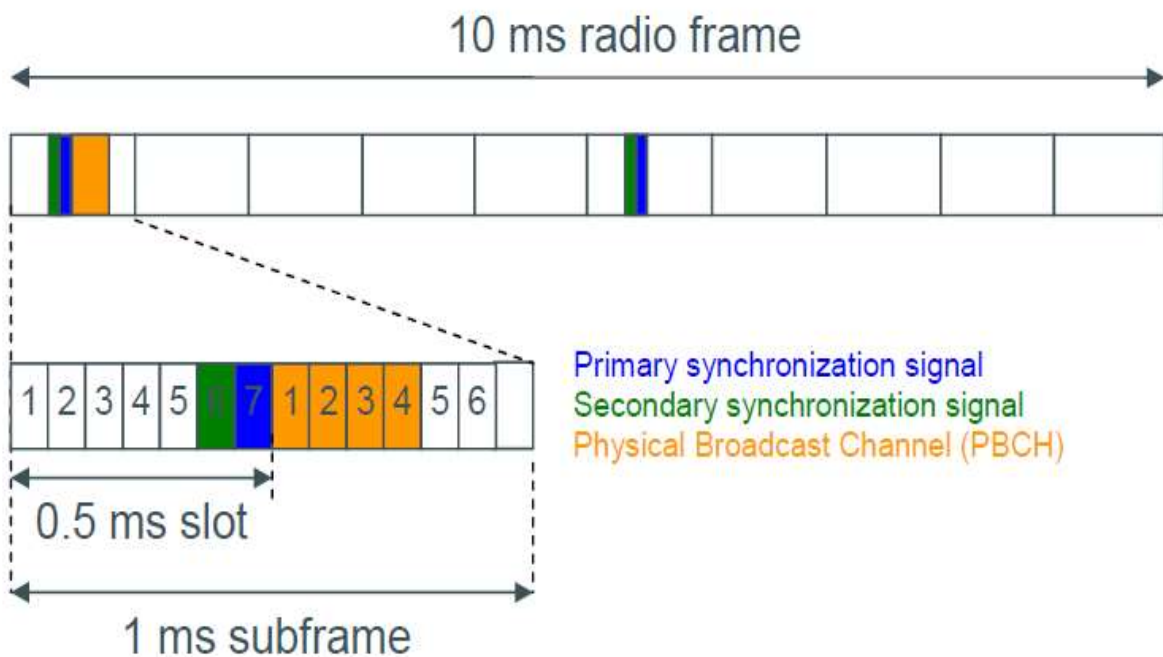
Figure 1.8: Primary synchronization signal and PBCH structure of frame structure type 1/FDD, normal, cyclic prefix [6]
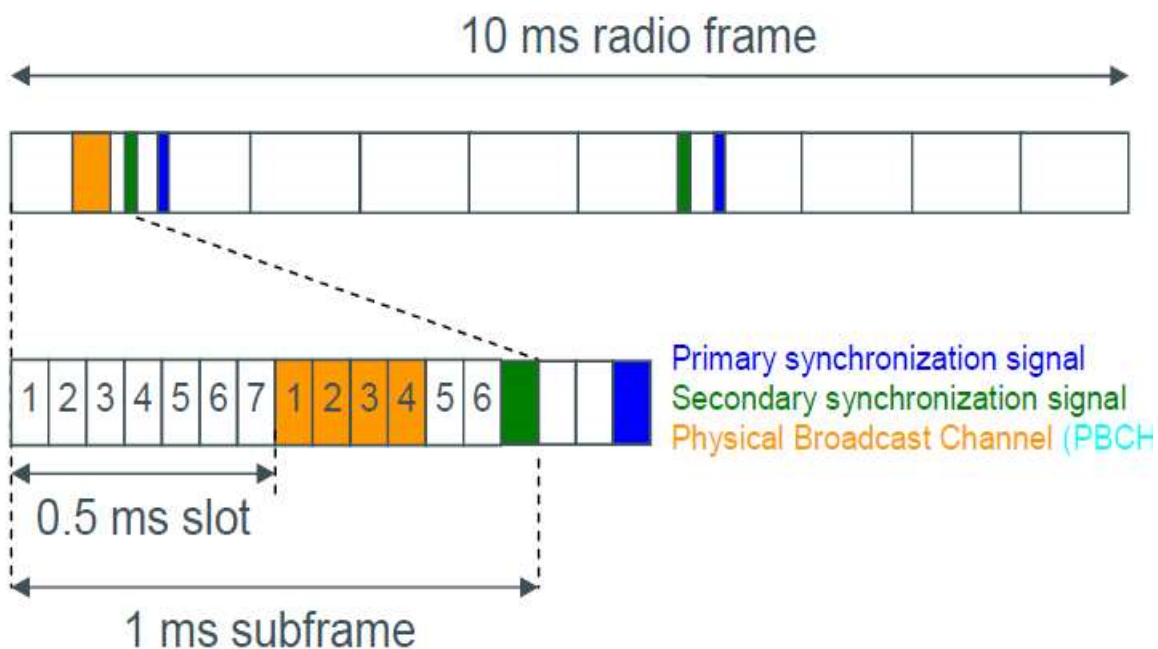
Figure 1.9: Primary/secondary synchronization signal and PBCH structure (frame structure Type2 / TDD, normal cyclic prefix [6]

The Master Information Block (MIB) carried by Physical Broadcast Channel (PBCH) provides information such as system bandwidth, PHICH configuration, and frame number it occupies for initial cell access [6].

1.2.5 Downlink Hybrid ARQ (Automatic Repeat Request)

Downlink HARQ is a retransmission protocol in downlink. It enables UE to request for retransmission of data packets if received incorrectly on PDSCH. The UE transmits ACK/NACK in the uplink using Physical Uplink Control Channel (PUCCH) or it multiplexes ACK/NACK within data transmission on Physical Uplink Shared Channel (PUSCH). As shown in Table 1.9 there are up to eight HARQ process in LTE FDD system [7].

Table 1.9: Total number of HARQ process TD-LTE (Downlink) [7]

TDD UL/DL configuration	Number of HARQ process for normal HARQ operation	Number of HARQ process for subframe bundling operation
0	7	3
1	4	2
2	2	N/A
3	3	N/A
4	2	N/A
5	1	N/A
6	6	3

1.3 LTE Uplink Transmission Scheme

1.3.1   SC-FDMA

At the time of standardization of LTE, various transmission schemes were considered for uplink. OFDMA filled the requirement for LTE in downlink. At the same time, OFDMA was found to be less favourable for uplink because of low Peak-to-Average Power Ration (PAPR). OFDM in uplink resulted in inferior performance in terms of coverage and power amplifier design for handsets due to its requirement for linear power amplifier. Thus, Single Carrier Frequency Division Multiple Access (SC-FDMA) was chosen for LTE uplink transmission scheme for both FDD and TDD modes. Compared to OFDMA, SC-FDMA offers better PAPR properties for cost-effective UE power amplifier design. The method of Discrete Fourier Transform (DFT) -Spread-OFDM (DFT-S-OFDM) was chosen to generate SC-FDMA signal for E-UTRA. The principle of DFT-S-OFDM is illustrated in the Figure 1.10. As illustrated, a size-M DFT is applied to a block of M symbols which are then modulated by QPSK, 16QAM, or 64QAM modulation schemes. The applied modulated symbols are converted into frequency domain and the result is mapped onto various available sub-carriers. The DFT transforms the applied modulation symbols into frequency domain and the result is mapped onto the available subcarriers and an N-point IFFT where N>M is then performed in OFDM which is followed by cyclic prefix and then serial to parallel conversion. In Release 8, localized transmission on consecutive subcarriers was allowed in uplink [4].
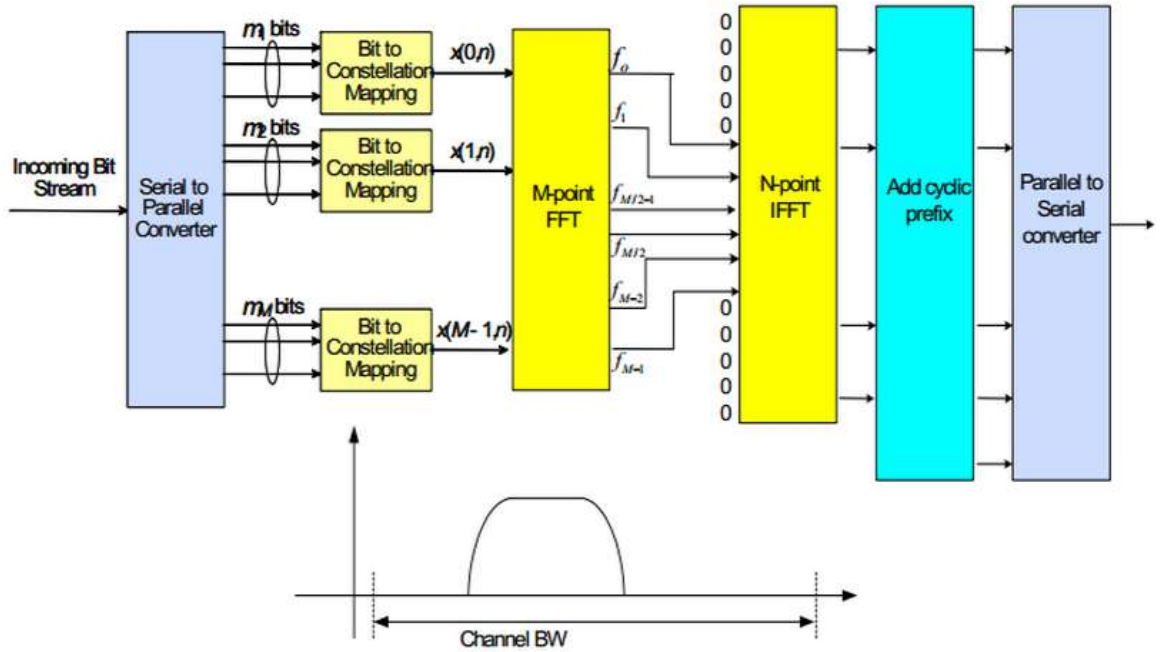
Figure 1.10: DFT-S-OFDM block diagram [4]

The fundamental difference between SC-FDMA and OFDMA signal generation is DFT processing and this is indicated by the term DFT-S-OFDM. In SC-FDMA signal, each subcarrier contains information of all transmitted symbols unlike OFDMA, since input data is spread by the DFT over the available subcarriers. In OFDMA, each subcarrier contains information related to specific modulation symbols. This spreading in SC-FDMA lowers the PAPR compared to OFDMA in downlink. In addition, it depends on the modulation schemes (QPSK, 16QAM, and 64QAM) and the applied filtering, which is not standardized as in WCDMA [4].

1.3.2   SC-FDMA Parameterization

The uplink is similar to downlink in LTE. The frame structure Type 1 consists of 20 slots of 0.5 ms duration and every two slots together form a subframe as shown in Figure 1.11. Frame structure type 2, consists of 1 or 2 special subframes such as DwPTS, GP, UpPTS for every 10 subframes. Each slot may carry 6 or 7 SC-FDMA symbols depending on the length of Cyclic Prefix (CP) normal or extended CP. Every 4th symbol in a slot (i.e.,

symbol number 3) carries Demodulation Reference Signal (DMRS) for channel estimation and coherent demodulation in eNodeB [4].
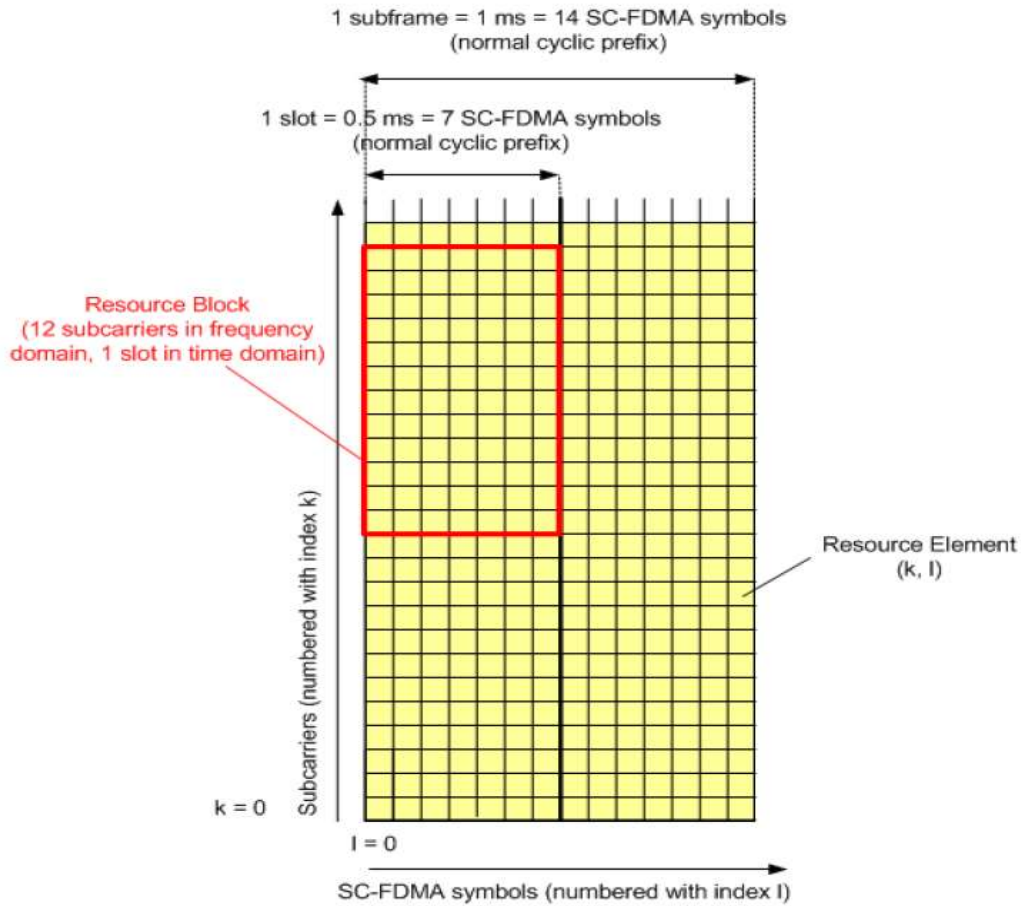
Figure 1.11: Uplink resource grid [4]

Table 1.10: Uplink frame structure parameterization (FDD and TDD) [4]

Configuration	Number of Symbols N_{symb}^{UL}	Cyclic prefix length in samples	Cyclic prefix length in μs
Normal cyclic prefix Δf=15kHz	7	160 for first symbol 144 for other symbols	5.2 μs for first symbol 4.7 μs for other symbols
Ext. cyclic prefix Δf=15kHz	6	512	16.7 μs

1.3.3   Uplink Data Transmission

The eNodeB assigns time/frequency resources to UE to perform scheduling in uplink and informs UE about the transmission format to be used. The eNodeB makes scheduling decisions based on various parameters such as QoS parameters, UE buffer status, uplink channel quality measurements, UE capabilities, UE measurement gaps etc. In uplink, data is allocated in multiples of resource block. The size of a resource block in uplink is 12 subcarriers in frequency domain which is similar to downlink. However, to maintain the simplicity of DFT design, not all integer multiples are allowed to be used. Table 1.11 shows the possible RB allocation for uplink transmission [4].

Table 1.11: Possible RB allocation for uplink transmission [4]

1	2	3	4	5	6	8	9	10	12
15	16	18	20	24	25	27	30	32	36
40	45	48	50	54	60	64	72	75	80
81	90	96	100						

The transmission time interval, in uplink direction is 1 ms, similar to downlink. The user data is carried on the PUSCH and DCI format 0 conveys uplink scheduling grant on PDCCH. Table 1.12 shows the contents of DCI format 0 [4].

Table 1.12: Contents of DCI format 0 carried by PDCCH [4]

Information type	Number of bits on PDCCH	Purpose
Flag for format 0 / format 1A differentiation	1	Indicates DCI format to UE
Hopping flag	1	Indicates whether uplink frequency hopping is used or not
Resource block assignment and hopping resource allocation	Depending on resource block allocation type	Indicates whether to use type 1 or type 2 frequency hopping and index of starting resource block of uplink resource allocation as well as number of contiguously allocated resource blocks
Modulation and coding scheme and redundancy version	5	Indicates modulation scheme and, together with the number of allocated physical resource blocks, the transport block sizeIndicates redundancy version to use
New date indicator	1	Indicates whether a new transmission shall be sent
TPC command for scheduled PUSCH	2	Transmit power control (TPC) for adapting the transmit power on the Physical Uplink Shared Channel (PUSCH)
Cyclic shift for demodulation reference signal	3	Indicates the cyclic shift to use for deriving the uplink demodulation reference signal from the base sequence
Uplink index (TDD only)	2	Indicates the uplink subframe where the scheduling grant has to be applied
CQI request	1	Requests the UE to send a channel quality indication (CQI) → aperiodic CQI reporting

The uplink scheduling grant contains 1 bit flag ON or OFF to enable or disable frequency hopping in uplink. By using frequency hopping in uplink on PUSCH, the effects of frequency diversity can be exploited and interference can be averaged. The UE obtains information regarding uplink resource allocation and frequency hopping by observing uplink scheduling grant received four subframes earlier. Both intra and inter-subframe frequency hopping are supported in LTE real time networks. The frequency hopping feature is configurable and is performed in higher layers of the cell. UE is advised about the type of frequency hopping (Type 1 or 2). Table 1.13 provides information regarding various hopping type and its associated hopping field and system BW.

Table 1.13: System BW vs. Hopping Field vs. Hopping Type

System BW	Hopping Bit Field	Hopping Type
1.4,3,5	0	Type 1
	1	Type 2
10,15,20	0	Type 1
	1	Type 1
	2	Type 1
	3	Type 2

In Type 1, frequency offsets is explicitly determined by the DCI0 and offset frequency between first and second slots is explicitly determined by DCI 0. In Type 2, the frequency offsets between first and second slot is configured by a predefined pattern and in case of multiple sub bands, hopping is performed from one sub band to another [4].

1.3.4   Uplink Control Channel PUCCH

The Physical Uplink Control Channel (PUCCH) carries control information such as ACK/NACK related to the data packets received in downlink, Channel Quality Indicator (CQI) information, Precoding Matric Information (PMI), rank indication for MIMO and Scheduling Requests (SR). The PUCCH RB is located at both the edges of the bandwidth. In 3GPP Release 8, a mobile device uses PUCCH when there is nothing to transmit on PUSCH. The PUCCH can carry different format of information as mentioned in Table 1.14 below.

Table 1.14: PUCCH formats and contents [4]

PUCCH format	Contents	Modulation scheme	Number of bits per subframe
1	Scheduling (SR)	N/A	
1a	ACK/NACK, ACK/NACK+SR	BPSK	1
1b	ACK/NACK, ACK/NACK+SR	QPSK	2
2	CQI/PMI or RI (CP), (CQI/PMI or RI)+ACK/NACK (ext.CP only).	QPSK	20
2a	(CQI/PMI or RI)+ACK/NACK (normal CP only)	QPSK+BPSK	21
2b	(CQI/PMI or RI)+ACK/NACK (normal CP)	QPSK	

The PUCCH formats specified in Table 1.14 are based on cyclic shifts from a Zadoff-Chu sequence, i.e. the modulated data symbol is multiplied with cyclically shifted sequence, which varies between symbols and slots. These formats carry three reference symbols per slot in case of normal cyclic prefix located on SC-FDMA symbol number 2, 3, 4. The RB can either be configured to support a mix of 2/2a/2b and 1/1a/1b or 2/2a/2b exclusively [4].

1.3.5 Uplink Reference Signal Structure

The uplink reference signal can be classified into two types namely Demodulation Reference Signal (DMRS) and Sounding Reference Signal (SRS).

Demodulation Reference Signal (DMRC) is used for channel estimation in eNB in order to demodulate control and data channels. This reference signal is located on the fourth symbol of each slot of normal cyclic prefix and spans the same bandwidth as allocated to the uplink data. The Sounding Reference Signal (SRS) provides uplink channel quality information which is used by the base station in making scheduling decision. SRS is sent in different parts of the bandwidth and it is transmitted in last symbol of the subframe. Both reference signals are derived from Zadoff-Chu sequence types [4].

1.3.6 Uplink HARQ

The HARQ is the retransmission protocol used in LTE uplink. The eNodeB requests retransmission of incorrectly received data packets and ACK/NACK for the retransmission is sent via Physical Hybrid ARQ Indicator Channel (PHICH) in the downlink. UE monitors PHICH resource in downlink after every PUSCH transmission in the uplink. In FDD, PHICH information is obtained after four subframes of PUSCH transmission. In TDD, the PHICH information is obtained from the uplink/downlink configuration and from PUSCH subframe number. The PHICH group consists of multiple PHICHs mapped to the same set of resource elements separated through different orthogonal sequences. UE obtains information about the PHICH group number and individual PHICH to be used inside that group through the lowest RB number PUSCH allocation, and the cyclic shift of the demodulated reference signal [4].

1.4 LTE Network Architecture

LTE, unlike its predecessor technologies such as 2G and 3G, is designed completely to provide seamless internet protocol connectivity between UE and Packet Data Network

(PDN). The term "LTE" includes the evolution of Universal Mobile Telecommunications System (UMTS) radio access through E-UTRAN. The evolution of LTE has resulted in the evolution of the term "System Architecture Evolution" (SAE). Together with SAE, LTE comprise of Evolved Packet System (EPS).

EPS route IP traffic between PDN and UE using EPS bearer service. The term bearer can be defined as the IP packet flow with defined QoS between gateway (PDN) and UE. E-UTRAN and EPC together are responsible for setting up and releasing bearers. EPS provides IP connectivity to UE for data and Voice over IP (VoIP) services. A single UE can be provisioned with multiple bearers to provide multiple QoS streams (such as voice call and web browsing at same time) and connectivity to multiple PDNs. The necessary QoS for the voice call would be provided by VoIP bearer, while for web browsing and FTP session, the necessary QoS would be provided by best-effort bearer. The LTE network architecture is designed so as to provide sufficient security and privacy to the users and protect against fraudulent usage of network. The overall network architecture of LTE is shown in Figure 1.12 and a brief explanation of different functionalities of LTE core network elements has been provided in Table 1.15.

At a high level architecture design, the LTE network is comprised of the Core Network (CN) namely EPC and the access network (E-UTRAN). While the CN is made up of many logical nodes, access network is comprised of eNodeB. Each network element in LTE architecture is interconnected by various interfaces and these are standardised by 3GPP. The standardization of these interfaces helps to facilitate interoperability between different service vendors. This opens up opportunities to service providers to source different network elements from different vendors. As a result, an open choice is provided to service providers to construct their network with a single vendor or multiple vendors depending on commercial considerations [1].

The CN is responsible for overall control of the LTE network and it establishes bearers for various services. The logical nodes of the EPC are:

• PDN Gateway (P-GW)

• Serving Gateway (S-GW)

• Mobility Management Entity (MME)

EPC includes other logical and functional nodes such as Home Subscriber Server (HSS) and Policy Control and charging Rules Function (PCRF). The EPS provides bearer for various QoS services and bearer for VoIP application is provided by IP Multimedia Subsystem (IMS), which is considered to be external to EPS architecture [1].
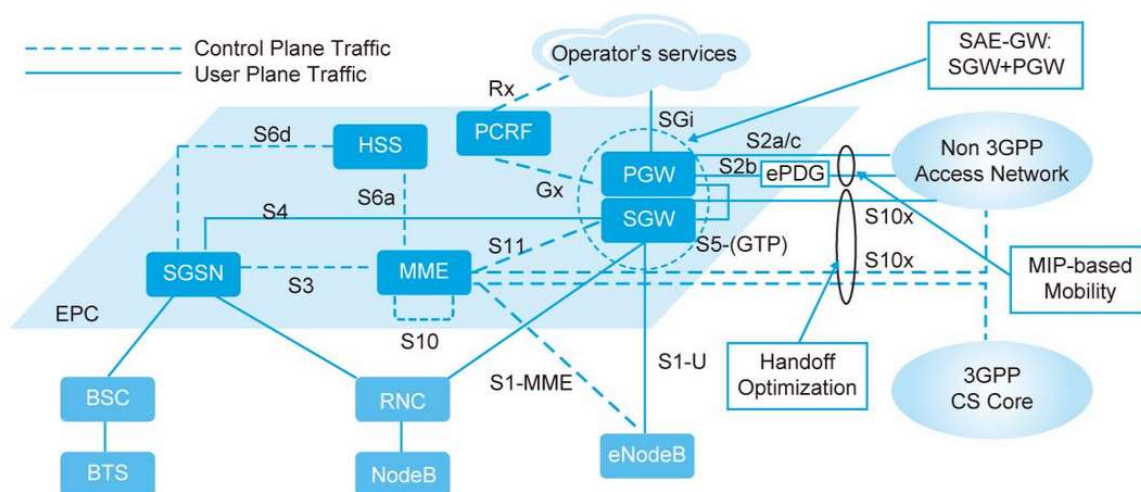
Figure 1.12: LTE architecture [1]

Table 1.15: Core functionalities of LTE network elements [1]

PCRF	PCRF performs policy control decision-making, control flow-based charging functionalities in Policy Control Enforcement Function (PCEF).
HSS	It is similar to Home Location Register (HLR) used in 2G and 3G. It contains users' subscription data such as the EPS-subscribed QoS profile and access restrictions for roaming.
P-GW	The PDN Gateway is responsible for allocating IP to UEs, QoS enforcement and flow-based charging according to the rules from PCRF.

S-GW	User's IP packets are exchanged through the Serving Gateway. SGW serves as the local mobility anchor for data bearers when the UE moves between eNodeBs.
MME	The Mobility Management Entity (MME) is the main control node which processes the signalling between UE and CN.

1.5 Intercell Interference in LTE

OFDMA actively combat interference and improve the system performance of LTE network. However, Inter Cell Interference (ICI) still poses a real challenge that limits the performance of LTE network. The UE located at cell edge are worst affected due to ICI. In OFDMA ICI is mainly caused when UEs in different cells use same resource at the same time. With such usage, the overall network performance is greatly impacted. Inter Cell Interference Coordination (ICIC) has been proposed by several researchers as a technique to effectively combat ICI. ICIC techniques are aimed to reduce such collision and mitigate the SINR degradation to improve the system performance. This in turn increases the overall bit rates of the cell, especially to the users at the cell edge.

ICIC techniques are classified into interference mitigation and avoidance techniques. In interference avoidance technique, the allocation of system resources such as time, frequency, and power is controlled to ensure ICI remains in acceptable limits. Interference mitigation techniques include 1) interference randomization, where cell specific scrambling, interleaving, or frequency hopping are introduced, 2) interference cancelation, where the interfering signals are detected and cancelled from to obtain the desired signal, and 3) adaptive beamforming, depending on the interference levels, the antenna can dynamically change its radiation pattern to control the interference levels.

In interference avoidance techniques various frequency reuse algorithms has been proposed to allocate resources in both frequency and time domain and different power levels to increase the SINR, to improve the system performance. These frequency reuse algorithms must satisfy power constraint to ensure that eNodeB in each cell transmits in allocated transmission power. The fundamental concept of this technique is to classify

users based on average SINR to the numbers users and apply different frequency reuse factors on based on different classes of users.

Various interference avoidance techniques are studied under various traffic conditions by several researchers. The techniques are classified mainly as static vs dynamic and centralized vs distributed. In static allocation, resources allocated to the users are computed during radio planning. The power levels and set of sub-carriers allocated to each cell is fixed. This technique is easy implement as they require no interaction with eNodeB. On the flip side, this technique does not offer the flexibility of performing modification in resource allocation. This technique does not meet the requirement of dynamic changes in the network. Figure 1.13 shows the classification of various ICIC techniques.
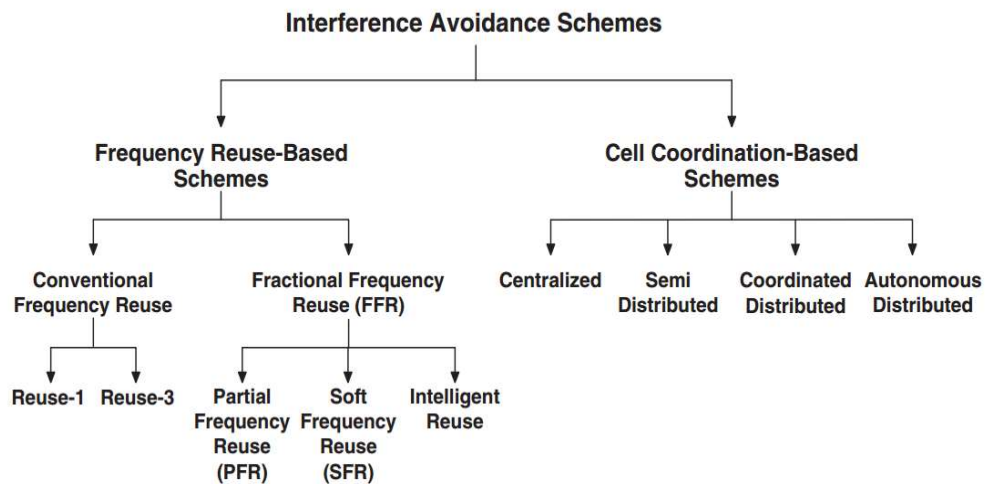
Figure 1.13: ICIC techniques

1.6 Motivation and Objectives

Convergence of mobile and internet exerts pressure on service providers to offer faster, efficient and cost effective mobile internet to the end user. This requirement has made service providers to roll out LTE network at greater speed than anticipated. In fact, several service providers are planning to shut down the existing GSM service and use the spectrum for LTE. Hence, it becomes pertinent to analyse the performance of LTE network. The research efforts of academia and industry in LTE over the years have led to

the standardization of several protocols and algorithms. These protocols and algorithms are implemented in real-time LTE networks. During the standardization process of LTE, it was decided to use IP as the key protocol to transport all services. Hence, it was decided to evolve EPC as packet core and not to have circuit switched domain that was used in GSM, GPRS, and 3G. The traditional RAN concept of BTS or NodeB controlled by BSC or RNC has been replaced with eNodeB. Majority of decision making capabilities are localised in LTE unlike legacy systems. The architecture of LTE has greatly simplified and at the same time the efficiency of the network has been greatly improved. These circumstances motivated to perform performance analysis study of LTE network. The performance analysis study was made based on simulations and by observing real-time LTE network.

The simulations were used to study the performance of packet scheduling algorithm in the downlink. These algorithms were simulated for various conditions such as a static user at various distances from eNodeB and a dynamic user travelling at various speeds. The simulations were carried out using LTE-Sim and NS-3. The main objective of this simulation is to analyse the performance of these algorithms in terms of throughput, Packet Loss Ratio (PLR), and latency under various user circumstances.

To further increase coverage and high data rates, heterogeneous networks are widely used in LTE. In heterogeneous network, small cells namely pico cells and femto cells work alongside the macro cells. Hence, in this study, heterogeneous network of pico cells working alongside the macro cells was simulated using LTE-Sim. The objective of this simulation is to study the performance of various LTE downlink packet scheduling algorithm and to analyse the impact of pico cells on macro cell network.

To further explore the possibility of analysing the performances of RAN and EPC network various tests were performed in real-time LTE network. The main objective of performing these tests is to analyse the performance of packet scheduling algorithm namely Proportional Fair (PF) algorithm in real-time network settings. Apart from testing the performance of PF algorithms, network coverage and network quality was tested by observing several KPIs. To the best of the knowledge, this thesis fills the gap in the performance analysis study of LTE network by analysing key LTE features through simulations and real-time LTE network settings.

1.7 Thesis Overview

A number of contributions were made in this thesis to study the performance of LTE network. The contributions and brief description of remaining chapters of this thesis are given below:

Chapter 2: Review and Simulations of Packet Scheduling Algorithms in LTE

In this chapter, a number of packet scheduling algorithms have been studied. These algorithms are simulated using NS-3 and LTE-Sim. The performance of these algorithms have been studied based on different user distance from eNodeB and based various user speed.

Chapter 3: Performance Analysis of Simulated LTE Networks

This chapter deals with performance analysis of simulated LTE network. LTE networks with macro and pico cells were simulated using LTE-Sim. The performance analysis of different packet scheduling algorithms was studied. The capacity and impact of pico cells on macro cells were analysed.

Chapter 4: Performance Analysis of Real-Time LTE Networks – Scheduling and RAN

After analysing the performance of scheduling algorithms in simulation environment, the performance of PF scheduling algorithm and RAN was analysed in real-time LTE network. The users are classified based on the subscription plans and there performance was analysed based on the throughput. A combination of various scenarios was tested as specified in Table 4.1. Since, the performance analysis was carried out in a real-time network, the factors affecting the throughput were not considered separately. It was assumed that all the factors affecting the throughput will be at play in practical environment. The performance analysis of LTE RAN of two leading service providers was made. The testing was performed in various locations and in various modes such as walking around the city centre, travelling in train, driving in the car and in indoor environments.

Chapter 5: Performance Analysis of Real-Time LTE Networks – EPC

As a continuation of the previous chapter, performance analysis of LTE EPC was carried out and presented. This performance analysis was based on real-time LTE network. Due to confidentiality, the service provider's network architecture was not explained. The KPIs obtained from the real-time network were analysed and an important issue was identified in course of the analysis and subsequently resolved. The strategy to resolve the issue is also discussed.

Chapter 6: Conclusions and Future Research Directions

The chapter summarizes the contributions made in the thesis and recommends some studies relevant for future research.

2. REVIEW AND SIMULATIONS OF PACKET SCHEDULING ALGORITHMS IN LTE

The contents of this chapter is based on the following publications
R. Subramanian, P. Ghosal, S. Barua, and S. C. Lam, "Survey of LTE Downlink Schedulers Algorithms in Open access simulation Tools NS-3 and LTE-SIM," International Journal of Wireless & Mobile Networks, vol. 7, no. 2, pp. 01–14, Apr. 2015.

The evolution process of LTE started from the earlier 3GPP system such as UMTS, which evolved from GSM. The standardization process for LTE was started in the year 2004 with the main objective of providing higher data rates with low latency. The LTE architecture was evolved as flat IP architecture and hence, the Circuit Switched Core (CSC) was replaced by Packet Switched Core (PSC). In LTE, PSC handles both traffics such as voice and data in LTE unlike in UMTS, where voice is handled by CSC and data is handled by PSC. The main objective of LTE is to improve peak data rates offered by UMTS to 100 Mbps in downlink and 50 Mbps in uplink. At the end of various LTE trials, the achievable data rate exceeded to 300 Mbps in downlink and 75 Mbps in uplink. In LTE, the communication between different frequency bands with different bandwidths is available. Furthermore, in LTE both paired and un-paired bands are used for communication. In paired frequency bands, the same frequency is used for both uplink and downlink transmission whereas in unpaired band, different frequency bands are used in uplink and downlink. In LTE downlink transmissions, 10 ms frame lengths are used and grouped by radio transmission. In LTE, both uplink and downlink frame are 10 ms in duration and each radio frame consists of 10 sub-frames of 1 ms duration. Furthermore, each subframe is further divided in to two slots of 0.5 ms duration. In this chapter, review of various Packet Scheduling (PS) algorithms in the LTE downlink has been performed through simulations. The simulations were performed using two popular simulators namely Network Simulator (NS) -3 and LTE-Sim. Both the simulators have implemented various PS algorithms. In general, LTE-Sim offers simplified models to suit academic needs and it is easier to customize. On contrary, the current NS-3 model is based on LENA, which follows 3GPP specification closely. Hence, the protocols are implemented in a detail manner as compared similar to LTE-Sim. On the flip side, it comes at the cost of increased complexity and it is harder to customize. Hence, NS-3 is more suitable for industrial type of simulation where more real time environment can be simulated and

accurate results can be obtained. These simulations were performed in various scenarios such as movement of user at various velocities (3 and 120 Kmph) and location of users at various distances (3 and 6 km) from eNodeB. Performance indices namely average system throughput, delay, Packet Loss Ratio (PLR) and fairness were analysed [9].

2.1 Radio Resource Management in LTE

Radio Resource Management (RRM) manages all radio related functions such as assignment of resources, resource management and sharing of radio resources among users. The main task of the packet scheduler in RRM is to perform optimal allocation of resource unit (frequency, time, power) to UEs so as to meet the required QoS requirements of the users. The LTE radio resource interface shares common channels namely control and logical channels with other users in the cell. The scheduling, in Up Link (UL) and Down Link (DL) is carried by eNodeB. The scheduler in eNB decides the number of RBs allocated to a UE based on factors such as channel quality and QoS requirements. In downlink, scheduler can assign RBs from different frequency bands and they need not be adjacent whereas, in uplink, the scheduler must assign RBs adjacent to each other because of single carrier property of the uplink channel (SC-FDMA). The scheduling decision in downlink is based on channel quality reports, which the eNB receive regularly from UE. Every UE in eNodeB calculates their respective Signal to Noise Ratio (SNR) and send the Channel Quality Indicator (CQI) value to host eNodeB to choose an appropriate Modulation Coding Scheme (MCS).

CQI reporting algorithms balances between the frequency of sending channel quality reports and minimum signalling overhead. Several CQI reporting techniques have been discussed in [8]. One of the main tasks of a PS algorithm is to provide fairness among users and maximize network utilization. Hence, appropriate PS must be employed to take care of QoS aspects in UL and DL. The PS is an entity of RRM which is present in the MAC layer of eNodeB. In multiuser environment, PS uses multiuser diversity and channel fading efficiently. At any given point of time, some users may have a good channel condition and thereby PS maximises the overall system throughout by allocating resources to those users to transmit in shared channel resources without compromising

on fairness [8]. The resource allocation decision for a UE is taken by PS algorithms. Hence, several factor such as QoS provisioning, throughout maximization, fairness, complexity and scalability is considered before making a decision. A number of PS algorithms are described in Section 2.3 in detail.

2.2 Introduction to LTE simulators

In this thesis, two popular LTE simulators namely NS-3 and LTE-Sim were used to simulate LTE downlink scheduling algorithms.

2.2.1 Network Simulator (NS) -3

NS-3 is a discrete event simulator that is publicly available for free for educational and research purposes. The simulator is licensed under GNU GPLv2 license. The main objective of the simulator is to design various network modules of LTE network to cater the needs of the student, research and industrial community. The complete development ecosystem of the simulator is based on open source model of community contribution, peer review, and software validation. NS-3 project is dedicated to build a 3GPP compatible simulation core with accurate documentation, easy to use and debug to cater the needs of the student and research community. Furthermore, NS-3 assists in developing models which are sufficiently realistic to be used as real-time network emulator and allowing reusing of many existing protocol implementations [9].

The core of the NS-3 supports simulation of both IP and non-IP based networks. However, the majority of NS-3 users focuses on simulating wireless and IP networks such as Wi-Fi, WiMAX, LTE (layer 1 and 2) for wireless and static and dynamic protocols such as Optimized Link State Routing Protocol (OLSR) and Ad hoc On Demand Distance Vector (AODV) for IP based applications. NS-3 supports several real-time schedulers that facilitate a number of use cases to interact with real network devices. NS-3 provides link effects between virtual machines by providing interconnection framework. Python and C++ were used to build NS-3, the libraries of NS-3 are wrapped by Python using pybindgen library which parses NS-3 headers to gccxml and pygccxml to automatically

generate C++ binding glue. These generated C++ files are compiled in to NS-3 Python module allowing users to interact with C++ NS-3 module and core using Python scripts [9].

The process of creating simulation in NS-3 can be divided into several steps such as:

1. Topology definition: The basic facilities and its inter-relationships are managed using containers and helps provided in NS-3.

2. Model development: Helpers in NS-3 handle adding simulation models such as UDP, IPv4, point-to-point devices and links.

3. Node and link configuration: The parameters of node and link configurations such as packets sent by an application or MTU are set with default values using attribute system.

4. Execution: Simulation generates data and events requested by users executing it.

5. Performance analysis: The simulation data is made available after execution in time-stamped format and the data can be analysed by using tools such as R to draw conclusion.

6. Graphical visualization: The graphical output of the collected data can be obtained by using tools such as Gnuplot, matplotlib or XGRAPH.

The LTE module of NS-3 comprises of 89 classes. Several modules of LTE are implemented in NS-3 [9]:

- UE and eNodeB
- Part of Radio Resource Control (RRC)
- MAC queues and RLC.
- Bearers for data traffic with QoS parameters.
- PHY layer is implemented with RB granularity.
- Outdoor channel model implemented for E-UTRAN.
- DL CQI management.
- Adaptive Modulation and Coding scheme implemented for downlink.
- PS algorithms in downlink.

The core component of LTE module comprises of both MAC and PHY layers of an LTE device. The LTE device implemented in the simulator has several entities such as IP

classifier, RRC, MAC and PHY layer. Figure 2.1 and 2.2 show the implementation of eNodeB network device and UE network device in NS-3.
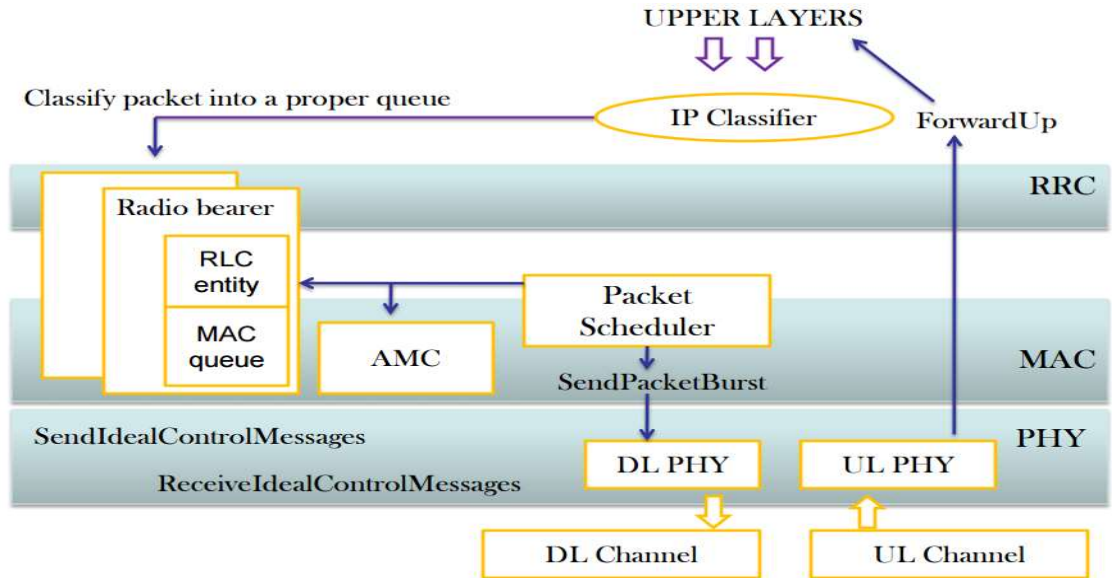
Figure 2.1: Implementation of eNodeB network device in NS-3 [9]
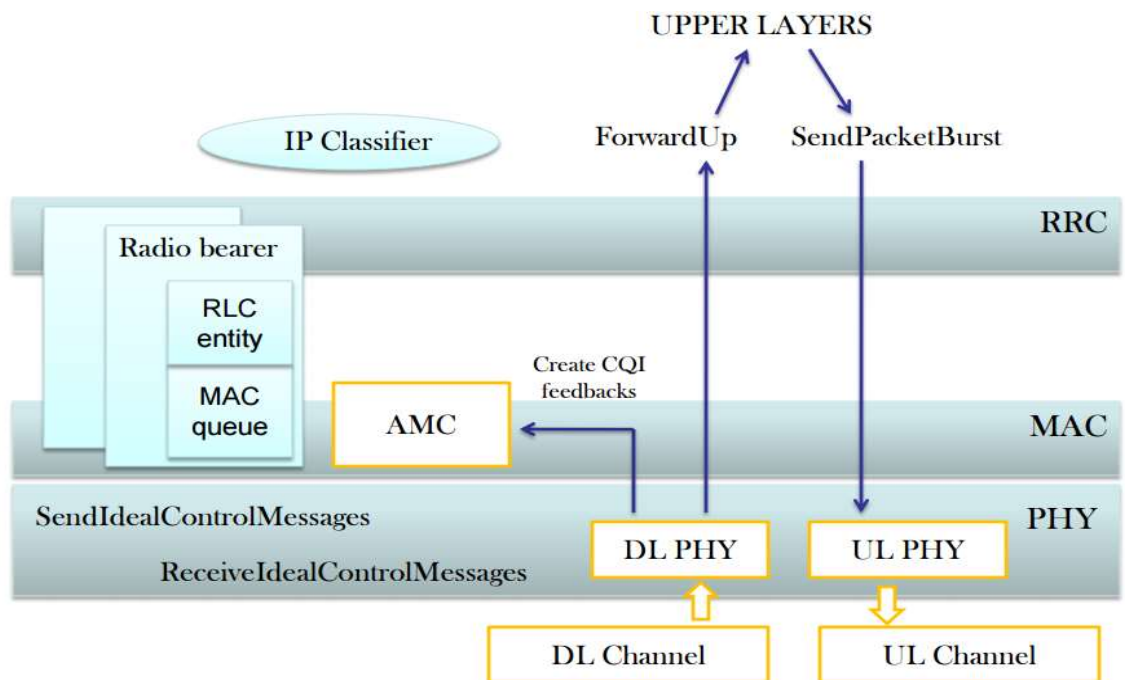
Figure 2.2: Implementation of UE network device in NS-3 [9]

Each flow in LTE network is mapped into a logical connection named bearer. The flow established between UE and eNodeB is mapped on to radio bearer. The different types of radio bearer can be established between UE and eNodeB such as:

- Default Radio Bearer vs Data Radio Bearer.
- GBR Radio Bearer vs non-GBR Radio Bearer.

Each of these radio bearers is associated with several QoS parameters such as target delay, minimum and maximum guaranteed bit rate, class identifier known as QoS class Identifiers (QCIs).

The PHY channel of NS-3 has been modelled based on spectrum framework. This framework allows implementing OFDMA PHY layer by:

- Defining the frequencies used at PHY layer.
- Modelling power spectral density of transmitted and received signal.
- By SINR computation of received signal.

The LTE channel model was implemented using SingleModelSpectrumChannel and LteSpectrumPhy by extending SpectrumPhy class in NS-3. The propagation model for E-UTRAN was implemented using PropagationSpectrumModel. The propagation loss was modelled using four components such as [9]:

- Pathloss:

  Path loss can be expressed in terms of

$$= 10 \; log_{10} \left(\left(\frac{4\pi df}{c} \right)^2 \right)$$

$$= 20 \; log_{10} \left(\frac{4\pi df}{c} \right)$$

$$= 20 \; log_{10}(d) + \; 20 \; log_{10}(f) + \; 20 \; log_{10} \left(\frac{4\pi}{c} \right)$$

$$= 20 \; log_{10}(d) + \; 20 \; log_{10}(f) - 147.55 \tag{2.1}$$

For d, f in GHz and Km, the path loss becomes$= 20 \; log_{10}(d) + \; 20 \; log_{10}(f) + 92.45$

For d, f in meters and megahertz, the constant becomes -27.55

For d, f in kilometres and megahertz, the constant becomes 32.45

- Penetration loss:

  $PN = \log normal \; distribution, \mu = 0db, \; \sigma = 8 \; db$
- Shadowing:

  SH = 10 db

- Fast fading is implemented using Jacks models.
- The received signal power at the receiver side is computed using propagation loss model.

Generally, when a PHY layer of UE receives a packet burst it performs the following:

- Computation of the received power.
- Computation of SINR for every sub-channel.
- Conversion of SINR to spectral efficiency value.
- Selection of CQI for each sub-channel.
- Sends CQI feedback to eNodeB.

The above information can be used by eNodeB to select appropriate MCS for downlink [9][12].

2.2.2   LTE-Sim

To the best of knowledge, LTE-Sim has complete LTE protocol stack, multi-cell environments with uplink flows and realistic applications compared with other simulators. LTE-Sim is written in C++ and is a well-known object oriented platform and it is an event driven simulator. The four main modules of LTE-Sim as defined in [8] are: a) the Simulator, b) the Network Manager, c) the Flows manager and d) the Frame Manager. The simulator performs the function of starting - scheduling - running and event management. Frame Manager defines LTE frame structure (starting and stopping of sub-frames). The Network Manager creates each node and devices (eNB, femtocell-picocell, UE), manages positioning, bandwidth and user mobility. The Flow Manager generates and handles applications such as VoIP and video. Separate class is created for each network element in LTE architecture such as eNB class, UE class, and MME class. The LTE protocol stack is implemented in its entirety with three network nodes such as UE, eNB, and MME. These network nodes maintain the flow of data through source and destination IP addresses. The data flow, resource allocation and maintenance of QoS are performed by packet schedulers that are located at eNB. LTE-Sim supports some of the well-known scheduling algorithms such as PF, MLWDF, ExPF, FLS and Log scheduling

schemes. CQI feedback is supported by LTE-Sim by utilizing channel quality estimation report from UE. In LTE-Sim application layer, four traffic generators namely trace-based, on-off, infinite buffer and constant bit rate have been developed. Simulator's channel module covers packet transmission and propagation models using path loss, penetration loss, shadowing, and fast fading due to multipath. All the aforementioned features provide flexibility and modularity to simulate a complete LTE network using LTE-Sim [10][13][15].

2.3 Packet scheduling in LTE

The QoS aspects in LTE downlink depend on several factors such as channel conditions, resource allocation policies, available resources, delay sensitive/insensitive traffic etc. The eNodeB allocates physical layer resources such as UL-SCH (uplink shared channel) and DL-SCH (downlink shared channel). The resource that is allocated for UL-SCH or DL SCH comprises of Physical Resources Blocks (PRB) and MCS. The bit rate is determined by MCS and capacity is determined by PRBs. The allocation of MCS and PRBs is performed for one or more TTIs and the duration of each TTI is 1ms. The downlink control channel is carried by LTE PDCCH. DCI has all information about the allocation of RBs, power control command, uplink grant and MCS to be used etc. The DCI messages are scheduled for every TTI and control overhead becomes a blockage during high traffic scenarios resulting in QoS degradation. To maintain a middle path and to prevail over this problem a concept called persistent scheduling is introduced. In this scheme, the idle and non-idle periods are pre-assigned by control overhead in the user specific RBs over a time sequence. The users know the allocation of TTI/RB in advance and the eNodeB is aware of this pre-assignment. This helps eNodeB to decode PDSCH (Physical Downlink Shared Channel), without any additional PDCCH overhead. The TTI/RB cannot be persistent in real-time because of several factors such as user mobility, channel quality, Doppler Effect and interference. In order to correctly decode at the receiver, an average RB requires multiple transmissions. For this reason, the research is on-going in semi persistent scheduling [8].

In semi persistent signalling, the control signalling is greatly reduced. In this scheduling, every allocation is not signalled and this will ultimately reduce signalling load. For example, in VoIP application, if each frame of duration 10 ms to 20 ms in the downlink is signalled then this will greatly increase the overall signalling load and it will consume more bandwidth. Semi-persistent scheduling allows setting up an ongoing allocation that persists until it is changed. Both uplink and downlink can be provisioned with semi-persistent schedules. Figure 2.3 shows generalized model of PS [8].
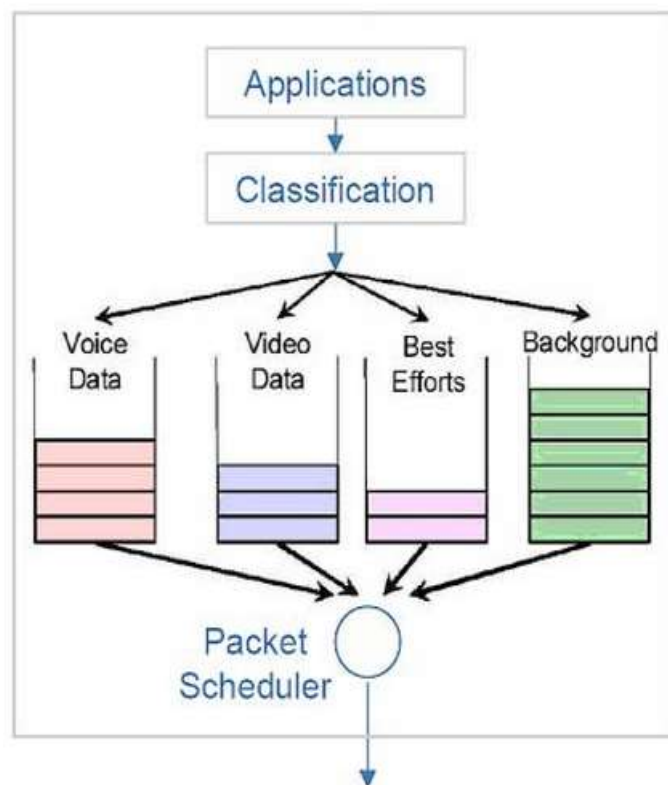
Figure 2.3: General model of PS [8]

The scheduling strategies in wireless networks can be broadly classified as channel independent scheduling and channel sensitive scheduling (as shown in Figure 2.4). The channel independent scheduling was first introduced for time invariant and error free wired networks. Some of the famous scheduling strategies introduced for wired networks are First-in-First-Out (FIFO), Round Robin (RR), Weighted Fair Queuing (WFQ), Earliest Deadline First (EDF), Largest Weighted Delay First (LWDF) [8].
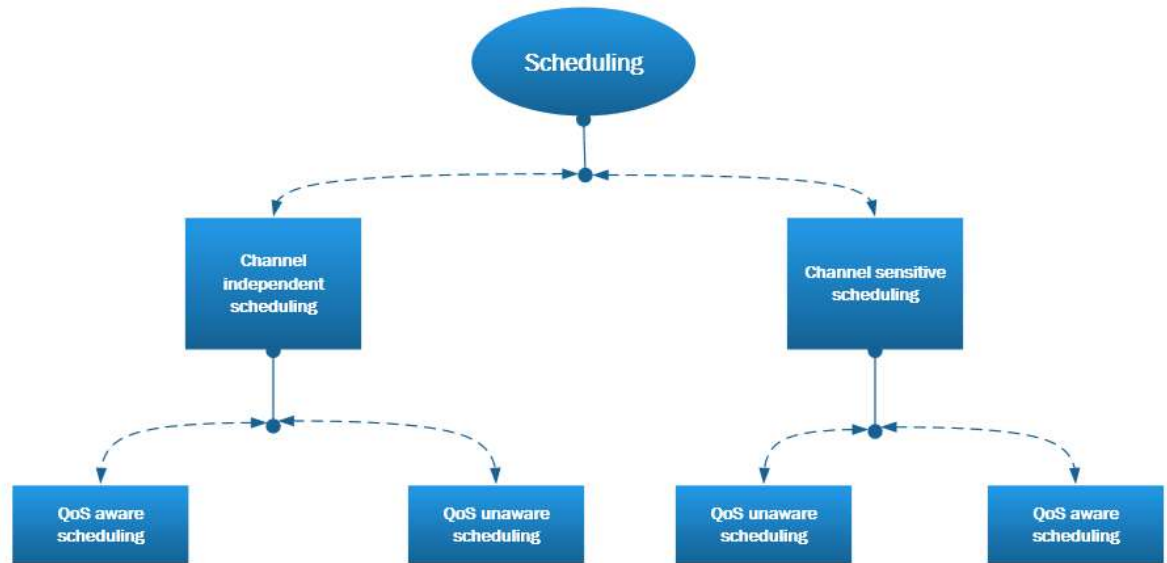
Figure 2.4: General classification of scheduling

In channel sensitive scheduling, the scheduler in eNodeB makes scheduling decisions based on channel quality estimated from the CQIs sent by UEs. In this type of scheduling, the scheduler tries to maximize the QoS requirements of each UE or provide fairness among the UEs. Some examples of channel sensitive scheduling are Maximum Throughput (MT), Proportional Fairness (PF), Throughput to Average (TTA), Exponential Proportional Fairness (EXP/PF), Exponential rule (EXP rule), Logarithmic rule (LOG rule) etc [8].

2.3.1   Downlink PS algorithms

2.3.1.1 Round Robin (RR)

This is one of the simplest algorithms. In this algorithm time slots (or resources) are assigned to every UE in an equal share in round robin fashion. In this algorithm, every UE is handled with equal priority. The excess flows will be allocated in a circular fashion in different subframes, since it cannot be allocated in the same subframe. The MCS will be decided depending upon the received CQI for each user [9].

2.3.1.2 Proportional Fair (PF)

In this algorithm, resources are allocated to UE when it has high instantaneous achievable data rate compared to average data rate [7]. Let the users be denoted as i, j, subframe index defined as t, and resource blocks are defined as k. The MCS is defined as $M_{i,k}(t)$ for the user i on the resource block k and let $S(M, B)$ be the Transport Block (TB) in bits for B resource blocks. The achievable rate that is represented as $R_i(k, t)$ in bit/s for user i on resource block k at subframe t is defined as [14]:

$$R_i(k, t) = \frac{S(M_{i,k}(t), 1)}{\tau} \tag{2.2}$$

where, τ is the TTI duration. Each user is assigned with resource block at the start of every subframe t. In detail, the index $\widehat{\iota_k}(t)$ to which RB k is assigned at time t is determined as

$$\widehat{\iota_k}(t) = argmax_{j=1,\ldots,N}\left(\frac{R_j(k,t)}{T_{j(t)}}\right) \tag{2.3}$$

where, $T_j(t)$ is denotes the past throughput performance of the user j. In scheduling algorithms, a user can be assigned with Resource Block Group (RBG) that can be adjacent or non-adjacent depending on present channel condition and previous throughput $T_j(t)$. At the end of the subframe t, the previous throughput performance can be determined by using the following exponential moving average approach:

$$T_j(t) = \left(1 - \frac{1}{\alpha}\right) T_j(t-1) + \frac{1}{\alpha}\widehat{T}_j(t) \tag{2.4}$$

where, α represents time constant in terms of number of subframes of exponential moving average, and the actual throughput is denoted as $\widehat{T}_j(t)$ achieved by user i in subframe t. $\widehat{T}_j(t)$ is measured as the following procedure. First, the MCS $\widehat{M}_j(t)$ is determined by user j:

$$\widehat{M}_j(t) = \min_{k:\widehat{\iota_k}(t)=J} M_{j,k}(t) \tag{2.5}$$

Then the total number of RBs $\widehat{B}_j(t)$ allocated to user j:

$$\widehat{B}_j(t) = |\{k: \widehat{\iota}_k(t) = j\}| \qquad (2.6)$$

where $|.|$ indicates the cardinality of the set;

Finally,

$$\widehat{T}_j(t) = \frac{S((\widehat{M}_j(t), \widehat{B}_j(t))}{\tau} \qquad (2.7)$$

2.3.1.3 Maximum Throughput (MT) Scheduler

The main idea of this algorithm is to provide the maximum throughput to a eNB [3][6]. In this algorithm, the RBG is assigned to each individual UE so as to attain maximum data rate in the current TTI.

Let the users be denoted as i and j. t is defined as the subframe index, and k can be specified as the resource block index. Let $M_{i,k}(t)$ be defined as MCS usable by user i on the resource block and let $S(M, B)$ be defined as the TB in bits for B resource blocks. The achievable rate is defined as $R_i(k, t)$ in bit/s for the user i on the resource block k at the subframe t

$$R_i(k,t) = \frac{S(M_{i,k}(t), 1)}{\tau} \qquad (2.8)$$

where τ is specified as TTI duration. At the beginning of every subframe t, every user is assigned with RB. In detail, the index $\widehat{\iota}_k(t)$ to which RB k is assigned at time t is determined as

$$\widehat{\iota}_k(t) = arg \max_{j=1,..,N}(R_j(k,t)) \qquad (2.9)$$

In case of multiple UEs with similar achievable rate, the present implementation always selects the first UE that is created in the script. Even though MT can provide maximum

cell throughput, it cannot provide fairness to UEs that are experiencing poor channel condition [9].

2.3.1.4 Throughput to Average Scheduler (TTA)

This algorithm can be assumed as an intermediate between MT and PF [3][6]. The metrics used in this algorithm can be deliberated as follows:

$$\hat{\iota_k}(t) = arg \max_{j=1,,N} (\frac{R_j(k,t)}{R_j(t)}) \tag{2.10}$$

Here, the achievable rate is denoted as $R_i(k,t)$ in bit/s for user i on resource block k at subframe t. The calculation methodology is already discussed in the MT and PF. Meanwhile, the achievable rate for i^{th} user at subframe t is denoted by $R_i(t)$ in bit/s. The difference in those two achievable rates is used to get MCS. For $R_i(k,t)$, MCS can be estimated by sub-band CQI while, $R_i(t)$ can be calculated by wideband CQI. Since, rate of particular RBG is related to Frequency Domain (FD), TTA scheduler is implemented in FD [9].

2.3.1.5 Blind Equal Throughput Scheduler (BET)

This algorithm does not take the channel condition into consideration for resource allocation. BET provides equal resources to all UEs in the same eNodeB [3][6]. Unlike MT and TTA, this algorithm is channel unaware scheduling algorithm. This algorithm uses wideband CQI in the scheduling decision in both Frequency Domain BET (FD-BET) and Time Domain BET (TD-BET).

The scheduling decision by BET can be best explained as follows:

$$\hat{\iota_k}(t) = arg \max_{j=1,,N} (\frac{1}{T_j(t)}) \tag{2.11}$$

where, user j past performance on throughput can be denoted as $T_j(t)$ and can be calculated similar to PF scheduler. In TD-BET, UE with highest priority metric is selected

by scheduler and all the RBGs are allocated to that particular UE. However, in FD-BET, UE with lowest average throughput in the past is selected by the scheduler and assigns one RBG to the UE and estimates the throughput of the UE. This throughput of the UE is compared with past average throughput $T_j(t)$ with other UEs. This is repeated until the expected throughput of the UE is better than the past throughput $T_j(t)$ of all UEs. The same method will be used by the scheduler to allocate RBG for a new UE that has lowest past average throughput $T_j(t)$ and this process continues until all RBGs are allocated to UEs. The principle of this algorithm is that, in every TTI, the scheduler tries to achieve equal throughput among all UEs in the best possible way [9].

2.3.1.6 Token Bank Fair Queue Scheduler (TBFQ)

This algorithm is designed from leaky bucket mechanism. TBFQ [4] is a downlink based QoS aware scheduling algorithm. The traffic flow of this scheduler is characterised by following parameters:

- t_i : packet arrival rate (byte/sec)
- r_i : token generation rate (byte/sec)
- p_i : token pool size (byte)
- E_i : This is the counter that records the number of token borrowed from or given to the token bank by flow *i*.
- E_i can be smaller than zero.

Each K bytes of data consumes k number of tokens. This algorithm, balance the traffic between different flows and maintains a shared token bank. If token generation rate r_i is greater than packet arrival rate t_i, then overflowing tokens from token pool are added to token bank, and E_i can be increased by the same amount. On the contrary, if the token generation rate is less than packet arrival rate, then flow *i* need to withdraw tokens from token bank based on the priority metric. Obviously, the user that contributes more tokens to token bank has the highest priority to borrow the tokens. On the other hand, the vice versa of low priority applies to the user who borrows more tokens from bank. Therefore,

in case of large number of users who are having similar token generation rate, traffic rate and token pool size, suffer with higher interference and have more opportunity to borrow tokens from the bank. In addition, TBFQ algorithm controls traffic by limiting the token generation rate to limit the throughput. Additionally, this algorithm can maintain the following three parameters for each flow [11]:

- Debt limit d_i: If E_i is below this threshold, user i cannot borrow tokens further from the token bank. This mechanism is designed for preventing malicious UE to borrow too many numbers of tokens.
- Credit limit c_i: This can be defined as the maximum number of tokens that a UE i can borrow from token bank at one time.
- Credit threshold C: Once the debit limit d_i is reached by E_i, the UE i should store C tokens in the bank for further borrowing from the bank.

2.3.1.7 Priority Set Scheduler (PS)

This is another scheduling algorithm where the algorithm combines both TD and FD packet scheduling algorithms into one algorithm [3]. The fairness among UEs is controlled, by defining a specified Target Bit Rate (TBR). In the TD, the UE with non-empty RLC buffer is chosen to be divided into two sets based on the TBR:

Set 1: UEs with past average throughput is lower than TBR; TD scheduler follow BET and calculates the priority metric $p_k^1(t)$:

$$p_k^1(t) = \frac{1}{Tj(t)} \tag{2.12}$$

Set 2: UEs with past average throughput is larger (or equal) than TBR; TD follow Proportional Fair (PF) scheduler to calculate its priority metric $p_k^2(t)$:

$$p_k^2(t) = \frac{Rj(k,t)}{Tj(t)} \tag{2.13}$$

Here, the $R_j(k,t)$ denotes achievable data rate for the UE j at time t, the kth RBG and $T_j(t)$ is the average past throughput of the UE j at time t. The UEs that are belonging to Set 1 are given higher priority than the UEs in Set 2. This algorithm selects the UEs with the highest metric in the two sets and forwards those UEs to FD scheduler [9].

2.4 Simulation Results of Various Scheduling Schemes in NS-3

In the previous section, a brief introduction to various scheduling algorithms was provided and in this section these algorithms are simulated and performance comparisons are made with theoretical performance in some reference scenarios. The decision of validating the scheduling algorithms against theoretical performance is mainly motivated by the lack of equivalent measurements from real time LTE deployments that could be used for the same purpose. A particular set of scenarios are chosen with simple assumptions so that it becomes possible to determine theoretical performance of scheduling and verify the accuracy of the implementations of the scheduler. We note that, because of simplified assumptions, these scenarios might not necessarily represent real world condition and deployments. For each scenario, the reference throughput from each UE is estimated and compared with the obtained throughput to verify whether simulated results match with reference throughput within a given tolerance (10% throughput) [12].

The simulation parameters that are common to all the scenarios have been provided in Table 2.1. Some of the assumptions made in the simulations are provided below:

1. Phenomenon of fading is not considered and UEs are assumed to be stationary, hence UEs will have same SINR throughout the simulation.

2. Both wideband and sub-band CQIs of UEs are assumed to be constants and their values are related to the distance between UE and eNB.

3. Since the allocation bitmap is coded in allocation Type 0, the minimum allocation unit in the simulation is RBG and that contains two RBGs in the test cases.

4. Different traffic patterns for QoS unaware and QoS aware schedulers were used. Specifically in schedulers such as MT, TTA, and BET which are QoS unaware, it is assumed that RLC buffer for each UE is saturated by using NS-3 RLC Saturation Mode (RLC/SM) model to reflect the RBG allocation behaviour for different scheduling algorithms.

5. For QoS aware schedulers such as TBFQ and PSS, UDP traffics with different but constant bit rates were generated to validate the unique features of those schedulers.

Schedulers mentioned here have been tested for two basic scenarios such as:

Scenario I: It is assumed that all UEs are separated at the same distance from eNodeB to have same CQI both wideband and sub-band.

Scenario II: UEs are separated to have different distance to the eNodeB in order to have varying CQI both wideband and sub-band.

The simulation time for all test cases is 10 seconds. This choice of the simulation time is acceptable due to stationarity (statistical properties such as mean, variance, autocorrelation are all constant over time) of CQI throughout the simulation, resulting in short convergence time of the performance of the scheduling algorithms. T_X^Y, is used to represent UEs reference throughput for scheduler X and in scenario Y and N denotes the number of UEs which is shown in each figure. The validation of schedulers is mainly focused throughput statistics since, the policies of all the algorithms are based on assigned resources in terms of bitrate. The work of analysing the performance of the algorithms in more realistic scenarios such as delay, jitter, and fairness have been left out for future work.

Table 2.1: Simulation parameters in NS-3

Parameter	Value
Number of RBs	25
RBs per RBG	2
AMC model	PiroEW2010
Error model of control	Deactivated
Error model of data	Deactivated
Path loss model	Friis spectrum propagation
Mobility model	Constant position
Transmission power	eNB:30 dBm, UE: 23 dBm
Noise figure	eNB: 5dBm UE: 5dB
TTI	1 ms
Number of UEs (N)	N $\leq$ 5
UE and eNodeB distance	0, 3, 6, 9, 12, 15 km
Simulation time	10 second

2.4.1 MT and TTA

Since wideband CQI and subband CQI are constant, the achievable data rate selected by Adaptive Modulation and Coding (AMC) is constant during the simulation. Therefore, in Scenario I, for FD-MT, TD-MT, and TTA all UEs have same priority metrics. In this case, all the RBGs are allocated to the first UE connected to eNodeB, which is the first UE defined in the script and served in Fist-in-First-Out (FIFO) order. In addition as defined earlier, wideband CQI and subband CQI are related to distance between UE and eNodeB, the UE closer to the eNodeB achieves high data rate in both wideband and subband. In Scenario II, schedulers allocate all RBs to the closest UE to eNodeB. In summary, the reference throughput T, in MT and TTA, in both scenarios is [9]:

$$T_{fdmt,tdmt,tta}^{I,II} = \frac{S(MCS,B)}{\tau} \tag{2.14}$$

In Equation 2.14, τ denotes TTI duration, B is total number of RBs that can be used (24 throughout this section because of transmission bandwidth configuration and RBG size), MCS represents modulation and coding scheme at given SINR, and $S(MCS,B)$ represents transport block size. According to the scheduler behaviour, $T_{fdmt,tdmt,tta}^{I,II}$ indicates the achievable data rate of the UE, while the reference throughput of other UEs is zero. Figure

2.5 shows the simulation results for FD-MT, TD-MT, and TTA for Scenario I with various distances between UE and eNodeB. The right three columns in the graph (brown, yellow and light blue bar) indicate the throughputs of TTA, TD-MT, and FD-MT for the UE receiving all the resources, while the reference throughputs of other UEs are zero hence, not shown in the figure.
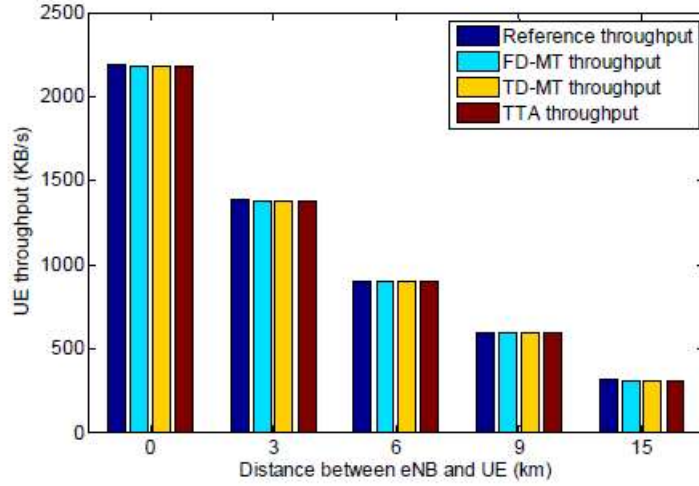
Figure 2.5: UE throughout in FD-MT, TD-MT and TTA schedulers

(scenario I and II, N=3)

2.4.2 BET

The expected behaviour of both TD-BET and FD-BET in long term for Scenario I and II is a fair division of resources among UEs which is independent of UE position or channel conditions. However, the reference throughput in scenario I and II are different. In Scenario I, because of identical wideband CQI, UEs achieve same data rate. In FD-BET, each UE is allocated with RBG until all RBGs are allocated to all UEs whereas, TD-BET, works in the principle of RR. All RBGs are allocated a single UE in the current TTI and assigns all RBGs to another UE in next TTI. If the number of RBGs is an integer multiple of N, then reference throughputs for FD-BET and TD-BET can be denoted as [9]:

$$T_{fdbet}^{I} = \frac{S(MCS, \frac{B}{N})}{\tau} \tag{2.15}$$

$$T_{tdbet}^{I} = \frac{S(MCS, B)}{\tau \; X \; N} \tag{2.16}$$
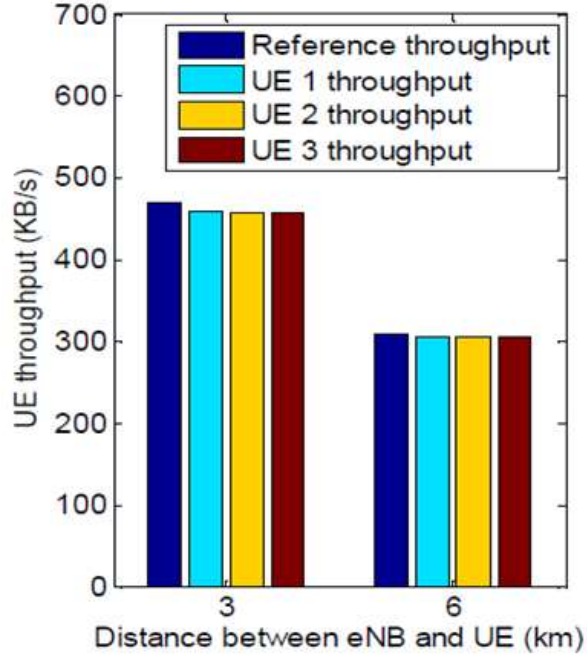
Figure 2.6: UE throughput of FD-BET schedulers (Scenario I, N = 3)

As illustrated in Equation 2.15 and 2.16, FD-BET allocates $\frac{B}{N}$ RBGs to a UE for every TTI while TD-BET allocates B RBGs for every N TTI. Figure 2.6 and 2.7 show the simulation results for Scenario I with all UEs have the same throughputs matching with the reference throughput [9].

In Scenario II, four UEs are placed in different location with different distance from eNB so that AMC assigns different achievable data rate to each UE in accordance with its wideband CQI. In this scenario, FD-BET assigns different number RBGs to each UE similar to TD-BET, where time slot between two scheduling events for each UE is variable. Hence, the same reference throughput equation used in Scenario I cannot be used for Scenario II. The modified reference throughput equations for Scenario II are denoted in Equation 16 and 17. Let us consider TD-BET in Scenario II, where F_i denotes fraction of time allocated to a UE i and R_i^{fb} full achievable bandwidth for a UE i in the simulation time. Let T_i be achieved throughput of UE i. Then we have:

$$T_i = F_i \times R_i^{fb} \tag{2.17}$$

In TD-BET, the sum of F_i for all UE equals one. The Equation 16 can be re-arranged as:

$$\sum_i \frac{T_i}{R_i^{fb}} = 1 \tag{2.18}$$

In long term, T_i will be same for all UEs, so it can be replaced by T. Then the final equation for reference throughput for TD-BET can be denoted as:

$$T_{tdbet}^{II} = \frac{1}{\sum_{i=1}^{N} \frac{1}{R_i^{fb}}} \tag{2.19}$$
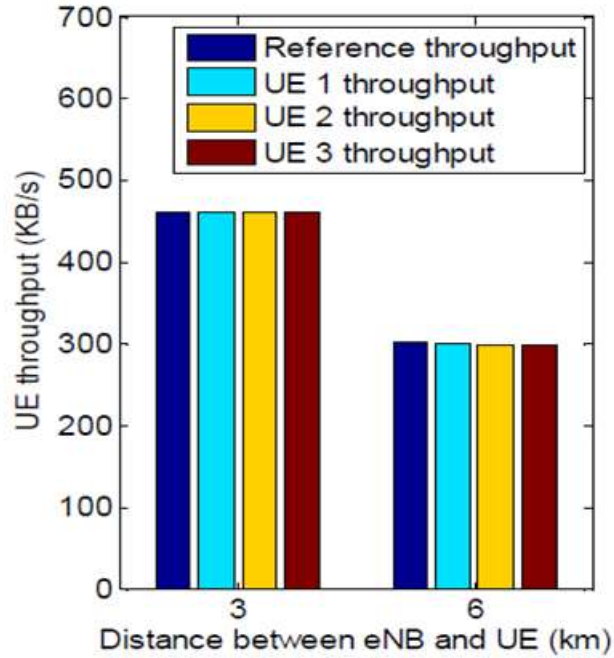
Figure 2.7: UE throughput of TD-BET schedulers (Scenario I, N = 3)

The reference throughput equation obtained in Equation 18 can be used for FD-BET in Scenario II. In the simulation, each UE obtains same amount of RBGs in both FD-BET and TD-BET. In addition, based on transport block size table in [9], we know that $\sum_i S(MCS, B_i)$ approximately equals to $S(MCS, B)$, where $B = \sum_i B_i$. B_i denotes the number of RBs allocated to UE i in FD-BET for one TTI. In other words, it can be explained as if UE can obtain same number of RBGs, then long term throughput for both FD-BET and TD-BET is very close to each other. Hence, Equation 18 can be used to calculate T_{fdbet}^{II}. The simulation results for TD-BET and FD-BET are shown in Figure 2.8. The results show the case of four UEs placed at different distance such as 0, 3, 6, and 9 kilometres (Km) from eNodeB. The results infer that obtained throughput matches with reference throughput.
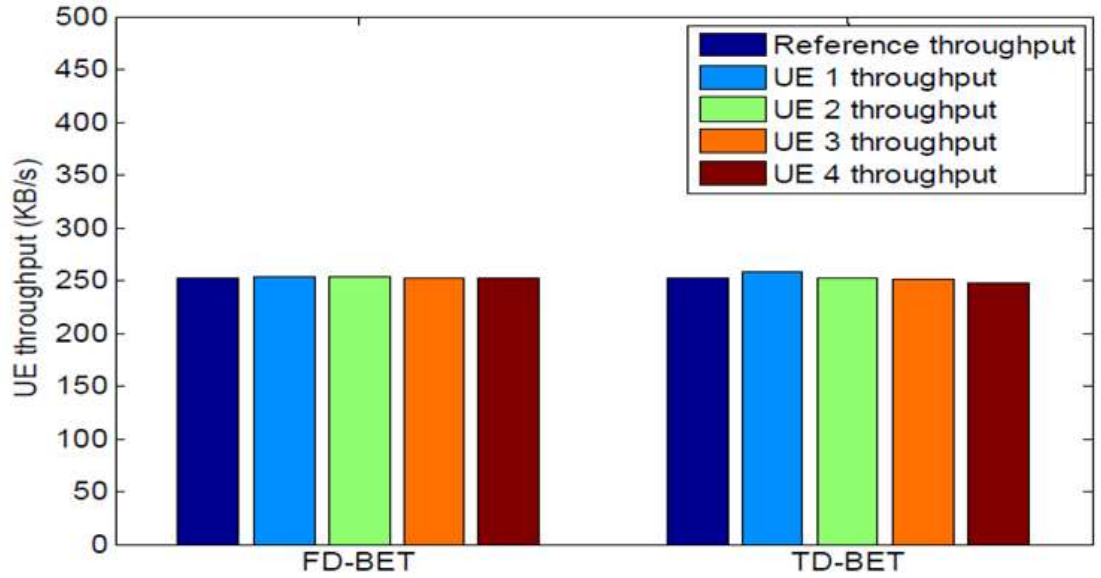
Figure 2.8: UE Throughout of FD-BET and TD-BET schedulers (Scenario II, N=4)

2.4.3 TBFQ and PSS

To test the QoS features of TBFQ and PSS (QoS aware schedulers), UDP flow with various but constant bit rates was simulated. The packet sending interval was set to 1 ms in order to keep TLC buffer non-empty. The performance of FD-TBFQ and TD-TBFQ algorithm are almost similar because of constant wideband CQI and subband CQI. In each simulation, the same UDP traffic rate and radio bearer specification among UEs were used. The token generation rate for each UE in FD-TBFQ and target bit rate in PSS were configured corresponding with UDP traffic rate. In Scenario I, the traffic flow for each UE has same traffic rate t_i and token generation rate r_i and FD-TBFQ scheduler guarantee similar throughput among UEs [11]. In addition, the exact throughput of LTE UEs depends on UDP traffic rate:

$$T_{fdtbfq}^{I} = t_i, if \ \sum_i t_i < T_t \tag{2.20}$$

$$T_{fdtbfq}^{I} = \frac{T_t}{N}, if \ \sum_i t_i \geq T_t \tag{2.21}$$

where, $T_t = \frac{S(MCS,B)}{\tau}$. T_t, is the total throughput which is equal to achievable data rate $\frac{S(MCS,B)}{\tau}$ when all RBGs are allocated to single UE and when total traffic rate $\sum_i t_i$ is

smaller than maximum throughput T_t. Then FD-TBFQ can police UDP traffic by token generation rate r_i, so that reference throughput of UE equals to its traffic (token generation rate is set to traffic generate rate in this simulation). On the other hand, if total traffic rate is greater than maximum throughput T_t, eNodeB can only serve one UE in one TTI. Therefore FD-TBFQ allocates all RBGs to one UE due to large RLC buffer size. When the UE is scheduled in current TTI, the token counter is decreased to prevent it from being scheduled in next TTI because each UE has same traffic generation rate t_i and FD-TBFQ serve only one UE for every TTI. Therefore the reference throughput of a UE in second condition equals to an even share of the maximum throughput of the system [11].
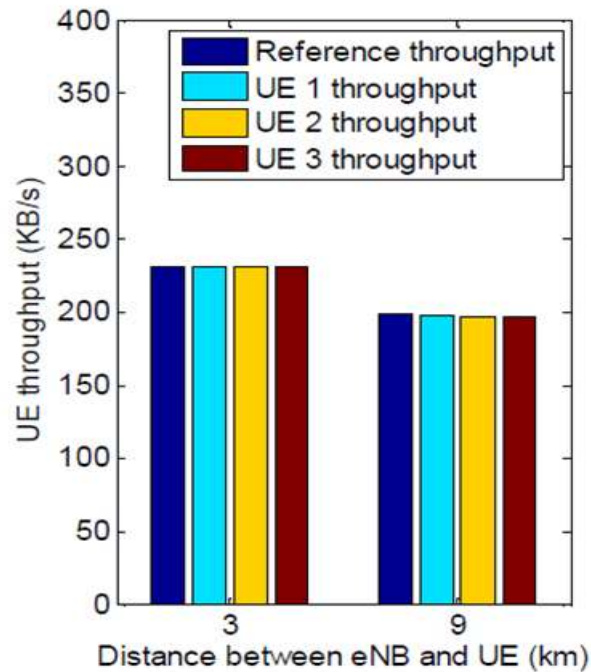
Figure 2.9: UE throughput of FD-TBFQ schedulers (scenario I, N = 3)

For PSS scheduler, in Scenario I, all UEs achieve the same data rate similar to BET Therefore, FD-TBFQ and PSS have the same maximum throughput. The equations in 2.20 and 2.21 can be used to calculate the reference throughput T_{pss}^I. Figure 2.9 and 2.10 show the simulation results of FD-TBFQ and PSS for Scenario I. In these two figures it can be observed that the throughput of UE at 9 km distance is similar to the traffic rate (232 KB/s). This is because of the fact that UDP traffic rate is higher than maximum total throughput. Similarly, for UE at 3 km distance, the obtained throughput is equal to the

traffic rate because UE throughput is limited by token generation rate in FD-TBFQ and by target bit rate in PSS scheduler.
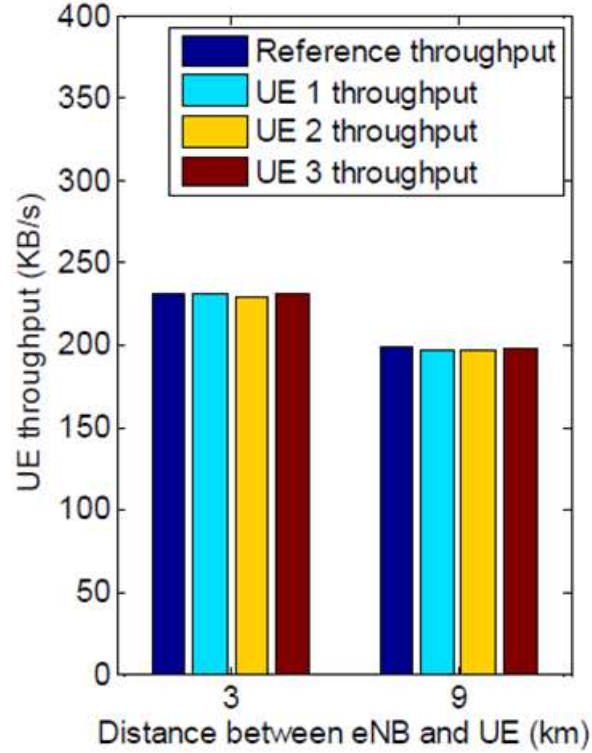
Figure 2.10: UE throughput of PSS schedulers (scenario I, N = 3)

Similarly, in Scenario II, reference throughputs of UEs in FD-TBFQ and PSS depend on maximum total throughput T_t. However, in this scenario, the maximum total throughput has different value compared to Scenario I. Similar to Scenario I, in this scenario FD-TBFQ and PSS perform similar to BET scheduler when total traffic is greater than maximum throughput. Therefore, $T_{pfdtbfqss}^{II}$ and T_{pss}^{II} can be calculated using same method similar to Equation 2.20 and 2.21, but considering different formulation for $T_t = \frac{N}{\Sigma_{i=1}^{N} \frac{1}{R_i^{fb}}}$ [11]. The simulation results for FD-TBFQ and PSS for Scenario II are shown in

Figure 2.11 and 2.12. In this simulation UEs are placed at various distances such as 0, 3, 6, 9 and 15 km from eNodeB. The UE throughput variance for PSS is higher than FD-TBFQ but still within the chosen tolerance setting. The reason for higher variance in PSS is due to slower convergence of PSS scheduler however, it largely decreases when longer simulations are conducted.
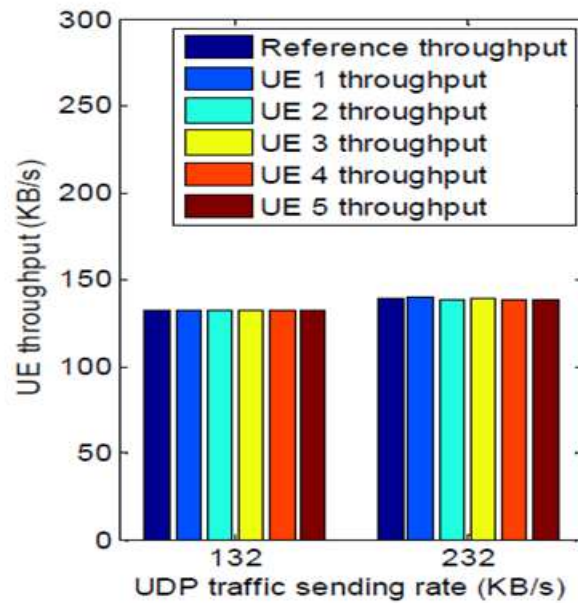
Figure 2.11: UE throughput of FD-TBFQ (scenario II, N = 5)
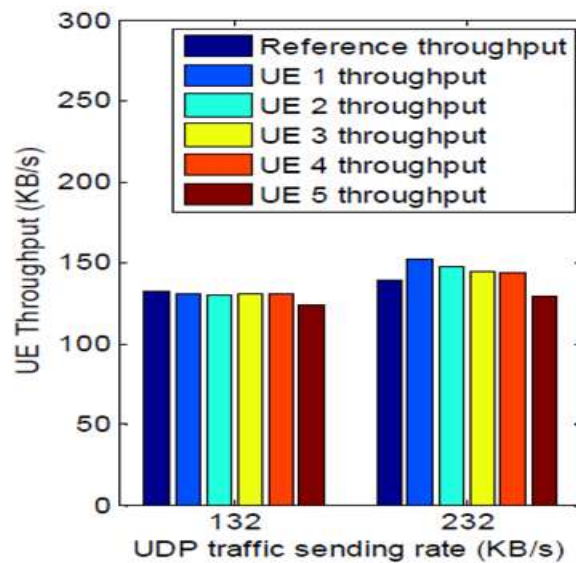
Figure 2.12: UE throughput of PSS schedulers (scenario II, N = 5)

2.5 Simulation Results in LTE-Sim

In this section simulation of various packet scheduling algorithms such as PF, M-LWDF and EXP/PF supported by LTE-Sim are performed in terms of packet loss Ratio, packet

delay, average throughput, fairness index and spectral efficiency with varying number of users and user speed. Simulation scenario is considered in an urban macro cell with cell coverage of 1 Km with the presence of interference and propagation loss. Fairness index is measured by Jain's fairness method. All the users experience single type traffic flow such as 50% of the users with VoIP traffic and the rest of the users have video traffic. Users (varied from 10 to 40) were moving with a speed of 3kmph or 120 Kmph. Simulation parameters are summarized in Table 2.2.

Table 2.2: Simulation Parameters

Bandwidth	10 MHz
Frame Structure	FDD
Cell Radius	1 KM
User Speed	3 Kmph, 120 Kmph
Flow Duration	80 sec
Maximum Delay	1 Sec
Video Bit rate	242 kbps

From Figure 2.13 and 2.14 it can be seen that for all schedulers, the average throughput (video and VoIP) is decreasing with the increase in user speed. With the increase in user speed, the channel quality deteriorates and becomes worse and lower order MCS are selected resulting in decreased average throughput of video and VoIP flow.
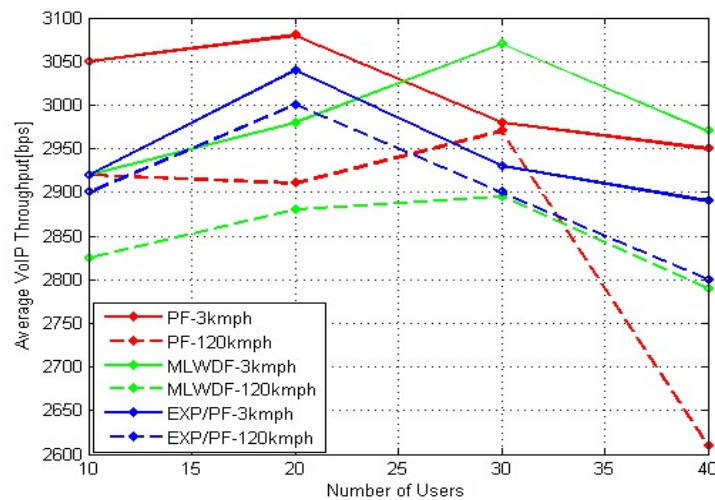
Figure 2.13: Average Throughput of VoIP
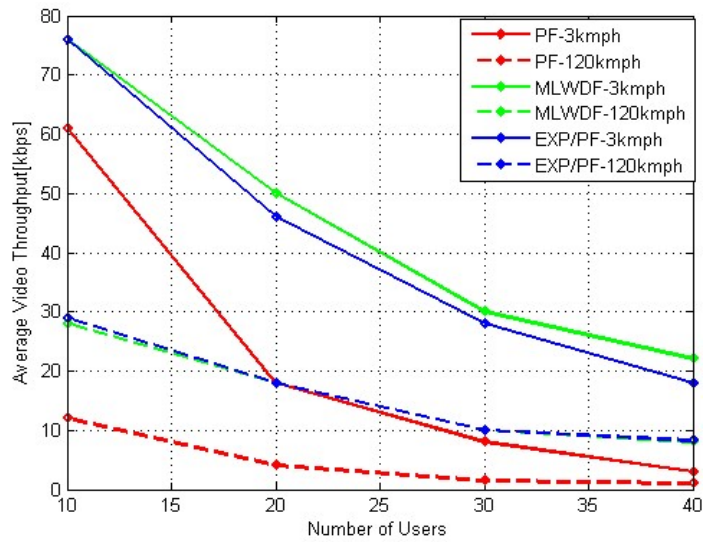
Figure 2.14: Average Throughput of video Flow with different schedulers at different speed

Figure 2.15 shows that for video flow, packet delay remains almost the same for M-LWDF and EXP/PF with increasing user number and speed while delay increases with PF. For VoIP, packet delay increases with speed and user number for all the scheduling algorithms shown in Figure 2.16.
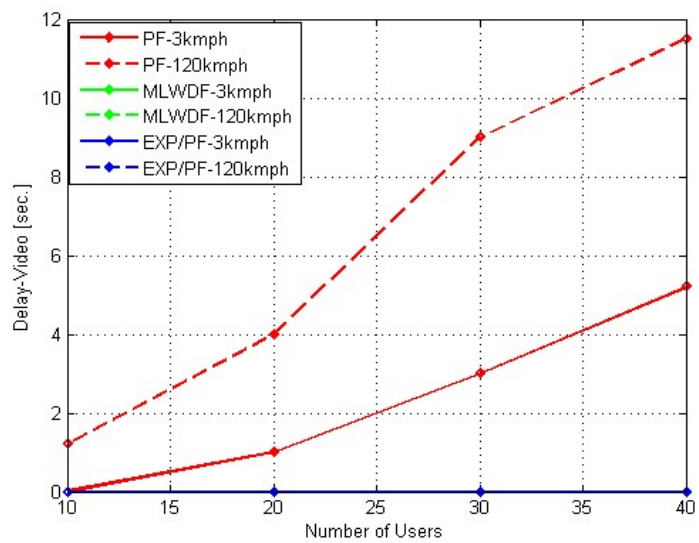
Figure 2.15: Delay in video flow with different schedulers at different speed
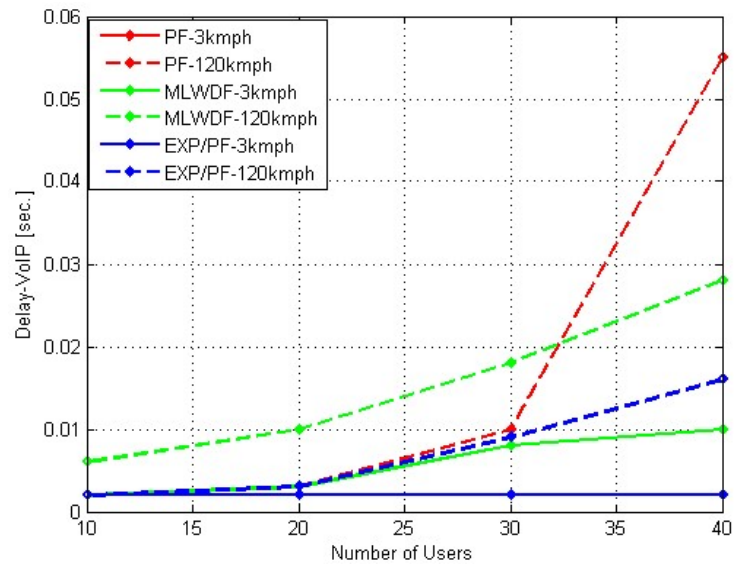
Figure 2.16: Delay in VoIP flow with different schedulers

In LTE, link adaptation becomes complex with increase in user speed and resulting in high packet loss as demonstrated in Figure 2.17 and Figure 2.18. As shown in the figure, all the schedulers suffer high packet loss with speed. Figure 2.19 shows degrade in spectral efficiency with user speed irrespective of scheduling algorithms used.
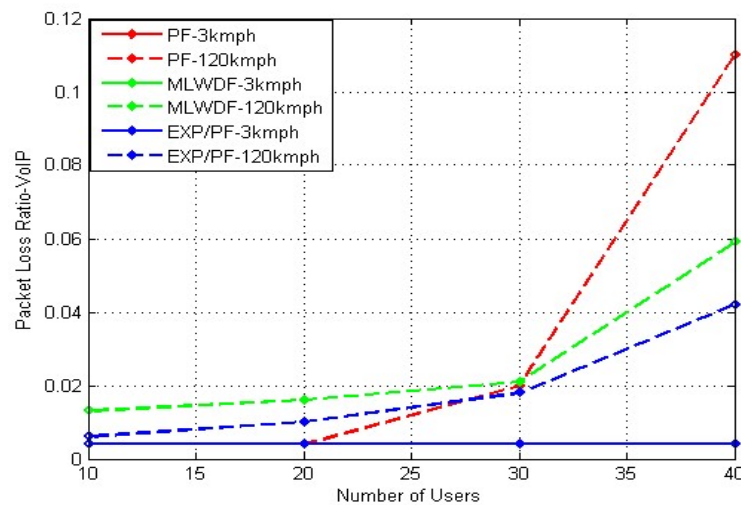
Figure 2.17: Packet Loss Ratio of VoIP flow with different schedulers at different speed
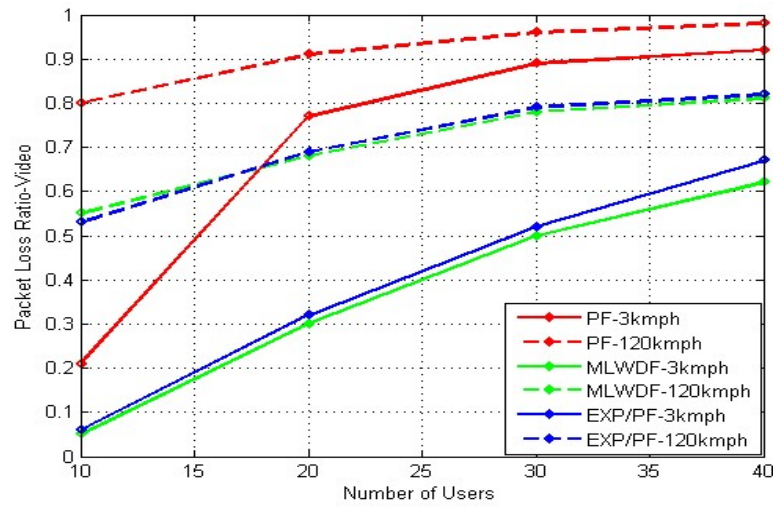
Figure 2.18: Packet Loss Ratio of Video Flow with different schedulers at different speed
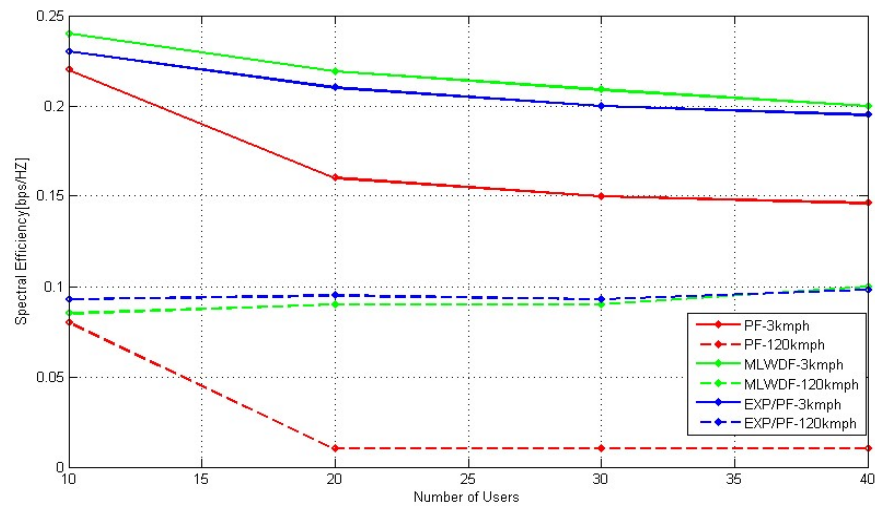
Figure 2.19: Spectral Efficiency of different schedulers in LTE-SIM

2.6 Summary

This chapter deals with the review and simulations of various PS algorithms. The performance of various PS algorithms were analysed against the theoretical performance. The method of comparing the simulation results with theoretical performance was mainly motivated due to the lack of equivalent measurements from real time LTE deployments that could be used for the same purpose. A particular set of scenarios were chosen with

simple assumptions so that it becomes possible to determine theoretical performance of scheduling schemes and verify the accuracy of the implementations of the scheduler. We note that, because of simplified assumptions, these scenarios might not necessarily represent real world condition and deployments. The PS algorithms were simulated by using two popular simulators knows as NS-3 and LTE-Sim. Both the simulators have implemented various PS algorithms. In general, LTE-Sim offers simplified models to suit academic needs and it is easier to customize. On contrary, the current NS-3 model is based on LENA, which follows 3GPP specification closely. Hence, the protocols are implemented in a detail manner than compared to LTE-Sim. On the flip side, it comes with increased cost and complexity, and it is hard to customize. Hence, NS-3 is more suitable for industrial type of simulation where more real time environment can be simulated and accurate results can be obtained. At the same time, it is user prerogative to use the simulator that suites them. In the subsequent chapters in this thesis, LTE-Sim was used for simulations.

3. PERFORMANCE ANALYSIS OF SIMULATED LTE NETWORKS

The work in this chapter is based on the joint publication [19]. [19] H.A. Kim, R. Subramanian, F. Afroz and K.Sandrasegaran, "Comparison of Performance of Packet Scheduling Algorithms in LTE-A HetNets," Wireless Personal Communication, vol 97, Issue 2, pp. 1947-1965, DOI 10.1007/s11277-017-4380-3.

Convergence of mobility and internet has put mobile service providers under tremendous pressure to offer faster and more efficient HSPA networks. Today, HSPA networks deliver high volume of data transaction in a cost-effective manner. However, the growth of smart phones has increased the ability of the customer to download large volume of video and has led to tremendous increase in data usage. However, to satisfy data thirsty customer, service providers require high capacity, large coverage area, high bit rates, and lower delay. Several advancements have been adopted in 4G mobile networks to improve the LTE system to meet the aforementioned requirement. The most cost-effective solution to achieve these demands is by introducing HetNets. HetNets can be defined as the mixture of maintaining small cells (such as pico and femto cells) cells working alongside the macro network [11]. The implementation of HetNets is classified as macro with pico and macro with femto [11]. In HetNets, both macro and associated small cells such as pico and femto use the same carrier frequency to efficiently manage channel utilization and thereby resulting in reduced operational cost. In LTE/LTE-A, the eNodeB is responsible for all functionalities of Radio Resource Management (RRM) such as Admission Control (AC), Power Control (PC), Handover Control (HOC), Congestion Control (CC) or Load Control (LC), Interference Coordination and Control (ICC) and PS. The most cost-effective solution to achieve these demands is by introducing HetNets. Hence, in this chapter, LTE network consisting of macro and pico cells is simulated and PS algorithms are evaluated based on this network setting. As seen in previous chapter, PS provides QoS guarantee because of efficient and best usage of available radio resources. Additionally, the responsibility of transmitting user's data packets in telecommunication system is manipulated by PS algorithms [2]. Generally, scheduling algorithms are vendor specific with no standardisations by 3GPP and therefore they are

based on network capability and user's demands. Consequently, this has led to the development of different PS algorithms according to the type of traffic, QoS requirement, vendor capability and applied services. Some of the most well-known PS algorithms such as PF, MLWDF and EXP/PF algorithms [17][18][19] are simulated in this chapter in HetNets environment in downlink direction.

3.1 LTE System Model in DL Direction

In LTE downlink, the basic element of radio resource is called Resource Block (RB). The UE is allocated a number of available RBs based on the user channel condition, required services, and agreed QoS requirements. RB could be defined in both TD and FD. In FD, RB is allocated with 12 of 15 kHz contiguous subcarriers consisting of 180 kHz as total bandwidth for one RB. On the other hand, in TD, RB is allocated with 7 symbols of OFDMA (Orthogonal Frequency Division Multiple Access) in a single 0.5 ms time slot [22].

As mentioned before, eNodeB performs PS besides other RRM operations in LTE system. The bandwidth (BW) that can be used in LTE system is in the rage of 5-20 MHz. In this study, the BW is 10 MHz. Since the same carrier frequency is used in macro and its associated micro (pico or femto), LTE suffers from ICI. In the simulation environment, ICI is modelled by calculating the SINR in downlink. The SINR calculation in downlink is performed for each RB assigned to data transmission by dividing the power of the desired from the eNodeB by the sum of noise power plus transmission coming from neighbouring eNodeB as interference signals. This is expressed as

$$\gamma = \frac{P_{signal}}{P_{noise} + \Sigma P_{interference}} \tag{3.1}$$

In general, different signals can be active during different time. Hence, in the simulation, a chunk is defined as the time interval between any two events or type. Let i be the generic chunk, T_i be its duration and $SINR_i$ its SINR. The average SINR $\bar{\gamma}$ obtained to be used as CQI feedback can be expressed as

$$\bar{\gamma} = \frac{\Sigma_i \gamma_i T_i}{\Sigma_i T_i} \tag{3.2}$$

The script in the simulator checks for the above calculation by recreating a number of random transmitted signals and interference signals to mimic the scenario where UE is trying to decode the desired signal from the eNodeB while facing interference other neighbouring eNodeBs. Macro UE SINR on a RB will be calculated using power from Macro BS and sum of all received powers when RB is used by neighbouring Pico cells. One way to limit this interference is Almost Blank Subframe (ABSF) where the interferer tier is not allowed to transmit data and vulnerable UEs are scheduled in ABSF with reduced cross-tier interference or operating Pico cells in different band to macro cells.

Packet scheduling operation is performed by eNodeB for every 1 ms TTI. Hence, two of 0.5 ms (1ms) is the time that the UE has to wait before it is allocated with new RBs. Each time the UE is assigned with two RBs because each RB is 0.5 ms in time domain. The eNodeB takes the scheduling decision at each TTI after considering the feedback CQI reports from UE in UL. The CQI mainly comprise of the channel condition, and more specifically, the SNR and the type of service requested. The SNR value is beneficial for the serving eNodeB to decide the downlink bit rate for each connected user in each 1 ms scheduling time. As an example, the number of bits involved in 2 contiguous RBs is calculated in [22].

The Equation 3.3 [23][24] determines user data rate as $dr_i(t)$ for the user denoted as *i* at subcarrier *j* at *t* time on the RB. The data rate as specified in Equation 21 is determined by the serving eNodeB on the basis of SNR values reported by UE in feedback reports.

$$dr_i(t) = \ nbs \ * nss \ * \ nst \ * nsr \qquad\qquad (3.3)$$

$$nbs = nbits_{i,j}(t)/symbol$$

$$nss = nsymbols/slot$$

$$nts = nslots/TTI$$

$$nsr = nsc/RB\text{rgg}$$

nbs is the number of bits per symbol. *nss* is the number of symbols per slot. While *nts* represents the number of slots per TTI, *nsr* represents the number of sub-carriers per RB.

Table 3.1 summarizes the mapping between SNR values and their associated data rates values.

Table 3.1: Mapping between instantaneous downlink SNR and data rates [23]

Minimum SNR level (dB)	Modulation and coding	Data rate (Kbps)
1.7	QPSK (1/2)	168
3.7	QPSK(2/3)	224
4.5	QPSK(3/4)	252
7.2	16 QAM (1/2)	336
9.5	16 QAM (2/3)	448
10.7	16 QAM (3/4)	504
14.8	64 QAM (2/3)	672
16.1	64 QAM (3/4)	756

As the user's packets arrive, the serving eNodeB buffers them in a particular buffer for each active user. In the buffer, the eNodeB assigns a timestamp for each queued packet in order to process them by scheduler or drop them, in case the maximum waiting time of a packet in the queue is reached. After that, First-In-First-Out (FIFO) technique is applied by eNodeB to transmit scheduled packets to their associated UEs in DL direction [23].

PS is responsible for scheduling operation in eNodeB. At each TTI, the scheduler prioritizes and classifies the packets sent by active users based on the applied scheduling algorithm. Various algorithms specify various criteria that are used to make scheduling decision. These criteria involve buffer status, channel condition, Head-Of-Line (HOL) packet delay, and service type. Based on the channel status, RBs are assigned for UEs

and high priority UEs are selected for scheduling and allocated with one or more RBs based on the requested service and status conditions [23].

3.2 Simulation Environment

The simulation was performed using LTE-Sim [15]. LTE-Sim V5 is the latest version simulator. LTE-Sim has not developed modules to deal macro with pico HetNets environment. Hence, to use LTE-Sim to simulate macro with pico HetNet environment, new pico module was developed on the basis of femto HetNet environment. LTE-Sim has developed substantial scenario that can be used to simulate and examine macro with femto HetNets environment. As shown in Figure 3.1, macro eNodeB is at the centre of the cell and it is surrounded by other small cells such as 2,4,6,8 and 10 with small and reduced power pico cells in the cell edge. As the number of pico cells is added to the cell edge, it is expected to enhance the system performance. However, by increasing the number of pico cells without appropriate planning may result in increased ICI, since the same carrier frequency is used in both macro and pico cells. The increase in ICI will confine the gain obtained by adding more pico cells in cell edge [18]. In this simulation, the radius of macro cells is assumed to be 1 km and pico cells are located 0.1 km on the macro cell. The simulation parameters and corresponding values are specified in Table 3.2. The simulation results on system performance are obtained by adding 2 pico cells and gradually increasing the number of pico cells by the factor two. Number of users served by pico and macro are not equal as pico cannot serve more than 30 users at a time [16]. Hence, if more than 30 users are added to a pico cell the system gain remains the same. Initially, all pico cells start with 10 users and gradually increased in steps of 10. The traffic of voice and video is assumed to be equally divided thereby making 50 % for voice and another equal half for video of the total system traffic. In this simulation, the two main criteria are considered for improving the system performance (1) increase the number of pico cells in steps of 2 and (2) increase the number of pico cells in steps of 10.

This network model is chosen since it has similarities with a real time network which is aimed to provide coverage to a large area and more number of users. Especially, the macro with pico setup provides better connectivity to cell edge users. The ICI is modelled, the handover is activated, unequal user distribution among cells is applied, and user is assumed to be in mobile with the speed of 3km/h. The other parameters such as path-loss,

penetration loss, multi-path loss and shadow fading which are summarized are applied in the simulation model [25][26]:

- Pathloss: The path loss expression for simulation for simulation is considered as in Equation 2.1, where *d* refers the distance between the eNB and the user in kilometers.
- Penetration loss: 10 *dB*
- Multipath loss: using one of the well-known methods called *Jakes model*
- Shadow fading loss (recently it could be used as a gain in LTE-A): log-normal distribution
  - Mean value of 0 dB.
  - Standard deviation of 10 dB.
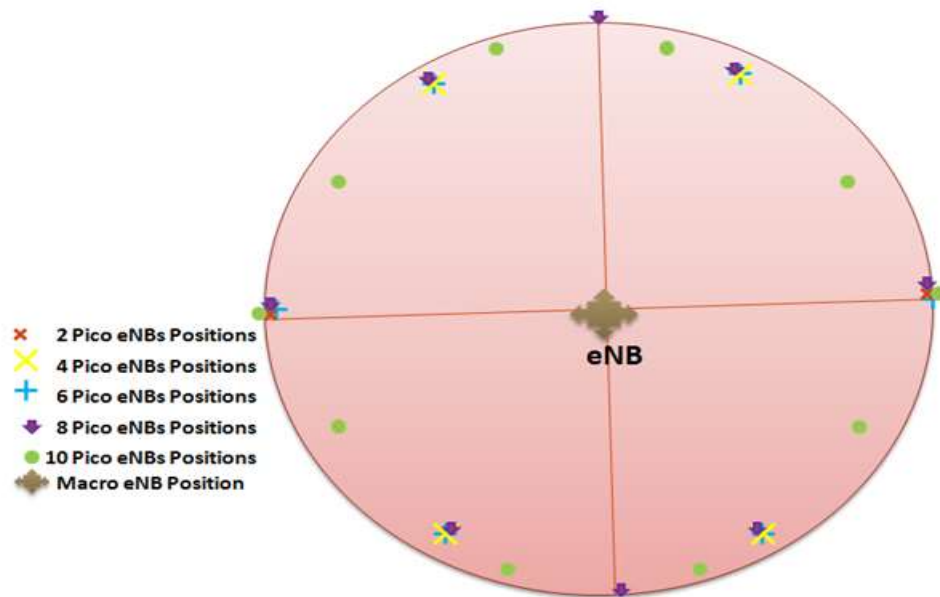
Figure 3.1: HetNets environment in simulation (Macro with Multiple Picos Scenarios) [19]

The system performance is evaluated in all aforementioned criteria based on packet throughput as seen in Equation 3.4, PLR as shown in Equation 3.5, packet delay (latency) and fairness index as seen in Equation 3.6. Fairness among users is implemented using Jain's method [16]. According to [30], the value of 1 is the best fairness value scenario among the scheduled users in which the resources are shared appropriately.

$$throughput = \frac{1}{T} \sum_{i=1}^{K} \sum_{t=1}^{T} ptransmit_i(t) \tag{3.4}$$

$$PLR = \frac{\sum_{i=1}^{K} \sum_{t=1}^{T} pdiscard_i(t)}{\sum_{i=1}^{K} \sum_{t=1}^{T} psize_i(t)} \tag{3.5}$$

$$fairness = 1 - \frac{ptotaltransmit_{max} - ptotaltransmi_{\ min}}{\sum_{i=1}^{K} \sum_{t=1}^{T} psize_i(t)} \tag{3.6}$$

The $ptransmit_i(t)$ refers to transmitted packet, $pdiscard_i(t)$ refers to discarded or lost packet size during the connection, $psize_i$ denotes to the summation of packets arrived and buffered in to eNodeB [23].

The size of the total transmitted packets (max -$ptotaltransmit_{max}$ and min - $ptotaltransmit_{min}$) is represented in Equation 3.6.

Table 3.2: Simulation parameters [19]

Simulation parameters	Values
Simulation time	40 s
Flow duration	30 s
Slot duration	0.5 ms
TTI	1 ms
Number of OFDM symbols/slot	7
Macro cell radius	1 km
Macro eNB Power	49 dBm
Pico cell radius	0.1 km
Pico eNB Power	30 dBm
User speed	3 km/h
VoIP bit rate	8.4 kbps
Video bit rate	242 kbps
Frame structure type	FDD
Bandwidth	10 MHz
Number of RBs	50
Number of subcarriers	600
Number of subcarriers/RB	12
Subcarrier spacing	15 KHz

To obtain more accurate results and reduce the probability of errors, simulations were performed for five times for algorithm (PF, MLWDF and EXP) with varying number of

users such as 10, 20, 30, 40, 50, 60, 70 and 80. In each user case 2, 4, 6, and 8 Pico cells are considered. This yielded a total of 2040 simulation (summation of 120,240,720 and 960) outcomes. The simulation values were averaged to obtain the graphs for each use case.

3.3 Simulation Results and Discussions

As previously mentioned, adding picos enhances system performance. The obtained simulation results prove that adding pico cells improve overall system throughput, PLR, delay, and fairness. Adding pico cells increases the number of users hence, it increases system throughput but at the same time increases the effects of ICI. Hence, sufficient care must be taken when adding pico cells to the macro. The simulations of various ICI algorithms are carried out in Section 3.3.5.

3.3.1 Throughput

The Figure 3.2 shows the average system throughput for all scenarios. As shown in the figure, adding two pico cells to macro increases the system performance in all scheduling schemes. Let's analyse this using PF algorithm as shown in Table 3.4. The number of user's increases by factor of 10 such as 10, 20 and 30 in vertical column. The gain value of 3.39 Mbps for 10 users doubles proportionally with increase in UEs. For example, the gain value is 6.78 Mbps for 20 users which is almost double than 3.39 Mbps for 10 users. The difference in average gain between 30 users to 20 users is 3.39 Mbps. This proves that by increasing 10 users to the pico cells increases the throughput in a constant value. However, the pico cells will not serve beyond 30 users and hence even if the users are accepted in pico cells, the system performance remains the same. However, macro cell can accept more users to the system that boosts the system throughput marginally by 1 Mbps. For instance, the overall system performance with 40 users is 16.41 Mbps and even when the number of users increases to 50, the overall system performance increases to 17.26 Mbps and thus increasing the performance by just 1 Mbps. As shown in Table 3.4, the increase in number of pico cells from 2 to 10 is shown in horizontal. The increase in pico cells increases the throughput of the system by10 Mbps. This value comes from the effect of adding two Pico cells to the system. That is, at the point of 40 users, at 2 Pico cells the total throughput of the system is 16.41 Mbps, whereas it is 26.44 Mbps with 4

Pico cells. Hence, the difference between these two cases is almost 10 Mbps. In Figure.3.3, throughput comparison is made between various scheduling algorithms with varying number of users.

The PF algorithm has the lowest throughput compared to MLWDF and EXP/PF. Figure 3.3 shows when number of user's increases, the throughput of PF is slightly degraded compared with the other algorithms. For example, while the number of users are 60, 70 and 80, the PF throughput is lower than the rest of the PS schemes. However, the behaviour of all schemes is similar to all Pico scenarios. It is easy to notice that the difference in gain between the scenarios such as 2 Picos and 4 Picos is the same as the difference in gain between the scenarios with 4 Picos and 6 Picos, 6 Picos and 8 Picos, and 8 Picos and 10 Picos.

Table 3.3: Throughput gain and averages [19]

PF								
		Picos (Y-axes)						
Throughput (Z-axes)		2	4	6	8	10	Average 2 Picos gain [Mbps]	
Users (X-axes)	10	5.09	8.48	11.88	15.28	18.67	**3.39**	Mbps increment
	20	10.17	16.95	23.74	30.53	37.32	**6.78**	Mbps increment
	30	15.124	25.21	35.36	45.46	55.64	**10.13**	Mbps increment
	40	16.41	26.44	36.57	46.52	56.56	**10.03**	Mbps increment
	50	17.26	27.11	36.93	47.05	57.19	**9.98**	Mbps increment
	60	17.55	27.41	37.37	47.45	57.44	**9.97**	Mbps increment
	70	17.29	27.14	37.35	47.46	57.8	**10.12**	Mbps increment
	80	17	27.13	37.43	47.55	57.91	**10.22**	Mbps increment
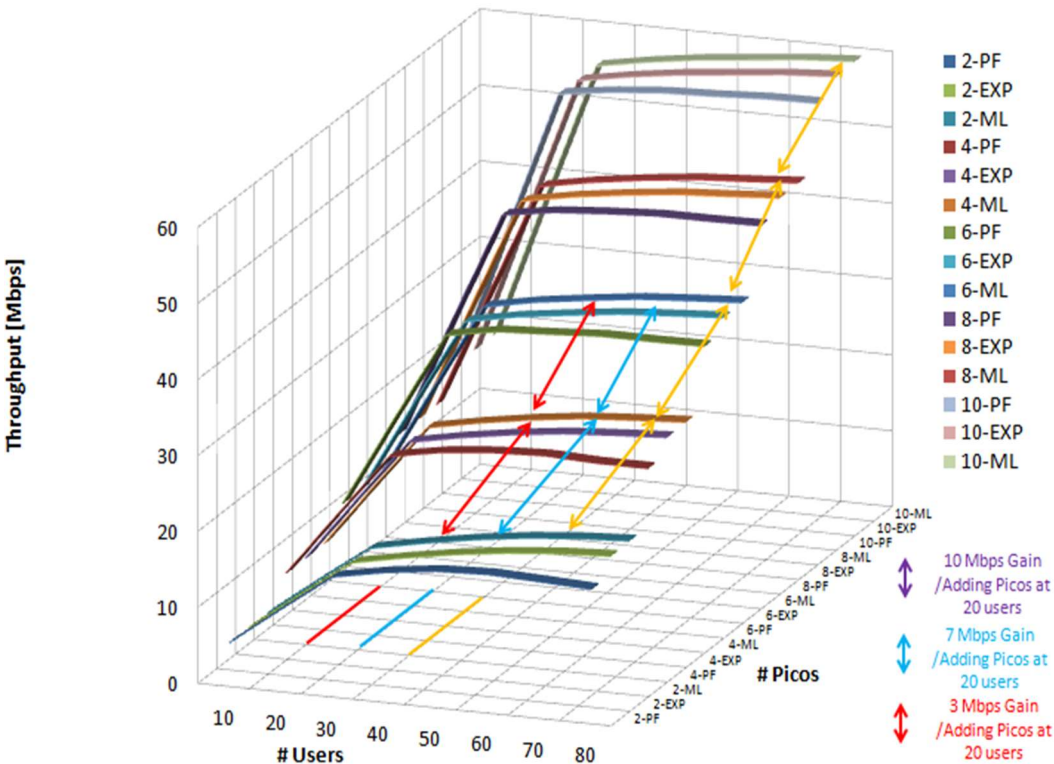
Figure 3.2: Throughput gain of video traffic in macro with 2-10 Pico scenarios [19]
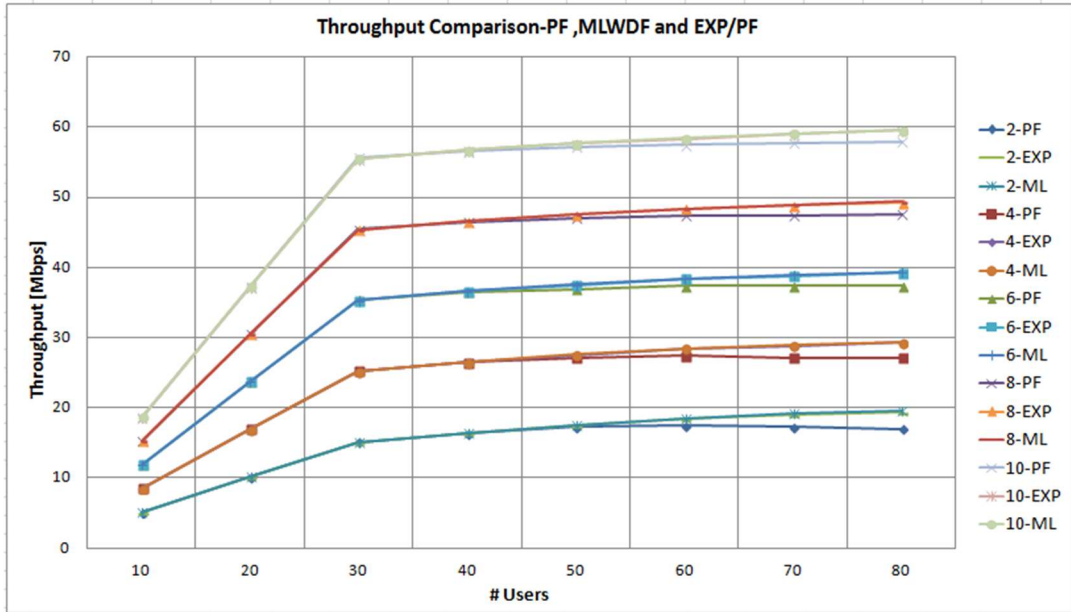
Figure 3.3: Throughput gain of video traffic in macro with 2-10 Picos scenarios [19]

3.3.2 Packet Loss Ratio (PLR)

The PLR increases as the number of users increase. The PLR starts to decrease with the increase in the number of pico cells. However, increasing the pico cells will increase the number of users and thereby increases PLR. Let's analyse PLR with the performance of PF algorithm. Since, the performance of PF algorithm is lowest compared with other algorithms in most cases the PLR starts to increase as the number of users in the system increases. The performance of PLR in the PF is shown in Figure 3.4. In this figure, it can be observed that, at 50 users and PF with 8 pico cells have PLR values similar to the PLR of other scheduling schemes namely MLWDF and EXP/PF with two Pico cells. This proves that adding more pico cells enhances system PLR under PF. Comparing various PS algorithms, the PF has the high PLR value in all pico cell scenarios. The highest and worst PLR value of PF is in two Pico cells scenario as shown in Figure.3.4. The PLR performance of PF is enhanced gradually by adding new pico cells to the system. Compared to PF, other algorithms such as MLWDF and EXP/PF have better PLR performance in the same scenario when the number of pico cells is 10.
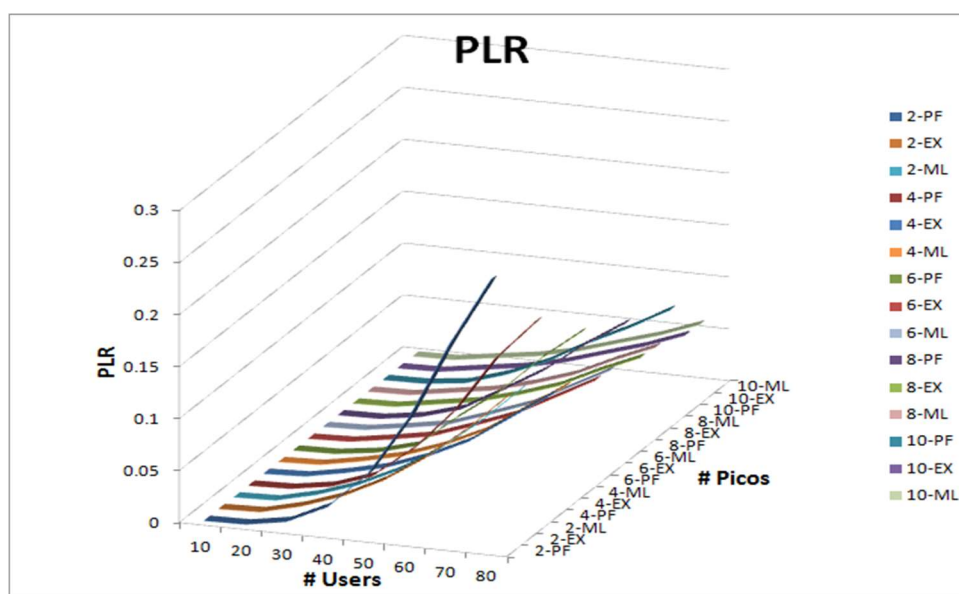
Figure 3.4: PLR video traffic comparison in Macro with 2-10 Picos scenarios [19]
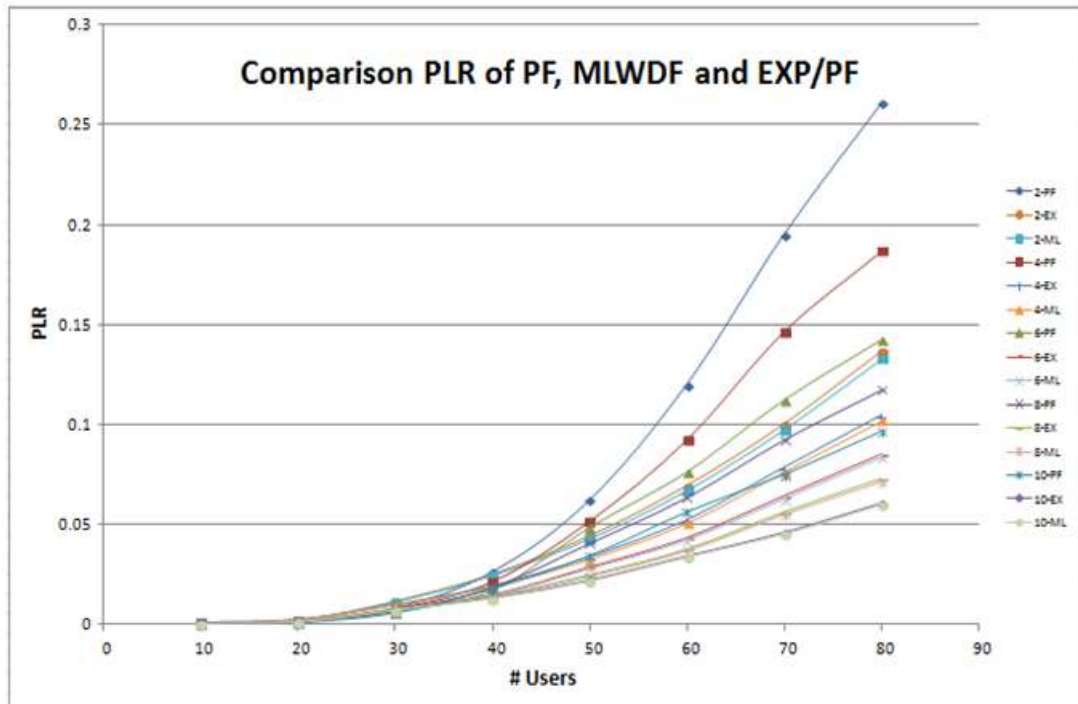
Figure 3.5: PLR of video traffic in macro with 2-10 picos scenarios [19]

3.3.3 Delay

Delay follows similar behavior to PLR. As the number of user's increases, the delay gets higher. Figure 3.6 and Figure 3.7 shows the simulation results of delay performance of various scheduling schemes. The delay in PF algorithm with 2 Pico cells at 80 users is the highest among other scheduling schemes. All the simulated PS schemes show an increasing trend of delay performance while the number of users increases. For example, at 10 users in two Pico cells scenario, the delay is 6 ms and at 20 users the delay is 10.32 ms in the same scenario. As the number of users increases, the delay increases too. Hence, adding more pico cells to the network reduces the overall system delay which is proved by simulation results. Horizontally, it is easy to notice that PF delay starts decreasing while the number of pico cells increases.

Table 3.4: PF delay values [19].

PF						
		Picos (Y-axes)				
	Delay (Z-axes)	2	4	6	8	10
	10	6	5.8	5.64	5.53	5.56
	20	10.32	9.89	9.67	9.56	9.59
	30	14.65	14.17	13.84	13.76	13.83
Users (X-axes)	40	16.57	15.39	14.71	14.48	14.41
	50	18.67	16.82	15.89	15.34	15.09
	60	20.86	18.12	16.75	16.04	15.7
	70	22.78	19.43	17.63	16.72	16.21
	80	24.35	20.32	18.25	17.17	16.63
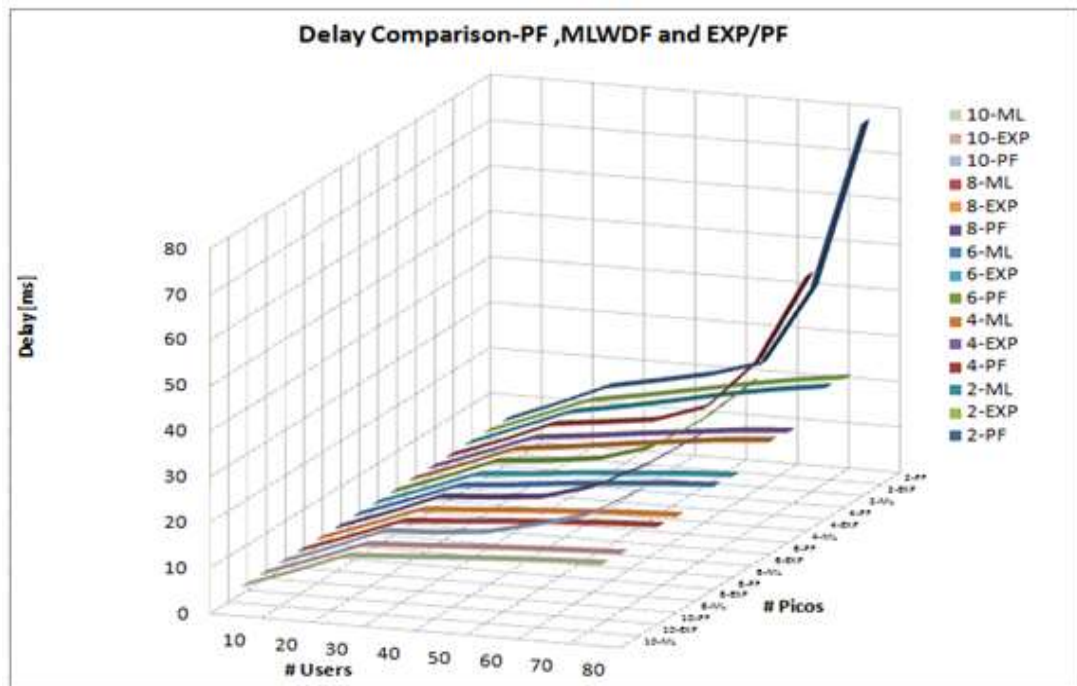
Figure 3.6: Delay of video traffic comparison in macro with 2-10 pico scenarios [19]
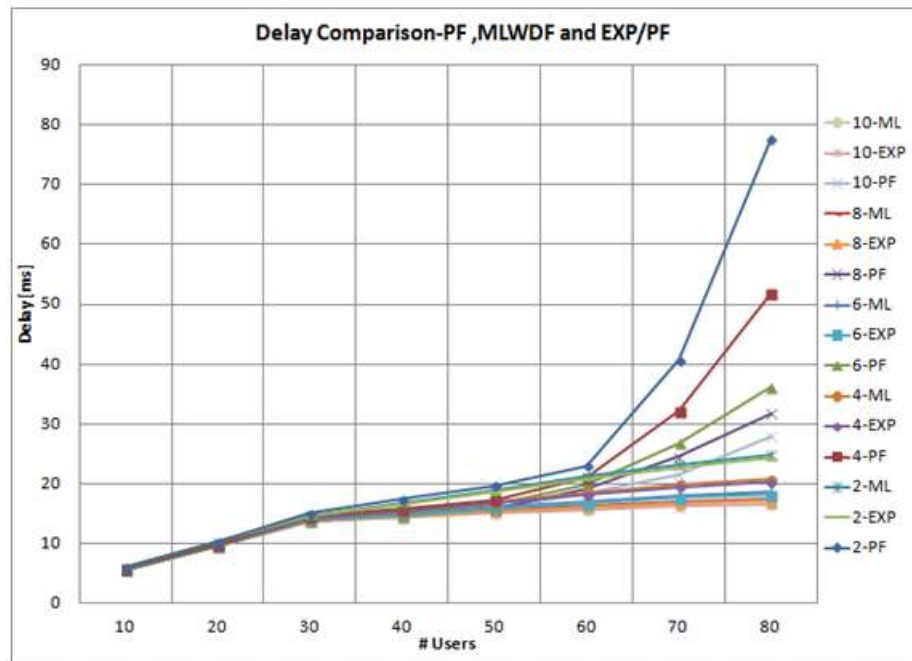
Figure 3.7: Delay comparison of video traffic in macro with 2-10 picos scenarios [19]

3.3.4 Fairness Index

Ideally, the fairness index has to be closer to the value of one. Adding more users affect fairness and it is indicated in Figure.3.8 as graph slopes down. Figure 3.9 illustrates the fairness index of macro with 2 to 10 Pico cells. In case of MLWDF and EXP/PF, the fairness index slightly decreases from one whereas, the PF suffers further drop. Adding more pico cells has limited impact on fairness as shown in Figure 3.8 and Figure 3.9. However, adding more pico cell slightly enhances the overall system fairness value. The results from simulations indicate that worst case scenario of fairness index is at 8 Pico cells. At this point, PF shows the lowest fairness value when the number of users is 80. The MLWDF and EXP/PF similarly suffer further drop at the same point as aforementioned in PF as seen in Figure.3.8 and Figure.3.9. In all schemes, the value of fairness index is more likely to be identical although PF has lower fairness values among the schemes. For example, MLWDF has similar values of fairness in 2, 4, 6, 8 and 10 Pico cells scenarios with number of users such as 10, 20, 30, 40, 50, 60, 70 and 80.
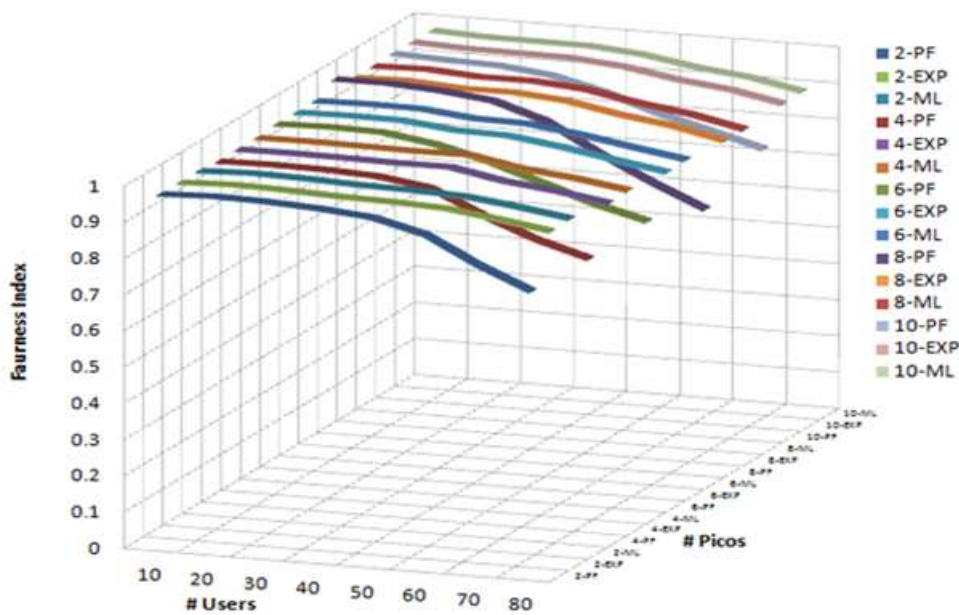
Figure 3.8: Fairness Index in macro with 2-10 picos scenarios [19]
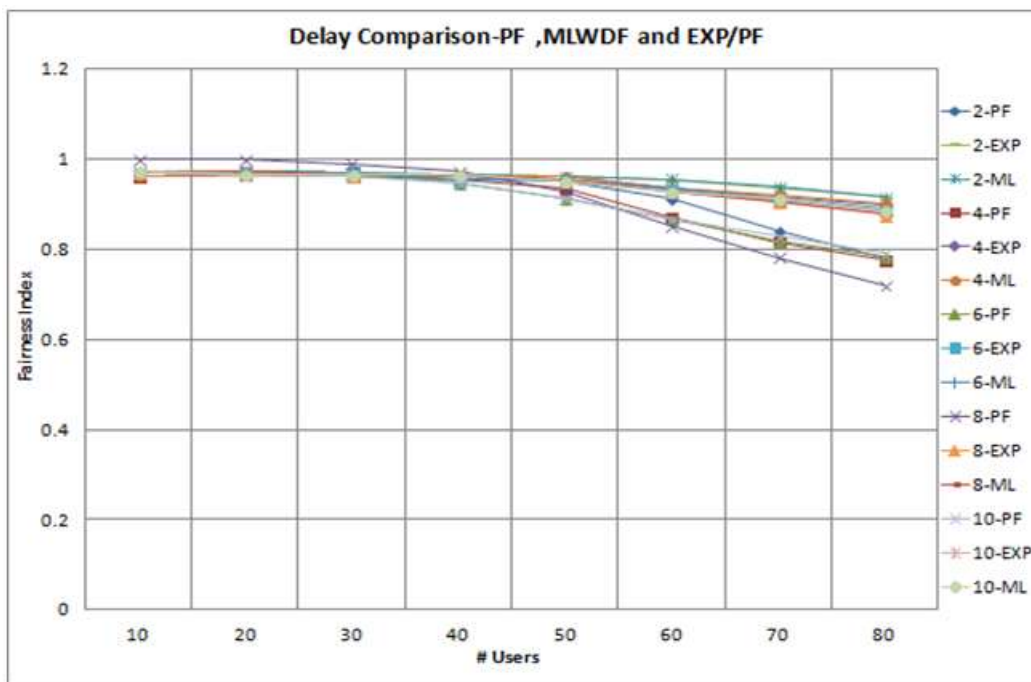
Figure 3.9: Fairness Index in macro with 2-10 picos scenarios [19]

3.4 Summary

The various PS algorithms proposed for LTE network have been analysed. The performance of these algorithms depends on type of traffic and number of users. Hence, different simulations were carried out for each algorithm. To improve the overall system performance, HetNets concept was used and small cells were added. The number of pico cells were gradually scaled up to 10 pico cells by the factor of two. This gradual scaling of pico cells enhanced the system throughput, decreased the PLR, reduced the delay and helped to maintain fairness level close to 1. However, saturation would be attained after reaching certain number of pico cells and users. This is because of the reason that, the ICI limits the performance, since the same carrier frequency is used throughout the cells. The results prove that MLWDF manifests the best performance for video flows followed by EXP/PF. In future research, several enhancement such as Almost Blank Subframes (ABS), enhanced Inter-Cell Interference Cancelation (eICIC), Cell Range Extension (CRE) concepts and using Carrier Aggregation (CA) and Coordinated Multi-Point (CoMP) will be added to the simulations to further enhance the performance of HetNets.

The work in this chapter is based on the joint publication [19].

4. PERFORMANCE ANALYSIS OF REAL TIME LTE NETWORKS – SCHEDULING AND RAN

The contents of this chapter are based on the following publications

- R. Subramanian, R. Heidari, K. Sandrasegaran, A. M. A. Dhanraj, and K. Srinivasan, "Benchmarking of Cell Throughput Using Proportional Fair Scheduler In A Single Cell Environment," International Journal of Wireless & Mobile Networks, vol. 7, no. 2, pp. 67–79, Apr. 2015.
- R. Subramanian, K. Sandrasegaran, and X. Kong, "Benchmarking of Real-Time LTE Network in Dynamic Environment," in IEEE Asia Pacific Communication Conference (APCC), Indonesia: IEEE.

This chapter discusses the performance analysis of real time networks. The first part of the chapter discusses the performance analysis of PF algorithm in a real time single cell LTE network. The second part of the chapter discusses the performance analysis of LTE RANs of leading service providers. The PF scheduling algorithm compromises between cell throughput and fairness [31]. Several researches have been published on PF algorithm based on mathematical model and simulations. The results discussed in this chapter are based on the tests carried out in a real time network. In this study, three types of user subscriptions namely Gold, Silver and Bronze schemes were used. Each subscription scheme was provisioned with a defined minimum throughput. Apart from subscriptions plans, channel condition plays a major role in determining the achievable throughput [28][29]. To ensure fairness among different subscriptions even in bad channel conditions and to deliver the provisioned throughputs, priorities are attached with the subscriptions [32][33]. As per the subscription plans, Gold subscribers are assigned with 50% of the bandwidth offered by the network (100 Mbps in DL and 50 Mbps in UL), Silver is assigned with 25% of the maximum bandwidth and Bronze is assigned with 12% of the maximum bandwidth. The priorities assigned to subscribers determine the fairness in unfavourable channel conditions - Bronze (high), Silver and Gold (medium). The benchmarking test has been performed with all three types of subscription plans for nearly two hours in a real-time single cell LTE network without any heterogeneous cells influencing the outcome. In the second part of the chapter, benchmarking of network

coverage was performed based on four different test scenarios namely walk test, train test, drive test, and indoor test. Walk test was carried out by walking around the city centre. Train test was carried out whilst travelling in train and passing through a small tunnel. Drive test was carried out while driving in a car inside the city, and indoor test was carried out inside the international airport.

4.1 System Model

In the system model, the downlink channel of a single cell wireless access network is considered. The downlink model PF is very much similar to IS-856 system where a single broadband channel is shared among all the mobile terminals in the cell. The BS transmits pilot signal at specified time slot which is received by all UEs in the cell and the feedback on the channel condition and transmission rate are constantly fed to the system. Based on the received information from UE, the BS decides to serve the next UE [35-40]. As specified in [42], the transmitting power at the BS is denoted as P_t, the power received at the mobile is given by:

$$P_k = |h_k|^2 P_t \tag{4.2}$$

The channel gain is denoted by h_k in Equation 4.2. The combination of various factors such as scattering, absorption, shadowing and multipath effect contributes to the channel gain. The channel gain between BS and user k can be written as:

$$h_k = \sqrt{cd_k^{-\alpha} S_k} m_k \tag{4.3}$$

In Equation 4.3, c is constant and it in-corporates the transmitting and receiving antenna gains, d_k denotes physical spacing between BS and user, α denotes path loss exponent which takes the value around 4.0 in urban environments [41], S_k represents the shadowing effect, m_k denotes multipath fading. The shadowing effect follows the log-normal distribution with zero-mean and variance σ_s^2 which is represented in decibels in the log scale. The multipath fading is modelled in second order chi-square or exponential random variable with mean 1.0, which represents Rayleigh fading channel. Since, single cell

scenario has been considered for benchmarking the parameter ICI is not considered in the system model. Therefore, the SNR of user k can be represented as:

$$Z_k = \frac{P_k}{P_n} \tag{4.4}$$

where P_n denotes background noise power that includes thermal noise and interference. In [41], the median SNR at the cell edge ρ represents the noise level of the wireless environment that is defined as:

$$\rho = cD^{-\alpha} \frac{P_t}{P_n} \tag{4.5}$$

where, D denotes the radius of the cell. The average SNR of the user k is defined as:

$$\overline{Z_k} = \rho(\frac{D}{d_k})\alpha S_k \tag{4.6}$$

Hence, the SNR is modelled as an exponential random variable.

4.2 PF Scheduler in Real-Time LTE Network

The several studies in the past on PF scheme have considered two states of channel model with the assumption that the transmission rate is fixed regardless of the channel state [37][38][40]. Due to bandwidth scarcity, cell throughput forms an important indicator to evaluate the wireless channel and this forms an important metric to evaluate the scheduling algorithms. With the given channel gain for each user, the BS serves the user k first, whose magnitude of the channel gain is greater than other users. The PF schedulers is designed in such a way that it allocates a considerable portion of time slots to each subscribers while giving preference to the subscribers in good channel state. In this study, the subscribers are broadly classified as Gold, Silver and Bronze based on the subscription and tariff. The channel state is sent as the feedback by each user at the beginning of the every time slot. The feasible rate to the average throughput is calculated for each user by BS which forms a key selection criterion, in turn, it forms the basis of the preference metric and based on this preference metric, the transmission for forthcoming timeslots will be decided. Figure 4.1 illustrates the fairness between the mobiles based on the

channel condition. This can be defined as the following. The possible user rate for user k in time slot n is $R_k[n]$, the moving average can be denoted as $\widetilde{R_k}[n]$. Then, user $k^* = argmax_k R_k[n]/\widetilde{R_k}[n]$ is served in n time slots. The throughput for each user can be updated as below:

$$\widetilde{R_k}[n+1] = \begin{cases} \left(1 - \frac{1}{t_c}\right)\widetilde{R_k}[n] + \frac{1}{t_c R_k}[n], & k = k^* \\ \left(1 - \frac{1}{t_c}\right)\widetilde{R_k}[n], & k \neq k^* \end{cases} \qquad (4.7)$$
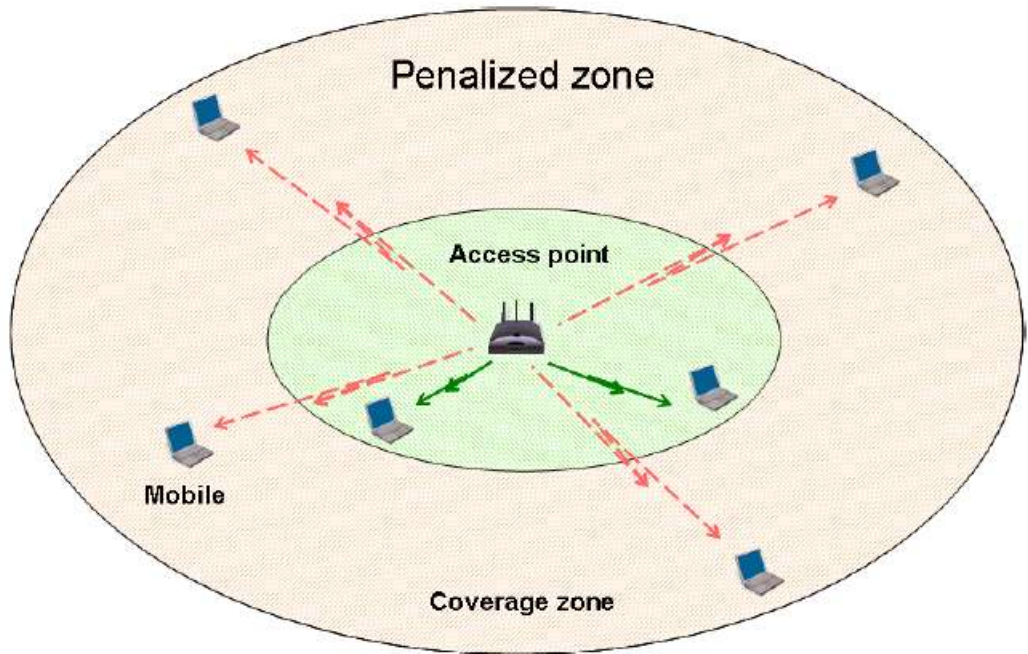
Figure 4.1: Illustration of Fairness

In Equation 4.7, t_c represents time constant for moving average. In the wireless environment, fading, which fluctuates in a random manner, has the greatest impact on channel state. When the number of users is small and if all the users are not in good channel condition, then the throughput will be very low regardless of whoever is scheduled. On the other hand, when the number of users is high, there is very high probability that some users can be in a very good channel state. Therefore, the cell throughout gain can be increased by scheduling them first to utilize the fast-fading

82

characteristics. The advantage of the multiuser diversity cannot be realised in RR scheduling. In RR scheduling, the scheduling order is determined well in advance. In this scheduling, each user is given equal amount of time. Based on the channel state, the transmitting data rate can be adjusted in RR but the order of service cannot be adjusted. The other schedulers such as Weighted Fair Queuing (WFQ), Channel Independent Fair Queuing (CIFQ), Server Based Fairness Approach (SBFA) and Weighted Fair Scheduling (WFS) select the users based on the channel condition although they have very less information on the channel state. These schedulers delay the service to the users in bad channel state temporarily and schedule the lagging users. As a result, the users can experience frequent packet drops and the lower throughput when compared with the opportunistic scheduler like PF [42-46].

In majority of real time networks, PF algorithm is implemented because of its simplicity. PF scheduler requires per flow queuing which is common to the scheduling algorithms. In core networks, there would be huge amount of per flow queues which creates a huge burden in the core network. Apart from this, PF requires channel state information from each user. The BS transmits broadcast pilot symbol periodically and collects the channel state information from each user regularly. Moreover, additional control channel is required to provide the feedback on the channel state, but this depends on the number of users. As the number of users increases the cost of implementing it increases.

4.3 Test Setup and Results

The benchmarking tests were performed in a single cell real time LTE network. Due to confidentiality, the name of the service provider cannot be revealed. In this testing more practical approach was considered. The APN Aggregate Maximum Bit Rate (APN-AMBR) applicable for EPS access is a QoS policing parameter that allows the network to control the maximum rate of payload traffic received or transmitted on a Packet Data Network (PDN) connection. The Maximum Bit Rate (MBR) is the corresponding parameter applicable for GPRS access. The Converged Packet Gateway (CPG) supports an APN-AMBR and MBR value between 4 kbps and 256 Mbps in both the uplink and downlink direction. Hence, maximum downlink speed will be 256Mbps instead of

300Mbps.For attaining this, there is a need to either disable the policing or use two APNs of each 256Mbps maximum. This is based on the subscription rent the subscribers pay to the operator for the service.

Apart from the subscription plans, the location of the subscriber and the radio channel play an equally important role in deciding the throughput for the subscribers. For example, assuming that the Gold subscriber travels to the cell edge, just because he has subscribed for the Gold service, it is not possible to negate the impact of the channel condition in the throughput and hence, a trade-off between the channel condition and subscription plan has to be made. The proportional fair is based on the trade-off between channel quality and average rate per user. In normal scenario, the users at good channel condition and with higher CQI will be allocated with large resources to achieve good throughput while, the users at cell edge and with poor channel condition will be allocated with fewer or no resources in-order to maintain optimum system performance. However, in PF algorithm, a trade-off between system performance and user fairness is delivered to keep the customers in the cell edge or in the bad radio environment satisfied. The following scenarios were tested by means of a script in the test environment:

Scenario 1: Gold, Silver and Bronze UEs are subjected to test by means of the FTP test

Scenario 2: Gold and Bronze

Scenario 3: Gold and Silver

Scenario 4: Silver and Bronze

Scenario 5: Gold only

Scenario 6: Silver Only

Scenario 7: Bronze only

Table 4.1 explains various testing scenarios. Each scenario is tested independently and with various combinations. Table 4.2 and Table 4.3 provide details about Radio Access Network (RAN) configurations made in the network exclusively for the benchmarking testing. Table 4.4 to Table 4.7 provide the benchmarking results in the tabular format. Figure 4.2 provides benchmarking results in the graphical form. The test results show that, when a Gold, Silver and Bronze users are tested individually in the good channel conditions, the throughput achieved is almost the same. However, in bad channel

conditions different priority is set for different subscription types. The Gold and Silver are set as medium priority, but the Bronze users are set as high priority. Apart from the subscription type, the channel conditions play a major part. Since, the Bronze users are set with 12% (least among the subscription plans) of the maximum bandwidth the channel condition will further bring down the throughput rate. That is why the Bronze users are set with high priority in bad channel condition. TEMS Investigation, Sony Xperia smart phones capable of LTE, scripts for testing various subscriptions and SIM Card configured with different ARP with Gold, Silver and Bronze profiles were used in this testing.

Table 4.1: Testing Scenario

No	Scenarios
1	Case1-Gold User
2	Case2-Gold User + Silver User
3	Case3-Gold User + Silver User +Bronze
4	Case4-Gold User + Bronze User
5	Case5-Silver User + Bronze User
6	Case6-Silver User
7	Case7-Bronze User

Table 4.2: RAN configuration for the testing

RAN parameters	Value
Downlink aggregate MBR for the UE in MME	10000000 kbps
Uplink Aggregate MBR for the UE in MME	10000000 kbps
Downlink aggregate MBR of an APN in MME	10000000 kbps
Uplink aggregate MBR of an APN in MME	10000000 kbps
Highest allowed ARP priority level for a non-GBR bearer in MME	1
Allowed value of PCI for a non-GBR bearer in the MME	Yes
Allowed value of PVI for a non-GBR bearer in MME	No
MBR downlink	256000 kbps
MBR uplink	256000 kbps
GBR downlink	256000 kbps
GBR uplink	256000 kbps
Highest allowed ARP priority level for a GBR bearer in MME	1
Allowed value of PCI for a GBR bearer in MME	Yes
Allowed value of PVI for a GBR bearer in MME	No

Table 4.3: Network Configuration for testing fairness

QCI	Parameter	Value	Remarks
QCI6	Scheduling algorithm	3	PFS_MEDIUM (Gold)
QCI8	Scheduling algorithm	3	PFS_MEDIUM (Silver)
QCI9	Scheduling algorithm	2	PFS_HIGH (Bronze)
QCI6	DL minimum bit rate	40000	kbps
QCI8	DL minimum bit rate	20000	kbps
QCI9	DL minimum bit rate	10000	kbps
QCI6	Relative priority	57	Relative priority keeping 100% as the max
QCI8	Relative priority	28	Relative priority keeping 100% as the max
QCI9	Relative priority	15	Relative priority keeping 100% as the max

Table 4.4: Benchmarking result and average values

Use case no	Scenario	QoS - Benchmarking results average values (kbps)		
		Gold user	Silver user	Bronze user
1	Gold user	27.75	-	-
2	Gold + Silver user	23.55	16.59	-
3	Gold+Silver+Bronze user	24.48	14.96	7.76
4	Gold + Bronze user	23.47	-	10.57
5	Silver + Bronze user	-	24.53	18.16
6	Silver user	-	30.62	-
7	Bronze user	-	-	26.78

Table 4.5: QoS for Gold subscription

Use case no	Scenarios	Gold subscription				
		Test 1	Test 2	Test 3	Test 4	Test 5
1	Gold user	27.3	31.59	29.08	26.26	24.52
2	Gold + Silver user	20.36	22.82	26.78	26.03	21.79
3	Gold +Silver + Bronze user	21.42	26.87	25.28	24.99	23.87
4	Gold + Bronze user	28.89	21.47	26.04	17.39	23.59
5	Silver + Bronze	-	-	-	-	-
6	Silver user	-	-	-	-	-
7	Bronze	-	-	-	-	-

Table 4.6: QoS for Silver subscription

Use case no	Scenarios	Silver subscription				
		Test 1	Test 2	Test 3	Test 4	Test 5
1	Gold user					
2	Gold + Silver user	19.05	17.03	10.19	16.06	20.66
3	Gold +Silver + Bronze user	16.11	16.27	14.24	14.05	14.14
4	Gold + Bronze user					
5	Silver + Bronze	26.51	24.95	22.8	22.32	26.08
6	Silver user	28.39	31.67	30.66	31.37	31.05
7	Bronze					

Table 4.7: QoS for Bronze subscription

Use case no	Scenarios	Silver subscription				
		Test 1	Test 2	Test 3	Test 4	Test 5
1	Gold user	-	-	-	-	-
2	Gold + Silver user	-	-	-	-	-
3	Gold +Silver + Bronze user	8.27	7.67	7.32	8.07	7.51
4	Gold + Bronze user	6.17	7.71	6.53	13.34	19.14
5	Silver + Bronze	17.71	18.41	18.45	20.7	15.55
6	Silver user	-	-	-	-	-
7	Bronze	26.72	30.7	15.32	30.17	31
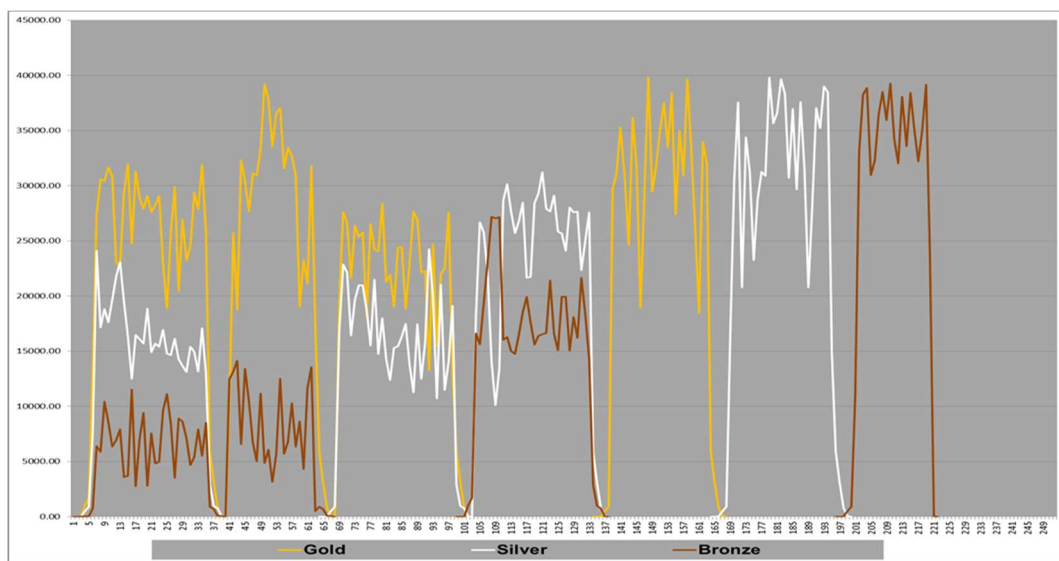
Figure 4.2: Benchmarking test results for different scenarios

(Subscription plan vs Throughput)

The performance analysis test were carried out in the cell with radius of 1 Km. The downlink channel slot length is 1.67 ms. The BS transmission power is fixed at 10 W. The standard deviation of shadow fading is around 8 dB and path loss exponent is around 4db. Figure 4.2 illustrates the performance test results of Gold, Silver and Bronze subscribers tested in different scenarios. In the performance test result, the number of subscribers is not shown explicitly like simulation. Since, the test is carried out in a real-time LTE network it is assumed that there will be fair share of subscribers in each plan (Gold, Silver and Bronze) trying to access data from the network.

In traditional setting, fairness was not considered because the cellular channels are assigned based on pre-reservation strategies, whereas in modern wireless technologies like in 4G technology, the reservation based allocation will not serve the purpose of the subscribers and network operators. These new technologies truly consider fairness and user throughput as one of the major requirements. Hence, several scheduling algorithms have been put forth by many researchers to achieve this feat. Among them, PF scheduling algorithm is very popular. Since, it offers various degree of flexibility for the operators to serve UEs based on location, channel environment, service subscription, etc. Among this, channel condition plays a vital role in user throughput and PF offers this required balancing.

4.4 Performance Analysis of LTE RAN in Dynamic Environment

LTE/LTE-A is a high speed wireless communication technology which evolved from 2G/3G. LTE provides very high throughput in uplink and downlink and hence, it is attracting more subscribers every day. This section analyses the performance of LTE RAN in real time LTE network of two different leading service providers through drive test. Test cases were performed under dynamic environment where the test user is dynamic or the environment around the test user is dynamic. The performance comparison of different Key Performance Indicators (KPI) such as Reference Signal Received Power (RSRP), Reference Signal Received Quality (RSRQ), Reference Signal Strength Indicator (RSSI) and throughput (uplink - UL and downlink - DL) are made

between the two LTE service providers. The performance tests were performed using Nemo tool in a real-time LTE network. Average values were obtained for different KPIs to study the performance of LTE network.

In these tests, the network performance of Operator A and B are compared. Both the service providers have an ambitious network roll out plan for future. Operator A for instance, is planning to shut down the 2G network operations by 2016 and is planning to allocate the spectrum used by 2G to LTE. Operator A has extended the 700 MHz TE trials in two major cities. Furthermore, to boost the data speed Operator A has introduced carrier aggregation using three bands to deliver data rate up to 450 Mbps.

On the other hand, Operator-B is aiming to cover 98.5% of the population with the LTE by end of 2016 where the initial service was started by Operator-B in the year 2013. Subsequent to the launch, the network was rolled out across various metropolitans in the country. The roll out was planned in such a way that new mobile sites were installed and some sites were upgraded to have combined 4G technologies of LTE-TDD (2300MHz) and LTE-FDD (1800 MHz). Operator B has plans to utilize 700 MHz and 2600 MHz for 4G.

4.4.1 Signal Power Measurement Indicators in LTE Network

The KPIs such as RSRP, RSRQ and RSSI provide information regarding quality of the wireless channel in LTE network. These measurements are conducted over Resource Elements (RE) that contains Reference Symbols (RS). The fourth and sixth REs contain RS, and RSs are transmitted in the first and fourth OFDM symbol of each RB [47]. RSRP is a cell specific metric denoting received signal strength that is used by LTE enabled UE for cell re-selection and handover. The definitions of KPIs are given below.

RSSI can be defined as the total power received in a single RE in a RB [48][49]. RE which is the smallest data unit in LTE standard represents 15 KHz in frequency domain and 1 OFDM symbol in time domain. Each RB constitutes 12 RE which corresponds to (12*15)180 KHz in frequency domain and 0.5 msec in time domain. RSSI includes all the power from neighbour, serving cells and noise. RSSI is expressed in dBm. RSRP can

be defined as power measured in a single RE. It is represented as the power of a single RE which contains reference signal. RSRP does not include noise or interference from serving or neighbouring cells. RSRP is expressed in dBm. The value of RSRP is given as Energy per Resource Element (EPRE) in every eNodeB. The unit of EPRE is defined as dBm/15 KHz, which is defined as power per 15 KHz or per RE. RSRQ can be defined as the quality of power received in RE that contains RS. It is an important KPI to assess the quality of received signal. It is defined as follows:

$$RSRQ = N \frac{RSRP}{RSSI} \qquad (4.8)$$

As seen in Equation 4.8, RSRQ is calculated using RSRP and RSSI. This is used as the reference signal by LTE network to make hand-off decision. N is the number of RBs and its value changes depending on the scheduling to the specific user. The CQI report by UE to the eNodeB is vital information used by eNodeB to take critical decisions regarding scheduling. The better the wireless channel, the higher will be the CQI from a UE. This is used to decide modulation formats, packet types, and pre-coding matrix types which affect the throughput delivered to a particular user [50][51].

4.4.2 Test Methodology

The main objective of the testing is to assess the performance of the various parameters of the LTE network with similar test cases and tools. The objective of our testing is:

- To analyse the 4G network measurement in different scenarios.
- To compare the network performance between Operator A and Operator B in a select locations in a huge metropolitan city.

LTE capable UE is used in real LTE network for all the test cases. All test cases where performed in 10 MHz LTE network. The tests were carried out in sub-urban environment. Testing consists of several scenarios such as walk test in urban city centre, drive testing in car, train testing while travelling in train and indoor testing inside the international airport. The LTE UE is connected to laptop and logs were collected using Nemo RF tool. The speed of the test UE was not controlled. The testing was designed in such a way that

testing scenarios reflect the user behaviour closed to the real world scenario as much as possible.

4.4.3   Test Scenarios

To verify LTE network performance, two service providers were selected: Operator A and Operator B. The below tests were performed as close as possible over the same routes and areas to provide an accurate performance comparison between Operator A and Operator B. In the real-time testing, scenarios considered for testing are:

- Walking test: Data was collected by walking around city centre.
- Train test: Data was collected whilst travelling in a train.
- Driving test: Data was collected by driving in a car.
- Indoor test: In order to test the performance inside the International Airport.

In our testing, the same script was used to test the various transmissions in different LTE environments.

The script includes:

- FTP transfer
- HTML Browsing
- Send SMS

4.4.4   Introduction to Nemo Test Tool

The testing is carried out by using Nemo hand held drive test tool. Nemo supports various technologies such as GSM, CDMA, EVDO, WCDMA, HSPA, HSPA+, LTE and Wi-Fi. It supports measuring and monitoring of QoS/QoE of various applications. The script to monitor and record various QoS parameters for voice call, SMS and HTTP accessing can be modified as per test case design. The interface options used in the testing:

- Carrier RSSI - values ranging from -140 to -10
- Serving SNR - Displays the SNR (signal to noise ratio) for the serving channel in db.

- Serving RSRQ - Displays the reference signal received quality for the serving channel in db. Range -30 to 0.

- Serving RSRP - Displays the reference signal received power for the serving channel in dBm. Range -140 to 0.

As previously stated, Nemo Handy allows the user to monitor and record measurements in different situations by creating scripts. Scripts can automate various features that include: voice call, text message, video streaming, HTTP accessing, etc. The files created from Nemo Handy is analysed using the Nemo outdoor analysis tool that can support over 280 terminals.

4.4.5 Experiments and Results

4.4.5.1 Experiment 1 – Walk test:

This test was conducted while walking in city centre, in the heart of the city. Table 4.8 and Table 4.9 provide KPI measurements of RSRP, RSRQ, RSSI and uplink/ downlink throughput (with minimum, maximum and average) for both Operator A and Operator B respectively.

Table 4.8: Operator –A KPI Measurement – Walk Test

Measurement parameter	Min value	Max value	Average
RSRP (dBm)	-109.3	-68.1	73.34
RSRQ	-22.6	-1.4	-6.7
RSSI	-82.9	-37.36	-58.6
Throughput in DL (bits/s)	0	320000	
Throughput in UL (bits/s)	0	1064000	

Table 4.9: Operator – B KPI Measurement – Walk Test

Measurement parameter	Min value	Max value	Average
RSRP (dBm)	-117.8	-64.2	-91
RSRQ	-23.3	-0.1	-12.2
RSSI	-90.2	-33.6	-70.2
Throughput in DL (bits/s)	0	280000	
Throughput in UL (bits/s)	0	1032000	

Figure 4.3: Operator A – Walk Test – Line Graph

Figure 4.4: Operator B – Walk Test – Line Graph

Table 4.10: Operator A walk test – Link Adaptation Table

Parameters	Reported value	Comments
Rank	3	Shows that three transmission layers are configured in serving eNodeB
Transmission standard	FDD	Two carrier frequencies were used, one for uplink and one for downlink transmission
Modulation type	QPSK	QPSK technique was used in air interface.
MCS index	up to 9	Up to 9 MCS index values were used and each value of MCS index matches with different modulation and coding schemes
Antenna port used	Port 0, Port 1	Two antenna ports were used in serving eNB to support MIMO transmission.

Table 4.11: Operator B walk test – Link Adaptation Table

Parameters	Reported value	Comments
Rank	3	Shows that three transmission layers are configured in serving eNodeB
Transmission standard	FDD	Two carrier frequencies were used, one for uplink and one for downlink transmission
Modulation type	QPSK, 16 QAM, 64 QAM	Three techniques were used in air interface.
MCS index	up to 27	Up to 27 MCS index values were used and each value of MCS index matches with different modulation and coding schemes
Antenna port used	Port 0, Port 1	Two antenna ports were used in serving eNB to support MIMO transmission.

Performance of Operator A in city centre was better than Operator B in terms of quality of received signal strength. The RSSI indicates effective signal to noise ratio, the average RSSI for Operator B is higher compared to Operator A, which indicates that quality of received signal in Operator A is better than Operator B. On the other hand, high RSRQ for Operator B indicates frequent hand-off while walking in city centre. During the test it was observed that, Operator A is using two ports (Port 0 and Port 1) in antenna to support MIMO in eNodeB. The benefit of using MIMO was evident in the KPIs. Figure 4.3 and Figure 4.4 indicate the line graph for walk test for Operator A and Operator B. Table 4.10 and Table 4.11 indicate the link adaptation table for the test.

4.4.5.2 Experiment 2 – Train Test:

This test was conducted while travelling in train from Station A to Station B. In the tables, it shows that for most of the time, the serving RSRP and RSRQ of Operator A maintains high level of network quality and coverage. However, the serving signal power reduces to -115 from -90 dBm inside a tunnel near the railway station. On the other hand, the

network coverage for Operator B varies between -74.4 dBm to -131.6 dBm. The variation in RSRQ of Operator B is higher than Operator A which resulted in more handoff. Figure 4.5 and Figure 4.6 indicate the train test for Operator A and Operator B. Table 4.12 and Table 4.13 indicate the KPI measurement for the test. Table 4.14 and Table 4.15 indicate the link adaptation table for the test.

Table 4.12: Operator – A KPI Measurement – Train Test

Measurement parameter	Min value	Max value	Average
RSRP (dBm)	-109.1	-65.2	-95.4
RSRQ	-14.3	-0.3	-6.3
RSSI	-82.4	-41.1	-59.8
Throughput in DL (bits/s)	0	280000	
Throughput in UL (bits/s)	0	142857	

Table 4.13: Operator – B KPI measurement – Train test

Measurement parameter	Min value	Max value	Average
RSRP (dBm)	-131.6	-74.4	-96.5
RSRQ	-25.2	-4.7	-14.9
RSSI	-94.3	-43.4	-70.2
Throughput in DL (bits/s)	0	280000	
Throughput in UL (bits/s)	0	1032000	
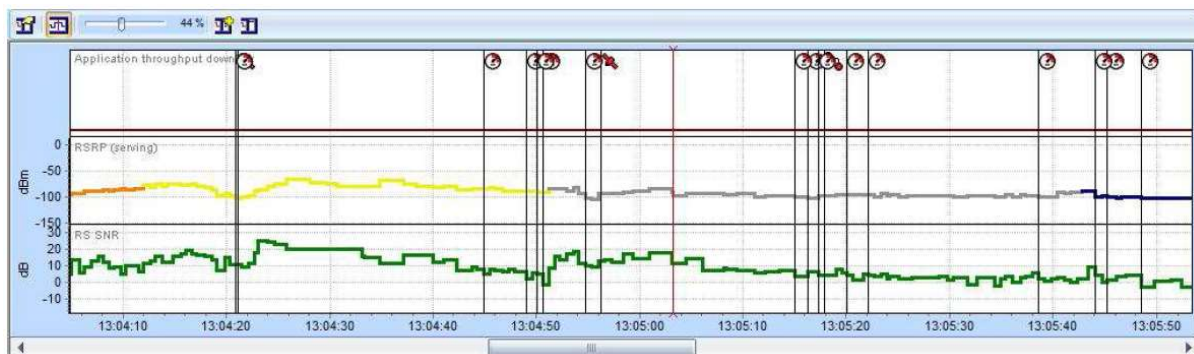
Figure 4.5: Operator A – Train Test – Line Graph

Figure 4.6: Operator B – Train Test – Line Graph

Table 4.14: Operator A Train test – Link Adaptation Table

Parameters	Reported value	Comments
Rank	3	Shows that three transmission layers are configured in serving eNodeB
Transmission standard	FDD	Two carrier frequencies were used, one for uplink and one for downlink transmission
Modulation type	QPSK, 16 QAM, 64 QAM	Three techniques were used in air interface.
MCS index	up to 19	Up to 19 MCS index values were used and each value of MCS index matches with different modulation and coding schemes
Antenna port used	Port 0, Port 1	Two antenna ports were used in serving eNB to support MIMO transmission.

Table 4.15: Operator B Train Test – Link Adaptation Table

Parameters	Reported value	Comments
Rank	3	Shows that three transmission layers are configured in serving eNodeB
Transmission standard	FDD	Two carrier frequencies were used, one for uplink and one for downlink transmission
Modulation type	QPSK, 16 QAM, 64 QAM	Three techniques were used in air interface.
MCS index	up to 28	Up to 28 MCS index values were used and each value of MCS index matches with different modulation and coding schemes
Antenna port used	Port 0, Port 1	Two antenna ports were used in serving eNB to support MIMO transmission.

4.4.5.3 Experiment 3 – Drive Test in a Car Inside The City

This test was performed while moving inside the city. The red patches in the Figure 4.7 for Operator A indicate that serving power was unstable in certain locations. Throughout the test, the majority of time signal quality was high to maintain high performance in terms of throughput. For Operator B, the received signal strength was better than Operator A and the quality of the link was similar to Operator A. At the same time, RSRP for Operator A is better than Operator B which indicates that Operator-A has less noise in the signal than Operator B from neighbouring cells. The same is reflected in RSRQ as well. This indicates that to boost the quality of the received signal, appropriate cell planning is the right strategy rather than increasing the number of eNodeBs. Figure 4.7 and Figure 4.8 indicate the drive test for Operator A and Operator B. Table 4.16 and Table 4.17 indicate the KPI measurement for the test. Table 4.18 and Table 4.19 indicate the link adaptation table for the test.

Table 4.16: Operator – B KPI Measurement – Drive Test in Car

Measurement parameter	Min value	Max value	Average
RSRP (dBm)	-110.9	-75.1	-82
RSRQ	-13.8	-0.3	-6.5
RSSI	-94.4	-30.4	-69.3
Throughput in DL (bits/s)	0	248000	
Throughput in UL (bits/s)	0	299200	

Table 4.17: Operator – B KPI measurement – Drive Test in Car

| Measurement parameter	Min value	Max value	Average
RSRP (dBm)	-131.6	-74.4	-96.5
RSRQ	-25.2	-4.7	-14.9
RSSI	-94.3	-43.4	-70.2
Throughput in DL (bits/s)	0	280000	
Throughput in UL (bits/s)	0	1032000	

Figure 4.7: Operator A – Drive Test in Car – Line Graph
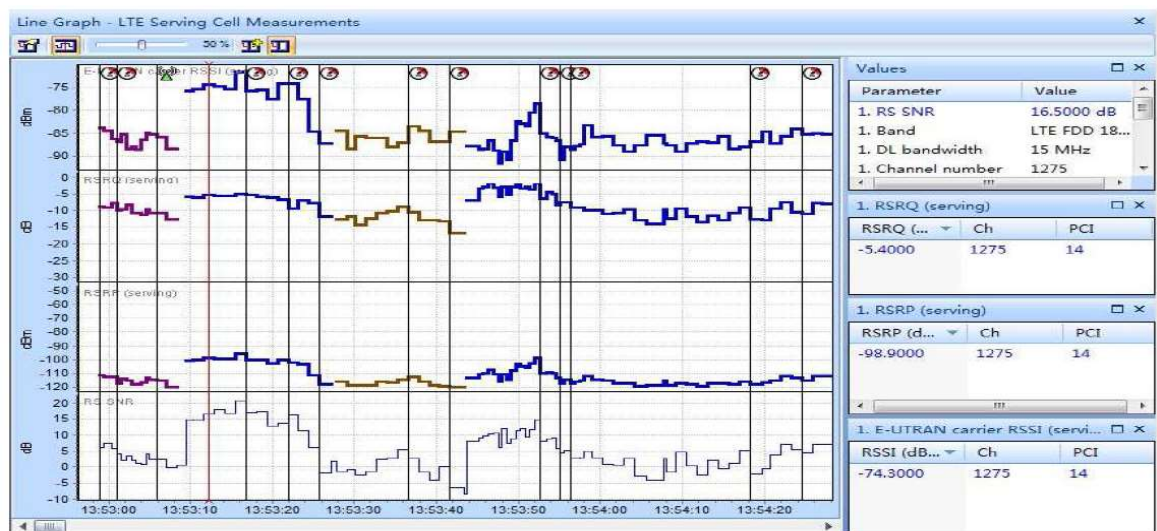
Figure 4.8: Operator B – Drive Test in Car – Line Graph
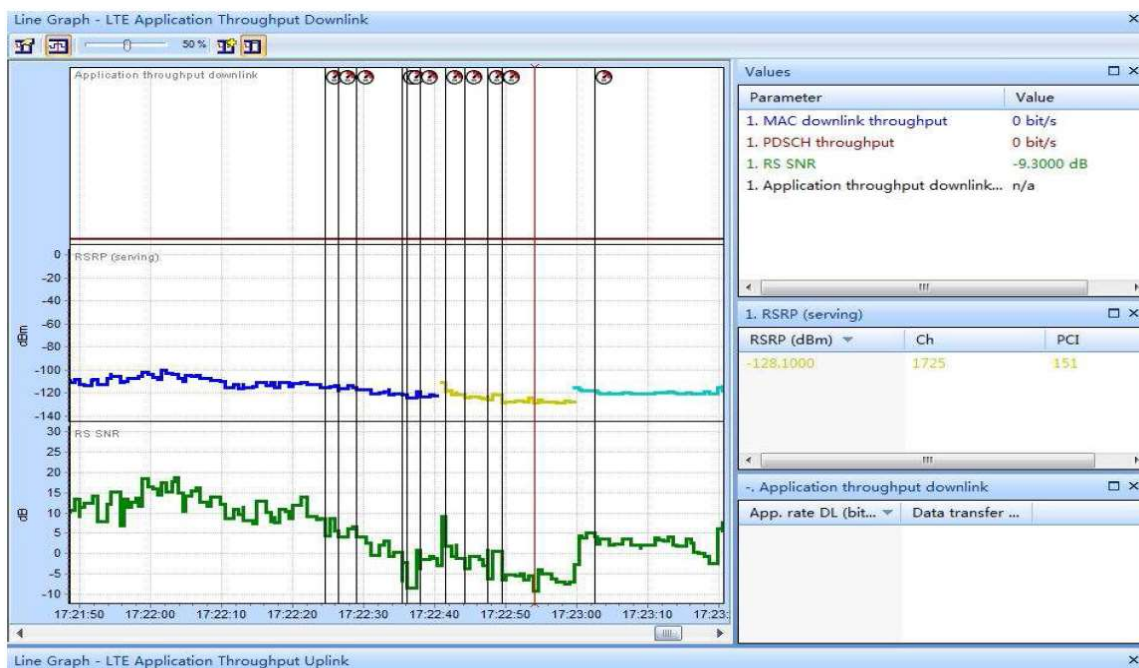
Table 4.18: Operator A Drive Test in a Car – Link Adaptation Table

Parameters	Reported value	Comments
Rank	3	Shows that three transmission layers are configured in serving eNodeB
Transmission standard	FDD	Two carrier frequencies were used, one for uplink and one for downlink transmission
Modulation type	QPSK, 16 QAM, 64 QAM	Three techniques were used in air interface.
MCS index	up to 20	Up to 20 MCS index values were used and each value of MCS index matches with different modulation and coding schemes
Antenna port used	Port 0, Port 1	Two antenna ports were used in serving eNB to support MIMO transmission.

Table 4.19: Operator A Drive Test in a car – Link adaptation table

Parameters	Reported value	Comments
Rank	3	Shows that three transmission layers is configured in serving eNodeB
Transmission standard	FDD	Two carrier frequencies were used, one for uplink and one for downlink transmission
Modulation type	QPSK, 16 QAM, 64 QAM	Three techniques were used in air interface.
MCS index	up to 27	Up to 27 MCS index were used and each value of MCS index matches with different modulation and coding schemes
Antenna port used	Port 0, Port 1	Two antenna ports were used in serving eNB to support MIMO transmission.

4.4.5.4 Experiment 4 – Indoor Testing – Inside the Airport

This test was conducted inside the international airport. The user remained stationary during the test. Since, it is an airport setting, there was constant movement of people and trolleys around the test user. Apart from this, airport is a closed environment with metal and glass structures which may affect the quality of the received signal. The impact of structures and reflections is evident in Table 4.20 for Operators A. The average RSSI is higher compared to RSRP which indicates that the noise level in the signal is high because of reflections and absorptions. Similar behaviour is observed in Operator B (Table 4.21). Hence, appropriate planning is required to negate the impacts of reflections and absorptions emanating due to the building structures. Figure 4.9 and Figure 4.10 indicate the indoor testing for Operator A and Operator B. Table 4.22 and Table 4.23 indicate the link adaptation table for the test.

Table 4.20: Operator – A KPI Measurement – Indoor Testing

| Measurement parameter	Min value	Max value	Average
RSRP (dBm)	-100	-112	-105
RSRQ	-5.4	16.3	-7.9
RSSI	-71.6	-93.9	85.3
Throughput in DL (bits/s)	0	248000	
Throughput in UL (bits/s)	0	112000	

Table 4.21: Operator – B KPI Measurement – Indoor Testing

Measurement parameter	Min value	Max value	Average
RSRP (dBm)	-122.4	-111.2	116.4
RSRQ	-28.2	-7.1	-17.65
RSSI	-94.7	-80.9	-86.2
Throughput in DL (bits/s)	0	232000	
Throughput in UL (bits/s)	0	218000	

Figure 4.9: Operator A – Indoor Testing – Line Graph
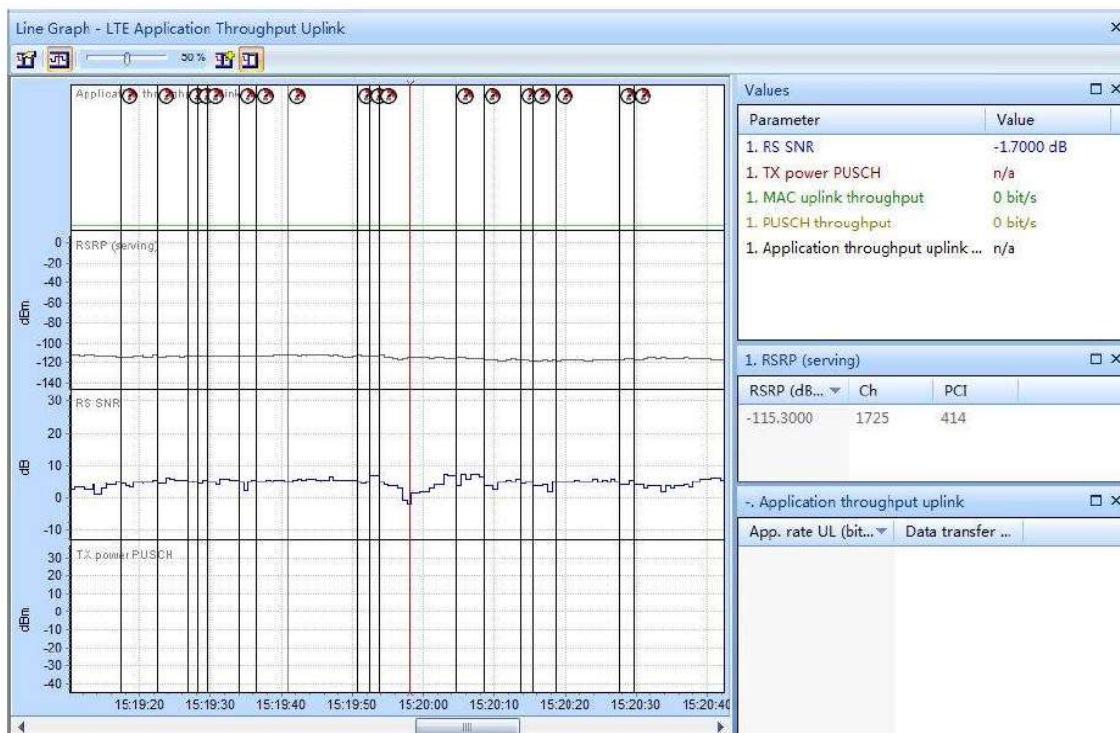
Figure 4.10: Operator B – Indoor Testing – Line Graph

Table 4.22: Operator A Indoor Testing – Link Adaptation Table

Parameters	Reported value	Comments
Rank	3	Shows that three transmission layers are configured in serving eNodeB
Transmission standard	FDD	Two carrier frequencies were used, one for uplink and one for downlink transmission
Modulation type	QPSK	Only one modulation technique was used in air interface.
MCS index	up to 8	Up to 19 MCS values index were used and each value of MCS index matches with different modulation and coding schemes
Antenna port used	Port 0, Port 1	Two antenna ports were used in serving eNB to support MIMO transmission.

Table 4.23: Operator B Indoor Testing – Link Adaptation Table

Parameters	Reported value	Comments
Rank	3	Shows that three transmission layers are configured in serving eNodeB
Transmission standard	FDD	Two carrier frequencies were used, one for uplink and one for downlink transmission
Modulation type	QPSK, 16 QAM, 64 QAM	Three techniques were used in air interface.
MCS index	up to 19	Up to 19 MCS index values were used and each value of MCS index matches with different modulation and coding schemes
Antenna port used	Port 0, Port 1	Two antenna ports were used in serving eNB to support MIMO transmission.

4.5 Summary

In the first part of the chapter, the performance analysis of PF algorithm in a real time single cell LTE network was performed. In this testing, slightly modified PF metric was adopted to analyse the performance of PF scheme. This approach supports the relationship between the transmission rate and SNR. In this performance analysis of PF algorithm, practical approach has been considered. The users were classified as Gold, Silver and Bronze based on the service subscription. A combination of various scenarios was tested as specified in Table 4.1. Since, the performance analysis was carried out in a real-time network, the factors affecting the throughput were not considered separately as in [11]. It is assumed that all the factors affecting the throughput will be at play in practical environment.

In the second part of the chapter, performance analysis of LTE RAN of two leading service providers was made. The testing was performed in various locations and in various modes such as walking around the city centre, travelling in train, driving in the car and in indoor environments. The main similarity between the Operator A and Operator B was that both were using 1800 frequency band and both were using FDD-LTE. According to the drive test results, we can conclude that the performance of Operator A in all test scenarios was better than Operator B (Table 4.24). Operator A's performance was much stable in high speed condition. However, the received signal strength for Operator A can be enhanced inside the indoor (airport) condition. For Operator B, the performance of the LTE network was stable in the CBD area and in the train. But the performance degraded while driving in the car in an urban environment. Furthermore, the Operator A and Operator B did not have sufficient coverage inside tunnels and underground passages.

Table 4.24: KPI summary between operators

Service Provider	CBD	Train	Driving	Indoor
RSRP				
Operator A	-73.34	-95.4	-82	-105
Operator B	-91	-96.5	-103.1	-116.4
RSRQ				
Operator A	-6.7	-6.3	-6.5	-7.9
Operator B	-12.2	-14.9	-15.1	-17.65
RSSI				
Operator A	-58.6	-59.8	69.3	-85.3
Operator B	-70.2	-75.3	-77.3	-86.2

The performance analysis enables us to analyse the performance of service providers. Another important point which was realised during the testing is the need for context aware simulation parameters. As the technologies continuously evolve from 2G to present LTE some of the simulation parameters have remained the same and this approach must be revisited. Some of the simulation parameters usually considered for packet scheduling are simulation time, flow duration, slot duration, TTI, number of OFDM symbols/slots, cell radius, eNodeB transmit power (macro and micro), user speed, VoIP bit rate, video bit rate, frame structure, number of eNodeB, no of subcarrier/RBs, and subcarrier spacing. But the context of the user is not considered. As seen in this benchmarking study four different contexts were considered which may result in different performance for the same tests. Some of the contextual scenarios that can be considered in future such as travelling in tunnel, modelling interference from non-cellular sources, harmonics, relative movements of mobile and surrounding environments, speed of the relative movements and many more are required to simulate near practical environment to study the performance of packet scheduling algorithms. Context aware parameters are required in simulation especially for 5G where densification, small cells, low power cells, high frequencies are expected to be used.

5. PERFORMANCE ANALYSIS OF REAL-TIME LTE NETWORKS - EPC

In this chapter, as a continuation of the previous chapter, performance analysis of LTE EPC has been presented. EPC stands for Evolved Packet Core and it is a complete packet core unlike in 2G and 3G systems where CS was involved in call setup procedure. The GSM architecture relies on CS to establish call between called and calling parties. In GPRS, the concept of duality was added to the core network comprising of both CS and PS. The voice was transported by CS core and data was transported in PS core and this duality was maintained in 3G systems. In LTE, the CS core was completely replaced by PS core. During the standardization process of LTE, it was decided to use IP as the key protocol to transport all services. Hence, it was decided to evolve EPC as packet core and not to have circuit switched domain that was used in GSM, GPRS, and 3G. This performance analysis was based on real time LTE network. Due to confidentiality, the service provider's network structure is not explained. The KPIs obtained from the real time network are analysed in forthcoming sections. An important issue was identified in course of the analysis and subsequently resolved. The strategy to resolve the issue is discussed. Figure 5.1 illustrates end to end LTE network architecture along with EPC [52-56][58].
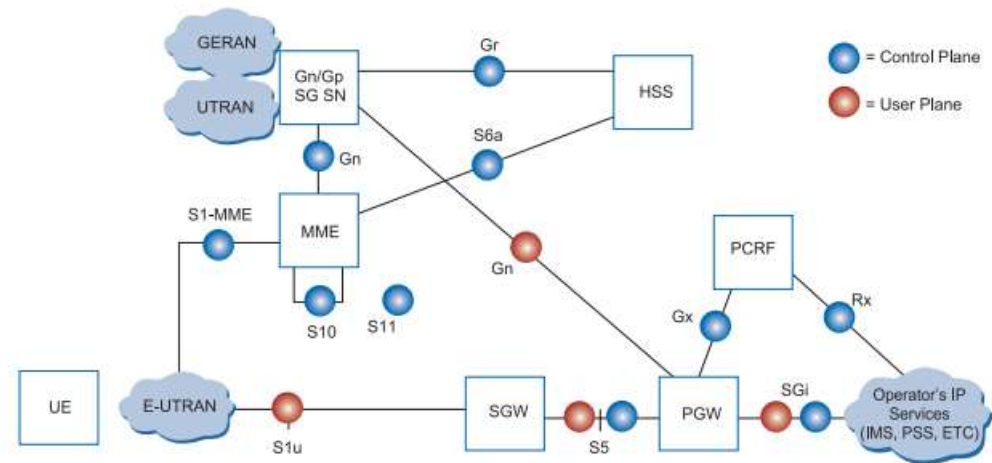
Figure 5.1: End to end LTE network components [52]

5.1 Architecture of EPC

Figure 5.2 illustrates a simple LTE EPC architecture.
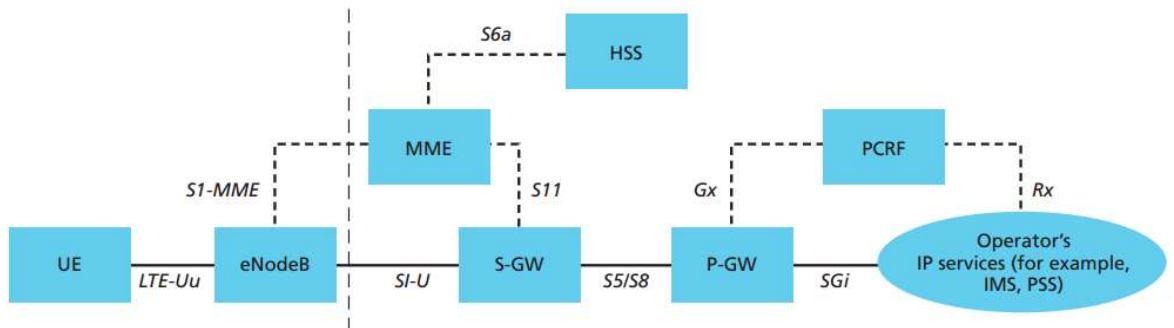
Figure 5.2: LTE EPC architecture [52]

The other components of EPC architecture such as Earthquake and Tsunami Warning System (ETWS), Equipment Identity Register (EIR) and Policy Control and Charging Rules Function (PCRF) are not shown in the figure.

The Core Network (CN) comprise of several logical nodes such as HSS, MME, SGW, and PGW. These logical nodes are connected by means of standardized interfaces namely as S1-MME, S1-U, S11, S5/S8, and S6a. The CN is connected to external PDN gateway through SGi interface. Thanks to 3GPP standardization of interface which provides the

service providers an opportunity to source nodes from different vendors to help check cost and complexity. The standardization efforts have provided the service providers to split or merge these logical nodes depending on commercial considerations. The Figure 5.3 illustrates the functional split between E-UTRAN and EPC network elements. The network elements are described in detail in forthcoming sections [1].
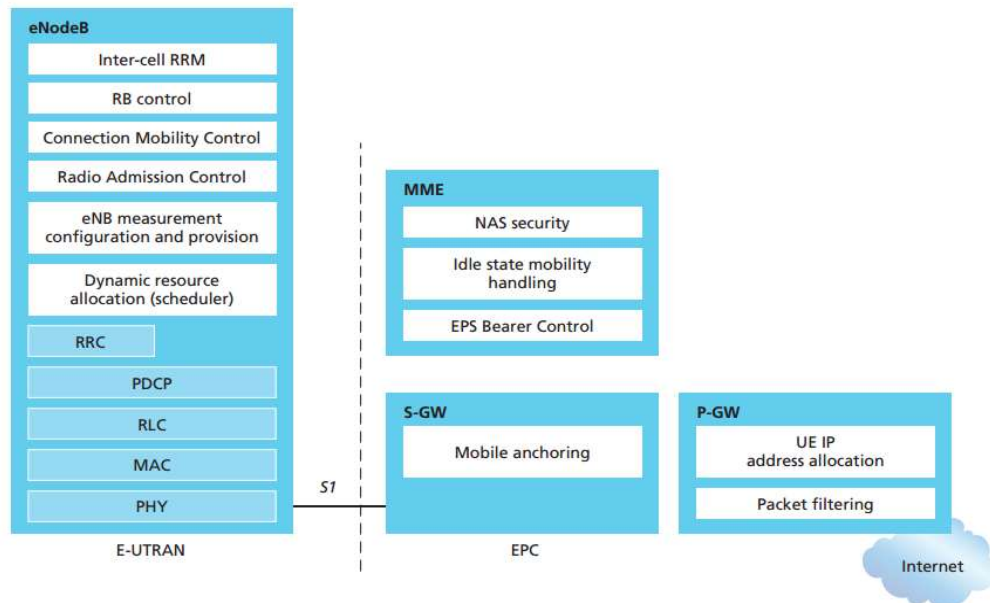
Figure 5.3: Functional split between E-UTRAN and EPC [52]

5.1.1   LTE Core Network Elements

The CN in LTE, which is known as EPC in SAE, is responsible for overall control of LTE network. Hence, the word CN and EPC will be used interchangeably in this chapter. It is responsible for the control of UE and bearer establishment procedure. The main logical nodes in EPC are:

- PDN Gateway (PGW)
- Serving Gateway (SGW)
- Mobility Management Entity (MME)

Apart from the above nodes, LTE CN includes HSS, PCRF, and the IMS which controls IP multimedia applications such as VoIP. The IMS is considered to be outside the EPC [1].

The logical nodes shown in Figure 5.2 are discussed in detail below:

- PCRF: This node is responsible for policy control and decision making as well as controlling flow-based charging functionality in Policy Control Enforcement Function (PCEF).

- HSS: HSS is similar to traditional Home Location Register (HLR). It consists of user details, subscription profile, and access restriction. It holds PDN information in the form of APN or PDN address to which PDNs the users can connect. In addition to this, HSS holds information such as the identity of MME to which the user is registered. The AUC, that generates vector authentication security keys, is integrated to HSS in most deployments [1].

- PGW: The PGW allocates IP address to UEs and enforces QoS and flow based charging according to PCRF rules. PGW comprises of Traffic Flow Templates (TFT) and based on which downlink IP packets are filtered into different QoS based bearers. It performs QoS enforcement for Guaranteed Bit Rate (GBR) bearers. It serves as an anchor to non-3GPP technologies such as CDMA 2000 and WiMAX [1].

- SGW: It serves as local mobility anchor where all users IP packets are transferred through SGW when the user moves from one eNodeB to another. The bearer information of a UE is retained in SGW when UE is in idle state and buffers downlink data temporarily while MME initiates paging to UE to re-establish the bearers. It plays an important role in roaming where it collects information for charging regarding volume of data sent or received by the user in the visited network. It is responsible for lawful interception and serves as mobility anchor to other 3GPP technologies such as GPRS and UMTS [1].

- MME: It is responsible for signalling between UE and CN. The protocols running between UE and CN are known as Non Access Stratus (NAS) protocols. The main functionality of MME is to maintain, establish and release of bearers through session management layer in NAS protocol. Apart from that, MME manages the security between UE and network [1].

5.1.2   Non Access Stratum Procedures (NAS)

The NAS procedure in LTE is similar to UMTS except that LTE allows concatenation of procedures for faster establishment of connection and bearers. Immediately after the UE is switched on, MME creates a UE context and attaches to the network. MME assign SAE – Temporary Mobile Subscriber Identity (S-TMSI) to the UE that identifies UE context. The UE context holds details such as subscription information which is downloaded from HSS. Storing UE information locally in UE context reduces bearer establishment time and results concatenation of procedures. To reduce overhead in E-UTRAN and processing in UE, all UE related information in an access network including radio bearers are released to MME. The MME retains UE context and information regarding bearer establishment in idle period. The MME needs to have updated location information of UEs in idle state to find out in which tracking area the UE is located and this procedure is called as Tracking Area (TA) update. MME is responsible to keep track of UEs in idle period. When MME has to send data to an idle UE, it pages all eNodeBs in the current TA over the radio interface. On the receipt of the message, appropriate UE responds to the message, and UE performs Service Request (SR) procedure which results in changing the status of UE from IDLE to CONNECTED [1].

5.2 EPC Performance Analysis

5.2.1   Test Methodology

The performance analysis of EPC was performed using three months of KPIs obtained from real time LTE network. The KPI results discussed in Section 5.2.2 of this chapter are obtained from real-time LTE network. Due to confidentiality, the network design of the service provider is not disclosed. The testing involved various EPC components such as MME, SGW, and PDN-GW together with eNodeB.

5.2.2   KPI Results and Discussion

To analyse the performance of EPC, KPIs such as accessibility, retainability, traffic, mobility, and Automatic Neighbour Relation (ANR) KPIs were analysed based on [53-58].

5.2.2.1 Accessibility

Accessibility success rate determines whether an end user can access the service. If an end user is unable to access the network, then end user may not get the service provided by the service provider and this may lead to end user changing the service provider. This may result in loss of income to the service provider. Hence, providing users a good accessibility to the service is critical from business perspective. This KPI assists the service provider to understand the accessibility provided to the end user. The accessibility of end user covers wide area including E-UTRAN and EPC. Hence, it is necessary to realize that E-UTRAN's KPI shall indicate the performance of the parts controlled by E-UTRAN and not the whole end-to-end service accessibility. The KPIs provided by E-UTRAN for accessibility are defined as E-RAB. The accessibility success rate is defined as percentage of success rate for the attempts. The accessibility success is defined as the ability of eNodeB to inform the requester about the successful completion of setup task by setting up resources resulting in E-RAB establishment. Accessibility is the first setup in providing end-user services to make sure that the user gets access to the system.
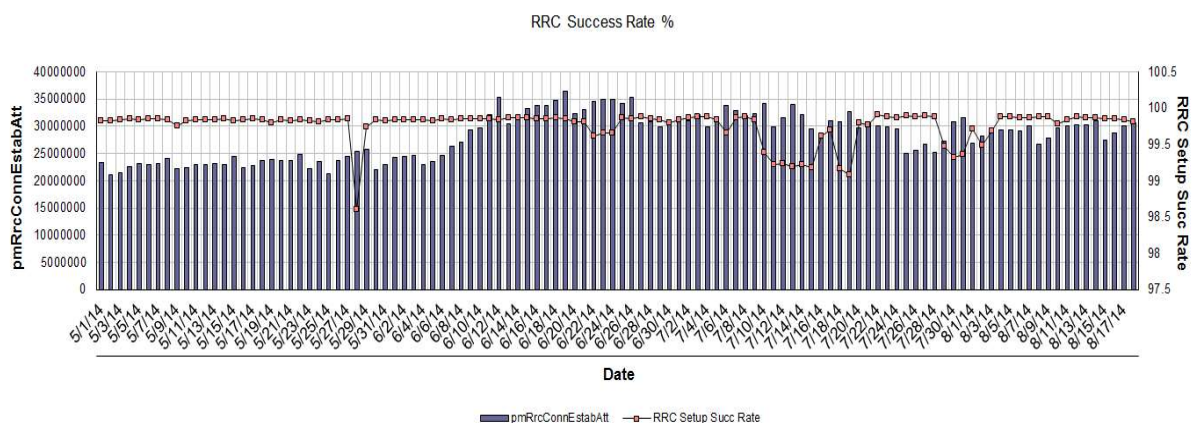
Figure 5.4: RRC success rate in percentage
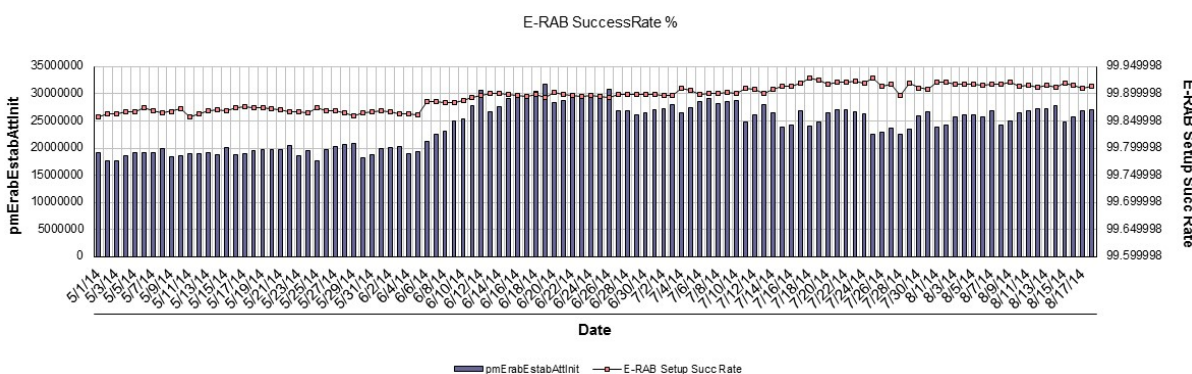
Figure 5.5: E-RAB success rate in percentage

The graphs are obtained from the data collected for three months. Figure 5.4 shows RRC success rate and E-RAB success rate in Figure 5.5. The similarity of peaks in the graphs in both the figures establishes the fact that the control plane (RRC) traffic is appropriately complemented with user plane (E-RAB) traffic. The percentage of success (99.5 % in both figures) indicates that end user accessibility was excellent in the network and a user could access to the service provided by the service provider. As seen in the graphs, accessibility KPI displayed an increase of 40 % in accessibility request in the month of June and July. The reason to this increase was attributed to increased retainability drops in the Figure 5.6.

5.2.2.2 Retainability

Retainability is defined as the ability to retain the established service for the end user. If the service to end user is interrupted or if it is aborted during use, the service provider

may find it hard to charge the subscriber for the time service was not available. If the interruption occurs often, then end user might change the service provider. Hence, good retainability is critical for service provider to retain the end user from business perspective. This KPI assist service provider with the statistics about the service offered to the end user. The retainability covers wider area including E-UTRAN and EPC. The KPIs shown in Figure 5.6 and Figure 5.7 provide E-UTRAN and CN (EPC) retainability. The KPI indicating E-RAB defines retainability offered in E-UTRAN. It is often required to keep E-RAB alive for long period than they are used for transmitting data because of the availability of Discontinuous Reception (DRX).
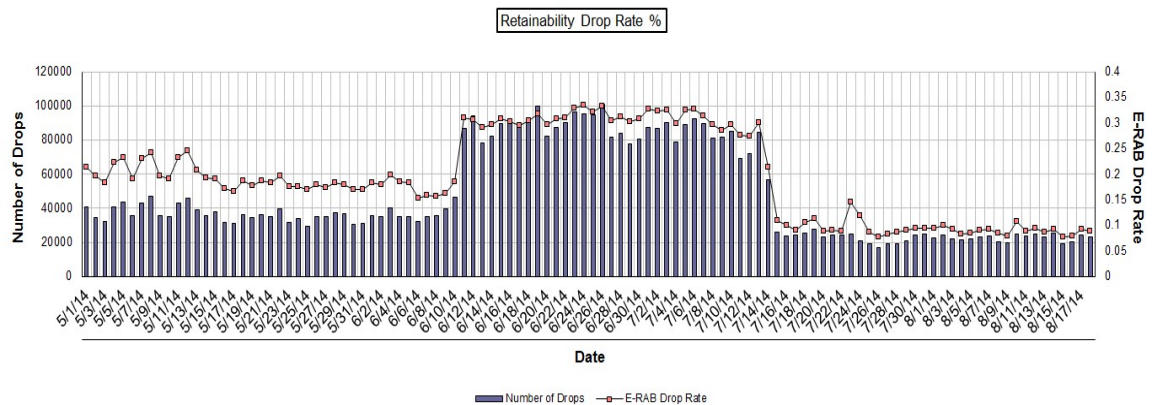
Figure 5.6: Retainability drop rate in %
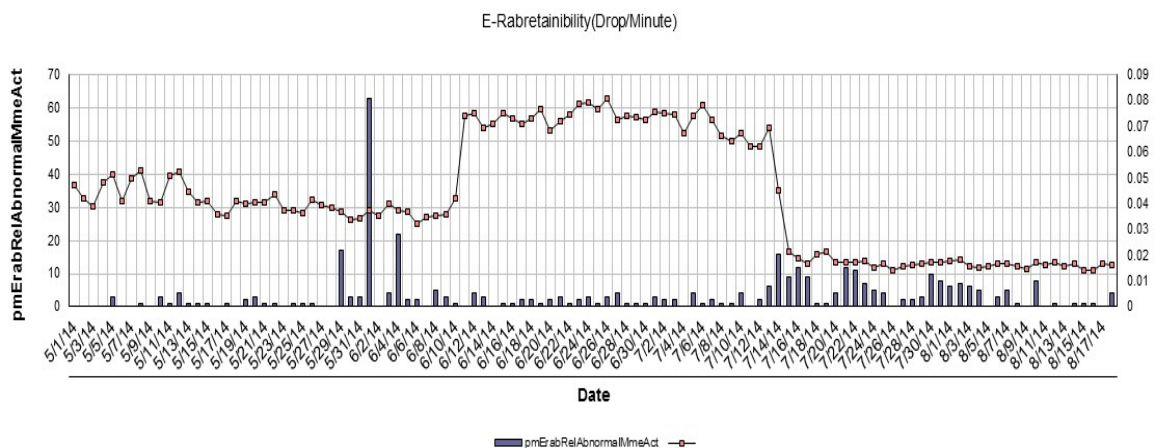
Figure 5.7: E-RAB-Retainability (Drop/Minute)

116

The noticeable aspect of the graph is the stats between the months of June to July. The graphs indicate high number of abnormal release between June and July. If the graphs of accessibility and retainability are correlated, the resulting increase in accessibility is due to high number of drops between June and July and the end user experienced high level of service drops during that period. The immediate analysis of the stats points out that MME releases connection abnormally and this leads to further investigation of traffic data to identify the source of the issue in MME.

5.2.2.3 Traffic and Mobility Analysis

The Figure 5.8 and 5.9 illustrates the data volume in UL and DL. The statistics show that the data volume was not impacted. The level of data volume has been maintained at approximately constant throughout the observation period.
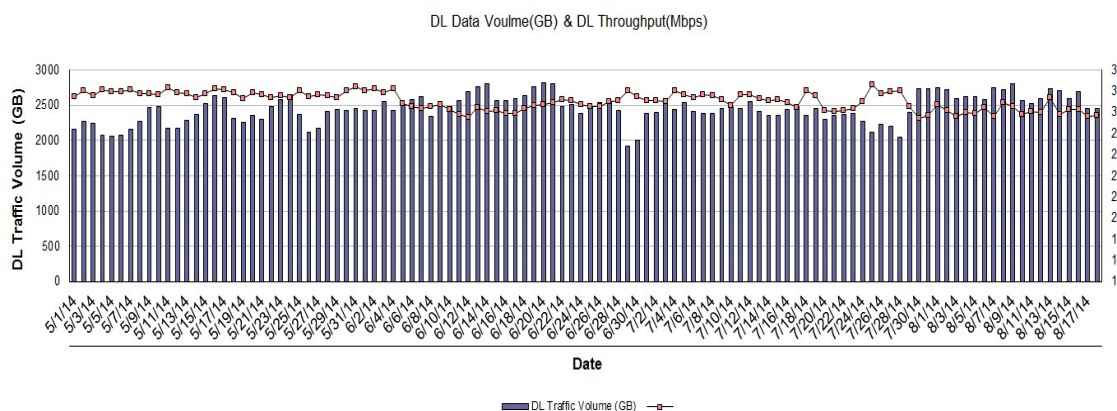
Figure 5.8: DL data volume (GB) and DL throughput (Mbps)
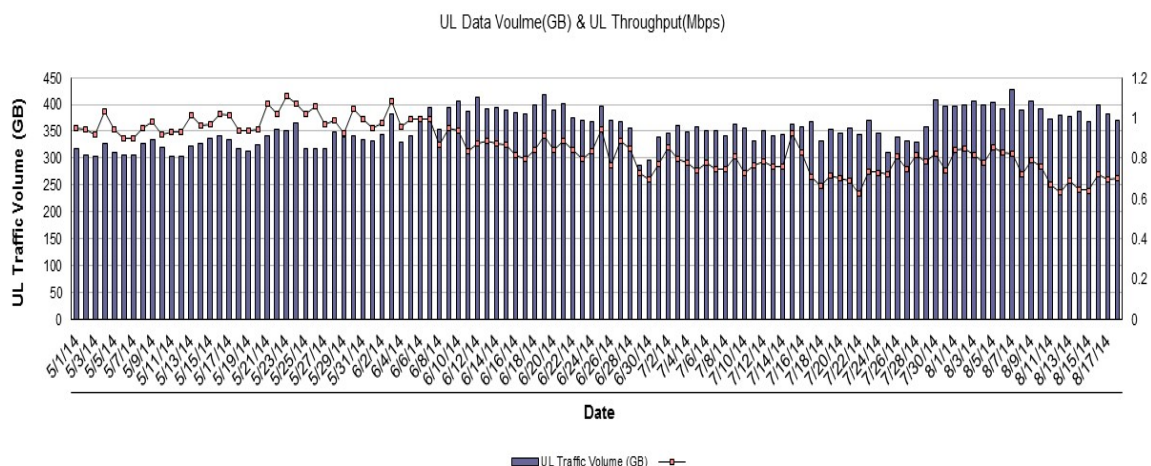
Figure 5.9: UL data volume (GB) and UL throughput (Mbps)

For in-depth analysis of retainability issue, mobility statistics was observed for the same period. Figure 5.10 illustrates handover success rate. The statistics include both Execution and Preparation Phase of handovers. In Preparation Phase in handover, eNodeB prepares resources in neighbouring cell for an UE which it is servicing currently. After Preparation Phase, the UE enters Execution Phase. In Execution Phase, the real handover takes place. The success of Execution Phase is defined as the time at which source eNodeB receives information that UE is successfully connected to the target eNodeB.
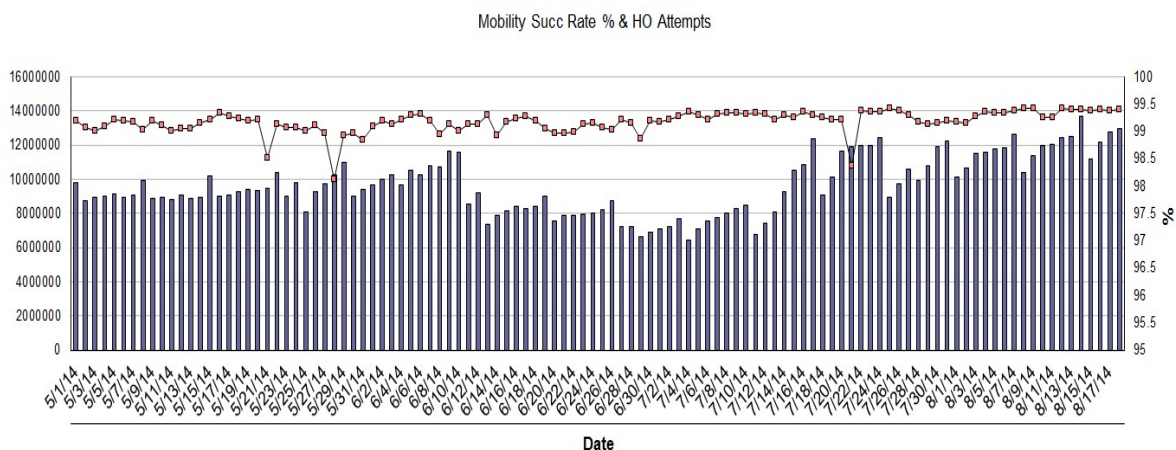
Figure 5.10: Handover success rate %

As shown in the Figure 5.10, the handover statistics show a significant dip in the month of June and July. This indicates the fact that when end user is trying to move from one

eNodeB to another eNodeB, the service gets dropped. Hence, further investigation was performed to identify the reasons for the failures in handover.
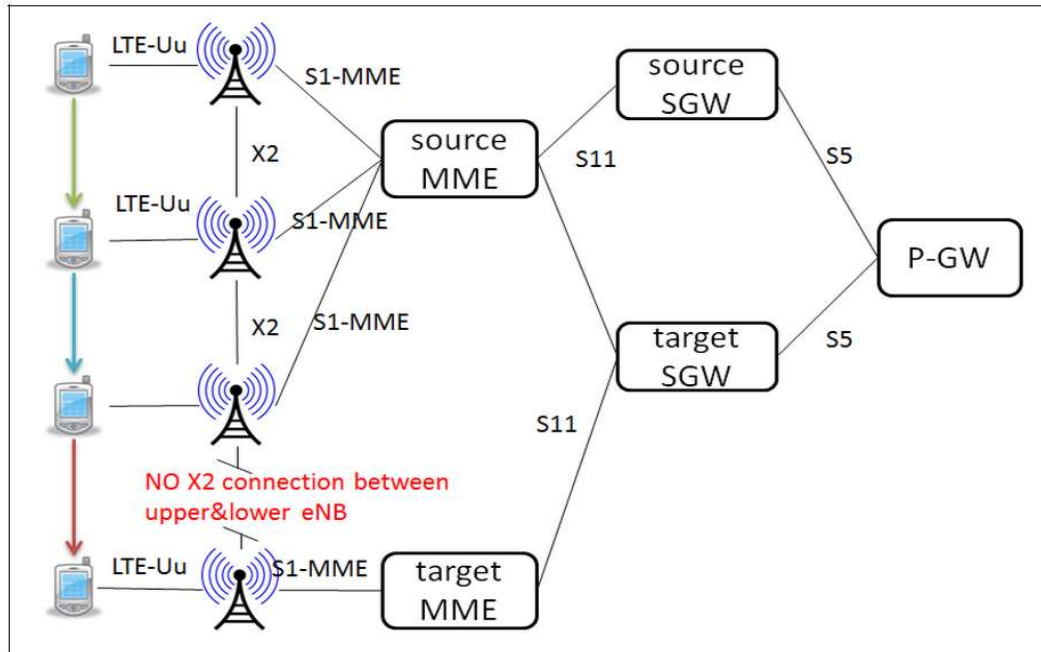
Figure 5.11: S1 handover scenario

In Execution Phase as shown in Figure 5.11, the *pathswitchrequest* message is sent from the target eNodeB to MME. In return, MME acknowledges eNodeB through *pathswitchaccept* and SGW relocation messages. The SGW relocation message is used to indicate eNodeB to relocate to new SGW for handover if multiple SGW servers are configured. However, in the test network only one SGW was configured. Ideally MME must be aware of the number of SGW configured and based on that information it should send SGW relocation message. However, in this case MME was not able to identify how many SGW was configured and hence, resulted in fake SGW relocation message. This fake SGW relocation message had resulted in a handover failure and hence, RRC release message was triggered affecting the retainability of the system. This can be observed in Figure 5.6 and Figure 5.7. This fake SGW relocation and subsequent handover failure was a critical issue which was identified for the UE trying to perform handover from source eNodeB to target eNodeB using X2 interface configured between the eNodeBs. The X2 handover is performed to handover UE from serving eNodeB to target eNodeB within the same MME. The target eNodeB sends *pathswitchrequest* message (including E-UTRAN Cell Global Identifier (ECGI) of the target cell and EPS bearers) to MME to

inform that UE has changed the cell. The MME is responsible for selecting the new SGW, since MME knows the service area of the UE to the TA granularity. This issue was identified in the performance analysis test of EPC network. To resolve the issue there are 3 ways to address this problem:

- Software upgrade in the Core is required to not to send SGW relocation when configured with the single SGW relocation.

- Introduce a patch in the eNodeB to ignore the fake request from the MME.

- Introduce a software add in the eNodeB for processing this fake request from the MME.

The third option was chosen, since it is future proof and in case if a real SGW relocation message comes from MME, the eNodeB will start working on the SGW relocation and hence, eNodeB software was upgraded to support the feature known as SGW relocation at X2. After this feature was introduced, the SGW relocation in *pathswitchaccept* message sent by MME to eNodeB was not ignored. Following this fix, stats starting from July 14 started improving and this issue was not observed.

5.2.2.4 Automatic Neighbour Relation (ANR)

In LTE strong emphasis was given to the simplicity of network management under Self Organizing Networks (SON). Several SON user cases were discussed for 3GPP LTE during the standardization process. The main SON feature was proposed in first LTE standard was ANR. ANR is a method of configuring neighbour relations automatically thereby performing handover ably assisted by RRC signalling. This feature is widely used in several deployments across the world. Figure 5.12 illustrates the performance of ANR in the network.
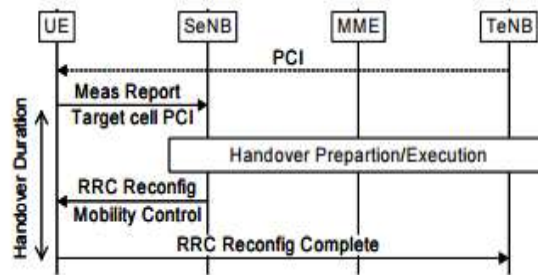
Figure 5.12: RRC signalling support for handover when PCI known

Figure 5.12 illustrates the support of RRC signalling for handover from source eNodeB (SeNB) to a target eNodeB (TeNB) when Physical Cell Identity (PCI) is known and when the neighbour relation is established. The target cell is identified by its PCI and handover is prepared and executed over X2 or S1 informing SeNB about the access information UE use when accessing the TeNB. Figure 5.13 illustrates the RRC support for handover when PCI is unknown sends the measurement report to the UE and UE reports the measurement information to SeNB. Figure 5.13 illustrates the RRC support for handover when PCI identity is unknown to the SeNB. The SeNB requests UE to decode and report Cell Group Identifier (CGI). The SeNB defines the discontinuous transmission cycles during which UE does not require to monitor the SeNB. Alternatively, UE uses autonomous gaps and during that time UE neglects the signalling from SeNB essentially to create a gap for TeNB CGI recovery.
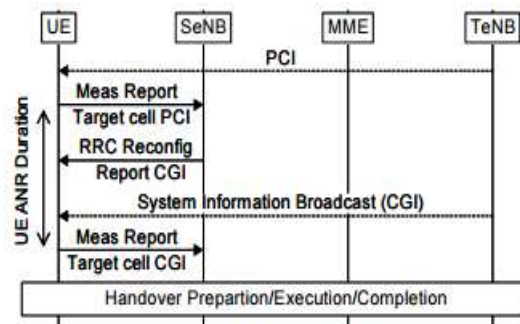
Figure 5.13: RRC signalling support for handover when PCI is unknown
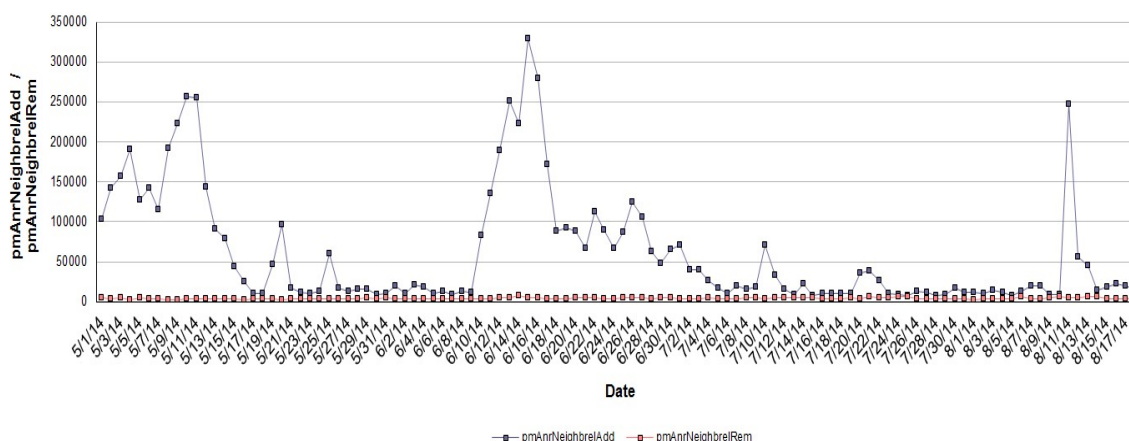
Figure 5.14: ANR statistics

The increased RRC success rate on 13th August as seen in Figure 5.14 illustrates that the increased number neighbours were added to the network. The ANR peaks in the graph are illustrated in Figure 5.14. Every corresponding spike in ANR graph is reciprocated with a similar corresponding spike in RRC success rate.

5.3 Concluding Remarks

In this chapter, performance analysis of LTE EPC network was analysed based on KPIs such as accessibility, retainability, mobility and traffic, and ANR. This performance analysis test helped to identify a critical issue which resulted in increasing the drops and impacting retainability. The issue was identified in MME software handling of SGW relocation resulting fake SGW relocation message sent to eNodeB despite the fact that only one SGW was configured in eNodeB. This issue fake of SGW relocation was fixed by introducing software upgrade in eNodeB. This option was chosen as future proof in case of a real request comes from the MME, eNodeB will start working on the SGW relocation. The eNodeB software was upgraded to support the feature known as SGW relocation at X2. The KPI graphs discussed in various sections played a vital role to understand the impact of this issue and helped to identify the issue. This testing helped to test the robustness of the KPIs and based on the obtained KPIs, the issue in network performance was identified.

6. CONCLUSIONS AND FUTURE RESEARCH DIRECTIONS

This thesis can be divided into three major areas: Firstly, the performance analysis of various scheduling algorithms such as PF, MLWDF and EXP/PF in LTE HetNets environment through simulations. Secondly, performance analysis of PF scheduler in a real time LTE network by segregating the subscribers based on the subscription and thirdly, performance analysis of RAN and EPC of real-time LTE network. Section 6.1 summarises the contribution of this thesis while Section 6.2 discusses relevant studies for future research and finally system implication is discussed in Section 6.2.

6.1 Summary of Thesis Contributions

The contributions made in this thesis are divided into three major areas as follows:

6.1.1 Performance Analysis of Scheduling Algorithms in Simulated LTE Network

A HetNet comprising of macro and pico was simulated using LTE-Sim simulator. In the simulated HetNet environment, performance analysis of different scheduling algorithms was performed. These scheduling algorithms were developed to enhance the LTE network performance by sharing radio resources fairly among users utilizing all available resources. These algorithms depend on the traffic class and number of users. Hence, different outcomes were presented for each algorithm. To further boost the overall system performance, in this simulation small cell such as pico cells were added from 2, 4, 6, 9 and 10 Pico nodes. The effect of this enhancement increases the throughput, reduces PLR, delay and fairness. In the case of throughput, the system gains more data rate while the user suffers less packet loss values in the PLR. Moreover, delay is decreased, and fairness stays similar. As the number of small cell increases, the system manifests more enhancements as seen in 2D and 3D graphs for throughput, PLR, delay and fairness. To

increase system throughput, it is appropriate to keep increasing the number of small cells. However, it is expected that a saturation state will be reached with increasing number of pico cells and the number of users. The reason is ICI will limit the performance since the same carrier frequency is used in all system's cells. Considering all scenarios, MLWDF has the best performance for video flows followed by EXP/PF. In another contribution, to the best of the knowledge LTE-Sim (simulator) has not yet developed any code for HetNets environment comprising of macro and pico cells. The code developed in this section could be considered as an enhancement in the future release of the LTE-Sim.

6.1.2 Performance Analysis of Proportional Fair Packet Scheduling Algorithm in Real Time Network

The PF scheduling algorithm compromises between cell throughput and fairness. In this performance analysis study of PF algorithm user subscriptions are differentiated as Gold, Silver, and Bronze schemes. In each scheme, the users are provisioned with certain bandwidths but apart from the subscription plans, channel condition plays a major role in determining the user throughput. To ensure fairness among users in bad channel conditions and to deliver the provisioned throughputs certain priorities such as 50% of the maximum bandwidth offered by network for Gold subscribers, 25 % of maximum bandwidth to the Silver subscribers and 12 % for Bronze subscribers are attached with the subscriptions In traditional setting in cellular system, fairness was not considered because channels are assigned based on pre-reservation strategies unlike in 4G, where reservation strategies will not serve the purpose. The throughput results obtained in this study was compared to the simulation results and found to be almost similar. Since, the tests were carried out in real time single cell setting factors affecting the throughputs were not considered separately as in the case of simulation because it is assumed that all the throughput limiting factors will be at play in real time single cell.

6.1.3 Performance Analysis of Real Time LTE Network – RAN and EPC

Performance analysis of real time network was carried out. During the performance testing, various KPIs such as throughput, RSRP, RSRQ, and RSSI were observed. The performance testing was carried out in four different scenarios such as walking in city centre, driving in car inside the city, travelling in train and inside the indoor environment. Based on the obtained measurements, the strengths and weakness of the network of both the service providers were analysed and ways to improve the network was discussed. After analysing the performance of RAN, three months of KPIs were analysed to evaluate the performance of accessibility, retainability, mobility, and ANR. Through KPI analysis, an important issue was identified and resolved.

6.2 Future Research Directions

Based on the performance analysis of LTE network and various packet scheduling algorithms performed in this thesis, a number of important issues were identified for future. Some of the issues are briefly discussed as follows:

- As per the study report released by Gartner, 6.4 Billion devices would be connected in 2016, up 30 % from 2015. The growing trend of connected devices is a potential challenge to the cellular system in terms of seamless coverage and scheduling. Hence, a new methodology of predictive performance analysis and benchmarking test is needed. The traditional methodology of performance analysis and benchmarking tests are reactive in nature. Hence, an effective analytics framework must be developed so that performance issue are identified well in advance.

- Predictive analytics of alarm management to improve node availability must be developed. The current alarm management report can provide detail about the nature of the issue and details about the issue. In order to improve node availability, technical issues must be identified well in advance to prevent node downtime. This predictive analytics framework can enhance the way alarm management is being handled at present.

- Centralized packet scheduling algorithm must be developed for HetNets. For example, the current packet scheduling algorithms implemented in macro or pico or femto cells work only in their respective systems and they do not work as centralized algorithm. Hence, if macro cells run out of resources, the users suffer even though pico cells might have un-utilized resources. The approach of centralized packet scheduling algorithm can have the knowledge of resource availability in macro, pico or femto cells and if users are available in the cell edge, these resources can be shared and allocated to these users. This helps in resource sharing among macro, pico or femto cells.

6.3 System Implications

This thesis dealt with four important areas such as (i) performance analysis of various packet scheduling algorithms in simulated LTE heterogeneous network, (ii) benchmarking of real time LTE network, (iii) performance analysis of proportional fair scheduling algorithm in LTE single cell environment, and (iv) interoperability testing of LTE network elements. The contribution of this thesis can benefit vendors and service providers in number of ways. Firstly, the pico cell module was developed in LTE-Sim simulator environment to help vendors to simulate LTE HetNets environment to analyse the performance of various packet scheduling algorithm before commercially rolling out the scheduling algorithm. This is evident from various simulation results presented in Chapter 3. The performance analysis of real-time LTE network results presented in Chapter 4 and 5 can help service providers to understand the issues in the network and help them to resolve it to provide better service to end user. The performance analysis of proportional fair algorithm in single cell environment presented in Chapter 4 helps vendors and service providers to understand how the scheduling algorithms perform in real-time environment. This result can help them to tune the network to achieve better performance.

The performance analysis of proportional fair algorithm discussed in Chapter 4 is limited to single cell environment. The heterogeneous structure was not taken in to account to reduce the complexity of analysis. The performance analysis of various packet scheduling

algorithms presented in Chapter 3 is limited to single macro cell. The neighbour relationship and other neighbouring macro cells were not taken in to account to reduce the complexity of analysis.

REFERENCES

[1] *IMA111_3E: HSPA+ Technology Introduction*, 2012.

[2] *Requirements for E-UTRA and E-UTRAN (Release 8)*, 2010.

[3] *3GPP TR 25.892; Feasibility Study for Orthogonal Frequency Division Multiplexing (OFDM) for UTRAN enhancement (Release 6)*, 2004.

[4] *3GPP TS 36.211; Physical Channels and Modulation (Release 8)*, 2009.

[5] *3GPP TS 36.101; User Equipment (UE) radio transmission and reception (Release 8)*, 2011.

[6] *3GPP TS 36.212; Multiplexing and Channel Coding (Release 8)*, 2010.

[7] *3GPP TS 36.304; User Equipment procedure in idle mode (Release 8)*, 2008.

[8] A. Ghosh, R. Ratasuk, B. Mondal, N. Mangalvedhe, and T. Thomas, "LTE-Advanced: Next-generation wireless broadband technology," *ACM Transactions on Multimedia Computing, Communications, and Applications*, vol. 17, no. 3, pp. 10–22, Jun. 2010.

[9] N. Baldo, "An Open Source Product-Oriented LTE Network Simulator based on ns-3," in *14th ACM International Conference on Modeling, Analysis and Simulation of Wireless and Mobile Systems*, FL, USA: ACM, 2011, pp. 293–297.

[10] F. Capozzi, G. Piro, L. A. Grieco, G. Boggia, and P. Camarda, "Downlink packet scheduling in LTE cellular networks: Key design issues and a survey," *IEEE Communications Surveys & Tutorials*, vol. 15, no. 2, Second Quater, pp. 678–700, May 2013.

[11] W. K. Wong, H. Y. Tang, and V. C. M. Leung, "Token bank fair queuing: a new scheduling algorithm for wireless multimedia services," *International Journal of Communication Systems*, vol. 17, pp. 591–614, 2004.

[12] D. Zhou, "NS-3 development tree," 2012. [Online]. Available: http://code.nsnam.org/dizhizhou/gsoc-lte-mac-scheduler/ns-3-dev. Accessed: 2016.

[13] "Small Cell Forum,". [Online]. Available: http://scf.io/en/documents/all_documents.php. Accessed: 2016.

[14] H. Seo and B. G. Lee, "A Proportional-Fair Power Allocation Scheme for Fair and Efficient Multiuser OFDM Systems," in *IEEE Globecom*, USA: IEEE, 2005, pp. 3737–3741.

[15] G. Piro, L. Alfredo, G. Boggia, F. Capozzi, and P. Camarda, "Simulating LTE Cellular Systems: An Open-Source Framework," *IEEE Transactions on Vehicular Technology*, vol. 60, no. 02, pp. 498–513, Feb. 2011.

[16] R. K. Jain, D.-M. W. Chiu, and W. R. Hawe, "A Quantitative Measure of Fainess and Discrimination for Resource Allocation in Shared Computer System," *ACM Transaction on Computer Systems*, pp. 1–38, 1984.

[17] H. A. Kim, S. Barua, P. Ghosal, and K. Sandrasegaran, "Macro with Pico Cells (HetNets) System Behaviour Using Well-Known Scheduling Algorithms," *International Journal of Wireless & Mobile Networks*, vol. 6, no. 5, pp. 109–121, Oct. 2014.

[18] I. Toufik, S. Sesia, "*LTE-The UMTS Long Term Evolution From Theory to Practice,*" (no. ISBN: 9780470660256), 2nd ed. OReilly, 2011.

[19] **H.A. Kim, R. Subramanian, F. Afroz and K.Sandrasegaran, "Comparison of Performance of Packet Scheduling Algorithms in LTE-A HetNets," *Wireless Personal Communication*, vol 97, Issue 2, pp. 1947-1965, DOI 10.1007/s11277-017-4380-3.**

[20] M. Andrews, K. Kumaran, K. Ramanan, A. Stolyar, R. Vijaykumar, and P. Whiting, "Providing Quality of Service over a Shared Wireless Link," *IEEE Communication Magazine*, vol. 39, no. 2, pp. 150–154, 2002.

[21] J.-H. Rhee, J. M. Holtzman, and D. K. Kim, "Performance Analysis of the Adaptive EXP/PF Channel Scheduler in an AMC/TDM System," *IEEE Communications Letters*, vol. 8, no. 8, pp. 497–499, 2004.

[22] *Overview of the 3GPP Long Term Evolution Physical Layer*, Freescale Semiconductor, 2007.

[23] R. Basukala, H. A. M. Ramli, and K. Sandrasegaran, "Performance Analysis of EXP/PF and M-LWDF in Downlink 3GPP LTE System," in *First Asian Himalayas International Conference on Internet*, Nepal: IEEE, 2009.

[24] X. Qiu and K. Chawla, "On the Performance of Adaptive Modulation in Cellular Systems," *IEEE Transaction on Communications*, vol. 47, no. 6, pp. 884–895, Jun. 1999.

[25] A. Alfayly, I.-H. Mkwawa, L. Sun, and E. Ifeachor, "QoE-based Performance Evaluation of Scheduling Algorithms over LTE," in *2012 IEEE Globecom Workshops (GC Wkshps)*, USA: IEEE, 2013, pp. 1–5.

[26] M. Iturralde, T. A. Yahiya, and A.-L. Beylot, "Resource Allocation Using Shapley Value in LTE," in *IEEE 22nd International Symposium on Personal, Indoor and Mobile Radio Communications*, IEEE, 2012, pp. 31–35.

[27] A.-H. Jaradat and K. Sandrasegaran, "On the Performance of PF, MLWDF and EXP/PF algorithms in LTE," *International Journal of Computers & Technology*, vol. 8, no. 1, pp. 698–706, Jan. 2013.

[28] H. Holma and A. Toskala, *LTE Advanced: 3GPP Solution for IMT-Advanced* (no. ISBN: 978-1-119-97405-5), 1st ed. Wiley, 2012.

[29] R. Q. Hu and Y. Qian, *Heterogeneous Cellular Networks* (no. ISBN: 9781119999126), 2nd ed. Wiley, 2013.

[30] H. A. M. Ramli, R. Basukala, K. Sandrasegaran, and R. Patachaianand, "Performance of Well Known Packet Scheduling Algorithms in the Downlink 3GPP LTE System," in *IEEE 9th Malaysia International Conference on Communications*, Malaysia: IEEE, 2009, pp. 815–820.

[31] F. Kelly, "Charging and rate control for elastic traffic," *European Transactions on Telecommunications*, vol. 8, pp. 33–37, 1997.

[32] S. Lu, V. Bharghavan, and R. Srikant, "Fair Scheduling in Wireless Packet Networks," *IEEE/ACM Transactions on Networking*, vol. 7, no. 4, pp. 473–489, 1999.

[33] A. K. Parekh and R. G. Gallager, "A Generalized Processor Sharing Approach to Flow Control in Integrated Services Networks: The Single-Node Case," *IEEE/ACM Transactions on Networking*, vol. 1, no. 3, pp. 344–357, Jun. 1993.

[34] T. S. E. Ng, I. Stoica, and H. Zhang, "Packet Fair Networks Queueing Algorithms for Wireless with Location-Dependent Errors," in *IEEE Infocom*, IEEE, 1998, pp. 1103–1111.

[35] S. Borst and P. Whiting, "Dynamic Rate Control Algorithms for HDR Throughput Optimization," in *IEEE Infocom*, IEEE, 2002, pp. 976–985.

[36] X. Liu, E. K. P. Chong, and N. B. Shroff, "Opportunistic Transmission Scheduling With Resource-Sharing Constraints in Wireless Networks," *IEEE Journal on Selected Areas in Communications*, vol. 19, no. 10, pp. 2053–2064, Oct. 2001.

[37] X. Liu, E. K. P. Chong, and N. B. Shroff, "A framework for opportunistic scheduling in wireless networks," *Computer Networks: The International Journal of Computer and Telecommunications Networking*, vol. 41, no. 4, pp. 451–474, Mar. 2003.

[38] Y. Lie and E. Knightly, "Opportunistic Fair Scheduling over Multiple Wireless Channels," in *IEEE Infocom*, IEEE, 2003, pp. 1106–1115.

[39] X. Qin and R. Berry, "Exploiting Multiuser Diversity for Medium Access Control in Wireless Networks," in *IEEE Infocom*, IEEE, 2003, pp. 1084–1094.

[40] P. Viswanath, D. N. C. Tse, and R. Laroia, "Opportunistic Beamforming using Dumb Antennas," in *IEEE International Symposium on Information Theory*, Lausanne, Switzerland: IEEE, 2004, p. 449.

[41] J.-G. Choi and S. Bhak, "Cell-Throughput Analysis of the Proportional Fair Scheduler in the Single-Cell Environment," *IEEE Transactions on Vehicular Technology*, vol. 56, no. 2, pp. 766–778, Mar. 2007.

[42] L. Massoulie and J. Roberts, "Bandwidth Sharing: Objectives and Algorithms," *IEEE/ACM Transactions on Networking*, vol. 10, no. 3, pp. 320–328, Jun. 2002.

[43] J. M. Holtzman, "Asymptotic Analysis of Proportional Fair Algorithm," in *12th IEEE International Symposium on Personal, Indoor, and Mobile Radio Communications*, IEEE, 2002, pp. 33–37.

[44] H. J. Kushner and P. A. Whiting, "Convergence of Proportional-Fair Sharing Algorithms Under General Conditions," *IEEE Transactions on Wireless Communications*, vol. 3, no. 4, pp. 1250–1259, Jul. 2004.

[45] S. Catreux, P. F. Driessen, and L. J. Greenstein, "Data Throughputs Using Multiple-Input Multiple-Output (MIMO) Techniques in a Noise-Limited Cellular Environment," *IEEE Transactions on Wireless Communications*, vol. 1, no. 2, pp. 226–235, Apr. 2002.

[46] A. J. Goldsmith and S.-C. Chua, "Variable-Rate Variable-Power MQAM for Fading Channels," *IEEE Transactions on Communications*, vol. 45, no. 10, pp. 1218–1230, Oct. 1997.

[47] *Evolved Universal Terrestrial Radio Access (EUTRA); Physical Channels and Modulations*, 3GPP Standard TS 36.211, 2011.

[48] *Evolved Universal Terrestrial Radio Access (EUTRA); Physical layer – Measurements*, 3GPP Standard TS 36.214, 2010.

[49] *Physical layer Measurements (FDD)*, ETSI Standard TS 25.215, 2006.

[50] *Evolved Universal Terrestrial Radio Access (EUTRA): Requirements for support of radio resource management*, 3GPP Standard TS 36.133, 2010.

[51] *Evolved Universal Terrestrial Radio Access (EUTRA); Radio Resource Control (RRC); Protocol specification*, 3GPP Standard TS 36.331, 2009.

[52] "LTE performance for initial deployments," Nokia Siemens Networks, Finland, White paper B301-00376-B-200902-1-EN. [Online]. Available: http://www.sharetechnote.com/Docs/LTE_measurement_A4_1302.pdf. Accessed: 2016.

[53] "Keeping the Customer Service Experience Promise – How to Meet the Service Assurance Challenge," *Ericsson white paper*. [Online]. Available: http://www.ericsson.com/news/110121 wp service assurance 244188811 c. Accessed: Oct. 2, 2015.

[54] *Key Performance Indicators (KPI) for Evolved Universal Terrestrial Radio Access Network (E-UTRAN): Definitions*, 3GPP Standard TS 32.450 version 8.0.0 Release 8, 2009.

[55] *Key Performance Indicators (KPI) for E-UTRAN: Definitions*, 3GPP Standard TS 32.450 V8.0.0 Release 8, 2009.

[56] *Study on Minimization of drive-tests in Next Generation Networks*, 3GPP Standard TR 36.805, 2009.

[57] O. Monkewich, "Conformance and Interoperability Testing Tutorial," ITU-T SG 17. [Online]. Available: https://www.itu.int/dms_pub/itu-t/oth/15/04/T15040000080001PDFE.pdf. Accessed: 2016.

[58] H. Moiin, "Next Generation Mobile Networks Beyond HSPA & EVDO," NGMN Alliance, Dec. 5, 2006. [Online]. Available: http://ngmn.org/uploads/media/Next_Generation_Mobile_Networks_Beyond_HSPA_EVDO_web.pdf. Accessed: May 10, 2016.